# Dynamics of Amyloid Plaque Formation in Alzheimer's Disease

A study in transgenic mice

**Dissertation of the Graduate School of Systemic Neuroscience**

Ludwigs-Maximilians-University Munich
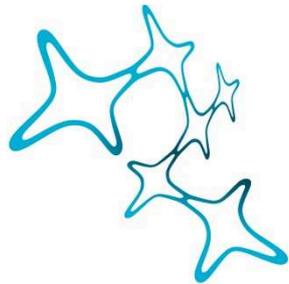
Graduate School of
Systemic Neurosciences

LMU Munich

Submitted by Joanna F. McCarter
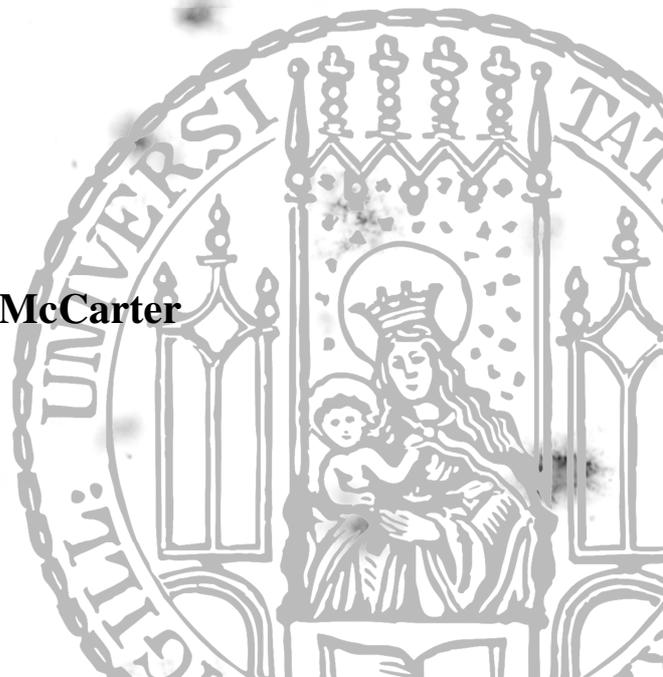
Supervisor: Prof. Dr. Melanie Meyer-Luehmann

2nd reviewer: Prof. Dr. Christian Haass

Date of the oral defense: June 2nd, 2014

Contents

List of Abbreviations

AD   Alzheimer's disease

AICD   APP intracellular domain

APP   Amyloid Precursor Protein

Aβ   Amyloid-β peptide

CAA   Cerebral Amyloid Angiopathy

CNS   Central Nervous System

CSF   Cerebral Spinal Fluid

DIAN   Dominantly Inherited Alzheimer Network

FAD   Familial Alzheimer's disease

FDG-PET   Fluorodeoxyglucose - Positron Emission Tomography

LTP   Long-term Potentiation

MAC   Membrane Attack Complex

MRI   Magnetic Resonance Imaging

MX   Methoxy-X04

PBS   Phosphate-buffered Saline

PIB   Pittsburgh compound B

PS   Presenilin

ROI   Region of Interest

SAD   Sporadic Alzheimer's disease

TAE   Tris-acetate EDTA

TBS   Tris-buffered Saline

TR   Thiazin Red

Summary

Alzheimer's disease (AD) is a fast growing global problem. AD is a form of dementia characterised by the progressive loss of cognitive abilities. Pathologically, the disease is defined by two neuropathological hallmarks: neurofibrillary tangles and amyloid-β plaques. Plaques appear to be toxic to brain tissue and are surrounded by activated microglia and astrocytes, dystrophic neurites and neurons under oxidative stress.

When plaques first develop, they are generally small, but in advanced AD, plaques can be much larger. How small plaques may develop into large plaques is still unclear. A number of studies have shown that small plaques grow uniformly over time to give rise to larger plaques. However, this study investigates an alternative hypothesis: that clusters of multiple small plaques merge over time to form large plaques. This hypothesis was inspired by a study that showed that plaques do not deposit in random locations within the brain parenchyma, but rather form in clusters and that these plaque clusters get bigger over time. The aim was to investigate the clustering of plaques in vivo, and follow these clusters over time to see whether they merge together to form a single, larger plaque.

This study employed a 2-stage staining technique to follow individual plaques in APPPS1 transgenic mice over time. The fluorescent, amyloid-binding dye Methoxy-X04 was injected into the mice at Day 0 of the experiment. Methoxy-X04 crosses the blood brain barrier and binds stably to plaques for several months and thus labelled the original plaque population. Following 1 day, 1 month or 4 month incubation periods, acute in vivo plaque imaging was performed or the mice sacrificed for post mortem analysis. Antibodies against amyloid-β labelled the state of the plaques at these later time points. Hence this procedure enabled comparison of individual plaque status at different time points and the identification of new plaques that had developed over the incubation time.

Detailed analysis of the new and pre-existing plaques revealed two key results. Firstly, that new plaques are more likely to form very close ($< 40\,\mu m$) to a pre-existing plaque than at further distances. New plaques depositing very close to other plaques formed clusters of plaques in the tissue. Secondly, that clusters of close plaques can fuse over time to form a

single large plaque. These two key results provide compelling evidence for a clustering hypothesis of large plaque formation and growth.

Together, these data provide in vivo support for the clustering hypothesis by which clusters of small plaques merge together to form single plaques over time. This work expands our understanding of how plaques form and develop in AD and could inform the understanding of plaque clearance strategies to combat AD pathological changes in the brains of patients.

Parts of this thesis were published in the following paper:

McCarter, J. F., Liebscher, S., Bachhuber, T., Abou-Ajram, C., Hübener, M., Hyman, B. T., Haass, C. & Meyer-Luehmann, M. (**2013**). Clustering of plaques contributes to plaque growth in a mouse model of Alzheimer's disease. *Acta Neuropathologica*, 126 (2), 179-188.

Introduction

1. Alzheimer's Disease

Alzheimer's disease (AD) is the most common form of dementia worldwide (Selkoe, 2001) accounting for 60-80% of all dementia cases (Thies & Bleier, 2011). Once over the age of 85, the chance of developing AD is 25-40% (Golde et al., 2011) and on a global scale, AD is currently estimated to affect 26.6 million people (Brookmeyer et al., 2011). As the human population ages, current projections forecast that, by 2050, a total of 100 million people will suffer from AD (Golde et al., 2011). This is a worrying prediction as the economic burden, in turns of palliative care and loss of economic contribution for so many patients and their carer-givers will be immense. To date there is no treatment for AD, only symptomatic relief in the mild to moderate stages of the disease (Holtzman et al., 2011). With the number of AD patients growing day by day, the need to find etiological clues and develop disease-modifying treatments is increasingly urgent.

AD is a disease recognised by the gradual worsening of memory, attention and other intellectual abilities. AD contains a long, pre-symptomatic phase and pathological changes in the brain are thought to begin decades before cognitive problems manifest (Jack Jr et al., 2010). The time course for AD from first clinical presentation to death is typically 7 to 10 years (Holtzman et al., 2011). AD patients generally first notice a loss of short-term and spatial memory, reduced attention and deficient problem-solving skills (Holtzman et al., 2011). Over the progression of the disease, memory, cognition and functional ability further diminish, frequently accompanied by symptoms of depression, anxiety and paranoia. In advanced stages of AD, patients are unable to perform basic everyday tasks and require intensive care, ultimately becoming entirely bed-bound. Patients often die of concomitant secondary complications associated with inertia, such as pneumonia (Thies & Bleier, 2011).

1.1. Pathological Hallmarks of Alzheimer's Disease

Alzheimer's disease was first identified as a unique neurological disorder in 1907 by Alois Alzheimer (Figure 1, (Alzheimer, 1907; Stelzmann et al., 1995)). He observed the two prominent cerebral hallmarks of the disease that are still used for post mortem diagnosis today – neurofibrillary tangles and amyloid plaques (Figure 2).
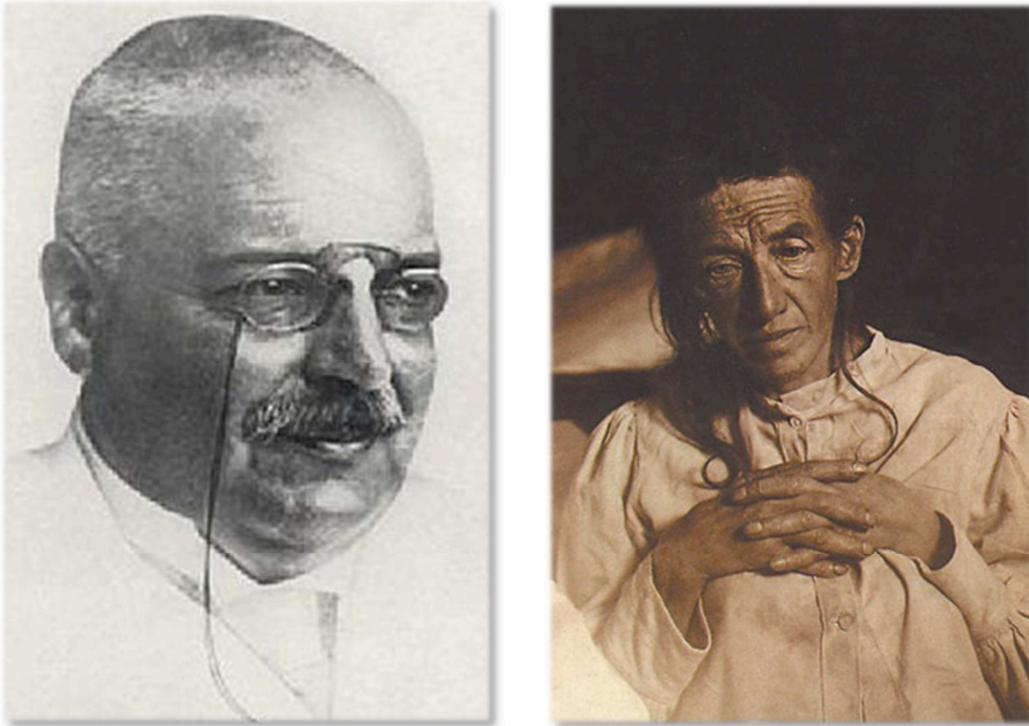
Figure 1: The identification of Alzheimer's Disease. Alois Alzheimer (left) and his first patient diagnosed with Alzheimer's disease, Augusta Deter (right). Images in the public domain.

Neurofibrillary tangles are abnormal intracellular structures mainly consisting of hyperphosphorylated tau protein (Grundke-Iqbal et al., 1986). Tau is a microtubule stabilising protein that is normally bound to the microtubules and forms an integral part of the cell structure. However, in AD, tau becomes hyperphosphorylated so that it no longer binds to microtubules (Drechsel et al., 1992) and aggregates inside the cell, eventually forming neurofibrillary tangles. Neurofibrillary tangles are often called the 'tombstones' of neurons as they are all that remains after the original cell has succumbed to the disease (Gendreau & Hall, 2013). What causes tau to be hyperphosphorylated and how amyloid-β (Aβ) peptide might be involved is still a matter of debate. Aggregated Aβ peptide is the main ingredient in the second hallmark of AD, amyloid-β plaques (Figure 2). Amyloid-β plaques are mainly found in the parenchyma, but also deposits around cerebral blood vessels to form cerebral amyloid angiopathy (CAA) (Attems et al., 2010). Amyloid plaques within the brain parenchyma are the main subject of this thesis and will be described in more detail in subsequent sections.
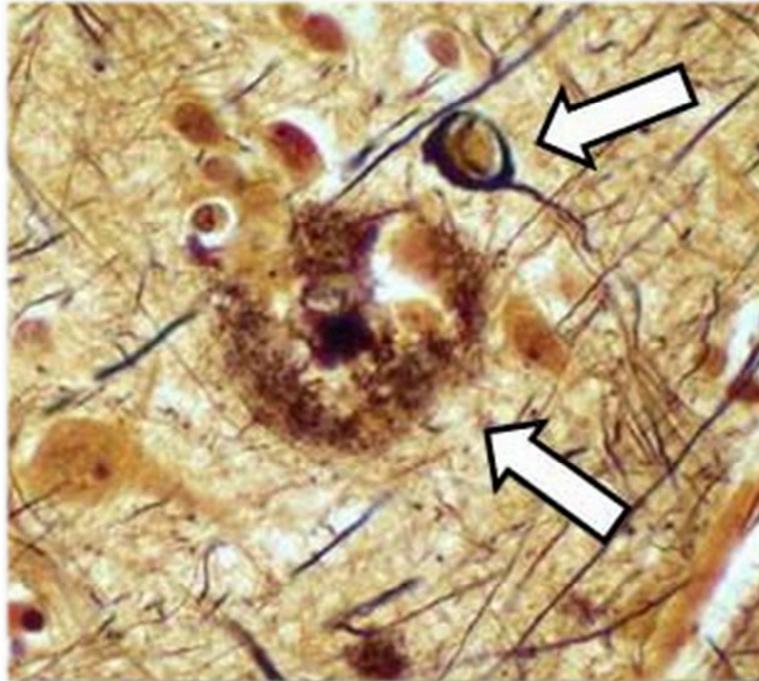
Figure 2: The pathological hallmarks of Alzheimer's disease. Neurofibrillary tangles (black semi-circle; upper white arrow) and amyloid plaques (dark brown, fibrous mass; lower white arrow) are the two major neuropathological hallmarks of Alzheimer's disease. Image taken from (Schellenberg & Montine, 2012).

1.2. Generation of Amyloid-β from its Precursor Protein

Aβ peptide, the major component of amyloid plaques, is produced by intramembrane cleavage of the Amyloid Precursor Protein (APP). APP (Figure 3a) is a highly conserved transmembrane protein and its cleavage follows two major enzymatic pathways; the non-amyloidogenic pathway and the amyloidogenic pathway (Figure 3).

In the non-amyloidogenic pathway, APP is cleaved at the cell surface by the enzyme α-secretase within the Aβ region to generate soluble APPα (sAPPα) and the α-c-terminal fragment (αCTF). As this cleavage occurs within the Aβ amino acid stretch, Aβ is not produced by this cleavage pathway (Figure 3b). The αCTF is further cleaved by γ-secretase to produce p3 and the APP intracellular domain (AICD, Figure 3c).

In the amyloidogenic pathway, APP is first cleaved in the endosomal compartment by β-secretase to generate the sAPPβ fragment and the βCTF (Figure 3d), and subsequently cleaved by γ-secretase to release the Aβ peptide into the extracellular space (Figure 3e) and the AICD intracellularly. The γ-secretase enzyme can cleave APP at different sites to give different species of Aβ: 38, 40 and 42 amino acids in length being the most common. Aβ is then released into the endosomal lumen or into the extracellular space (O'Brien & Wong, 2011). $A\beta_{40}$ is the most abundant Aβ species produced (Seubert et al., 1992). However, in AD patients, $A\beta_{42}$ is the most abundant Aβ species found in plaques (Roher et al., 1993). $A\beta_{42}$ has the greatest propensity to aggregate of all the Aβ species as shown by *in vitro* experiments (Snyder et al., 1994) and these aggregated Aβ species can form fibrils that give rise to plaques. Therefore, an increase in $A\beta_{42}$ could directly promote AD pathological processes.
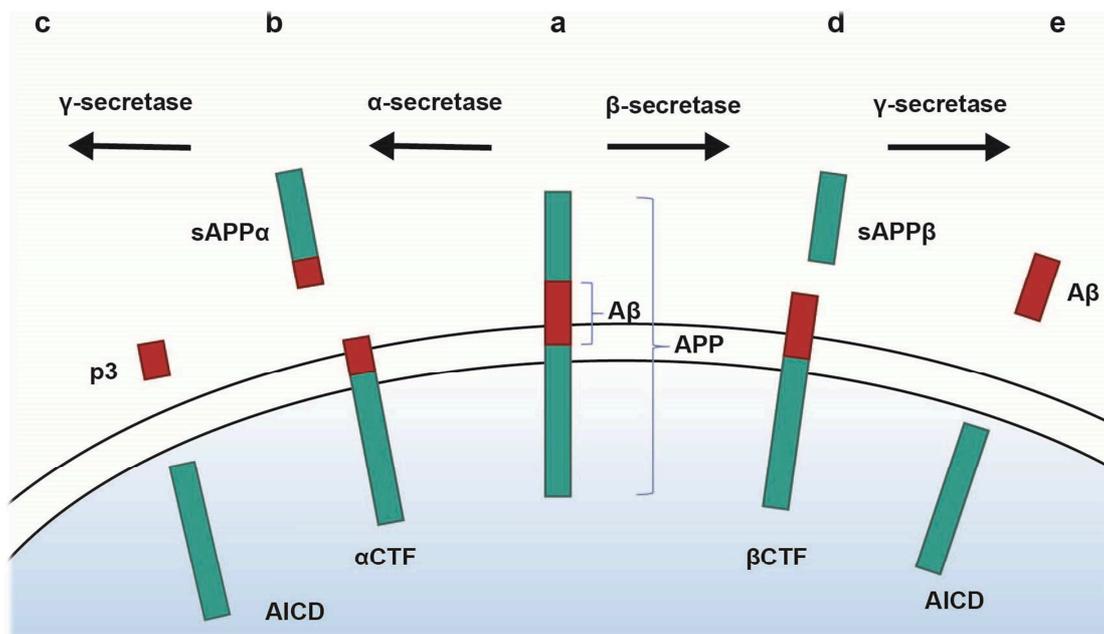
Figure 3: Processing of APP by the 3 secretases. In the non-amyloidogenic pathway, APP (a) is cleaved by α-secretase to generate sAPPα and αCTF (b) and then by γ-secretase to release p3 and the AICD (APP intracellular domain). In the amyloidogenic pathway, APP (a) is cleaved first by β-secretase to generate sAPPβ and the βCTF (d) and subsequently by γ-secretase to release Aβ into the extracellular space and AICD intracellularly (e).

The three secretases have been characterised molecularly. ADAM10 was identified as an α-secretase (Kuhn et al., 2010; Lammich et al., 1999) and, when over-expressed in APP transgenic mice, increase sAPPα and decrease $A\beta_{42}$ production and plaque deposition (Postina et al., 2004). BACE1 is a β-secretase (Willem et al., 2009) and BACE1 knock-out APP transgenic mice do not deposit any plaques (Luo et al., 2003). γ-secretase is a complex of 4 different proteins: presenilin (PS), Nicastrin, APH-1 and PEN-2 that are all required for its enzymatic function (Edbauer et al., 2003).

The physiological functions of APP and its cleavage products are largely unknown or highly debated. APP is a ubiquitously expressed protein and highly conserved, yet the role of this protein remains elusive. Mice overexpressing APP have enlarged cortical neurons, suggestive of a neurotrophic effect (Oh et al., 2009), while APP knockout mice had reduced brain weight, deficient LTP and impaired spatial navigation in behavioural tests (Ring et al., 2007). sAPPα also appears to be beneficial to neurons; sAPPα protects neurons against stress (Mattson et al., 1993) and reduces neuronal damage following traumatic brain injury (Thornton et al., 2006). CTFα and –β have no known physiological function (Chow et al., 2010). Research suggests a role for AICD in transcription, apoptosis and cytoskeletal dynamics, but the data are inconclusive and many questions remain open (Müller et al., 2008). It is important to continue research into the physiological functions of these proteins as any therapy aimed at altering these cleavage pathways could have unintended side-effects.

1.3. Genetics of Alzheimer's Disease

There are two main categories of AD: familial and sporadic. Familial AD (FAD) accounts for <1% of all AD cases (Morris et al., 2012) and is associated with heritable autosomal dominant mutations. The majority of AD cases are classified as sporadic AD (SAD) where no clear genetic cause is implicated.

Familial AD (FAD) patients have an earlier onset and faster progression than SAD cases. Some forms of FAD are caused by mutations in the amyloid precursor protein (APP) from which Aβ is cleaved. All 31 FAD APP mutations are found in a 54 amino acid segment in and around the Aβ peptide sequence and effect the amount or type of Aβ produced; this generally leads to increased Aβ aggregation and plaque formation (Schellenberg & Montine, 2012). For example, some mutations lead to an increase in the amyloidogenic processing of APP (Haass et al., 1994). Many APP mutation sufferers have specific neuropathological

characteristics; they may develop more plaques than SAD patients (Ishii et al., 2001) or display overly CAA-dominated pathology (Natté et al., 2001).

Mutations in subunits of the γ-secretase enzymatic complex that cleaves APP – called Presenilin 1 or 2 (PS1 or PS2) - are also known to cause FAD. These mutations primarily alter the transmembrane domains of these proteins (O'Brien & Wong, 2011) and effect the enzymatic processing of APP. PS mutations can also increase the amount of plaques (Ishii et al., 2001) and tau deposits (Shepherd et al., 2004) found in the brains of patients carrying these mutations compared with the more common SAD neuropathology.

Sporadic AD (SAD) patients generally have a later onset of the disease than patients with FAD, typically first presenting symptoms after the age of 65, and the specific cause of SAD is largely unknown. Genomic studies have, however, identified a number of risk factors that alter the chance of developing SAD. The most common risk factor for SAD is the *APOE4* allele (Strittmatter et al., 1993) which is present in 10-20% of the population (Singh et al., 2006). Heterozygous carriers have three-fold increase in risk of AD, while for homozygous individuals, the risk increases 12-fold (Kim et al., 2009). The ApoE4 protein degrades Aβ less than other APOE variants (Small & Duff, 2008), thereby most likely increasing the rate of AD pathology. Indeed, expression of APOE4 in APP transgenic mice exacerbated the AD pathology of these mice compared to control mice (Hudry et al., 2013). A correlation was also found between sortilin-related receptor 1 (SORL1) mutations and SAD risk (Reitz et al., 2011; Rogaeva et al., 2007). SORL1 is involved in a cellular transport pathway important for Aβ generation (Lane et al., 2010), although exactly how this would then increase the risk of AD is still unclear.

Rare heterozygous mutations in the TREM2 protein have been linked to an increased risk of SAD (Guerreiro et al., 2013; Jonsson et al., 2013). TREM2 is expressed in microglia and regulates microglial phagocytosis (Guerreiro et al., 2013). If TREM2 function is impaired by these SAD-linked mutations, then impaired microglia phagocytosis reducing the clearance of Aβ could explain the increased risk of SAD.

A recent meta-analysis of genome wide association studies (GWAS) involving over 70,000 individuals' genomes discovered a number of new AD risk factors. These genetic risk factors implicate a number of factors in the susceptibility to AD; e.g. inflammation, synaptic function

and axonal transport (Lambert et al., 2013). These new factors could yield some exciting lines of investigation into the etiology and modification of AD.

Genetic analysis also revealed a mutation protective against AD; a study of an Icelandic population found that an APP mutation decreased the risk of developing AD (Jonsson et al., 2012). This study sheds light on a cellular mechanism that protects against AD, and may lead to new insights into preventative therapies.

1.4. Mouse Models of Alzheimer's Disease

There are many different transgenic animals used to investigate AD; from fish, flies and worms to rats and mice. Although useful for investigating certain questions, fish, fly and worm models are very physiologically different to AD patients. Rodents have a much more comparable physiology and, of particular interest when studying AD, a similar gross brain anatomy. Mice are easy to breed and house and the technology to create transgenic mouse lines is well established. Transgenic mice are therefore an extremely useful model to investigate aspects of AD.

Knowledge about FAD-causing autosomal dominant mutations has been used to recapitulate AD pathology in mice. The first transgenic mouse models used to study AD expressed human APP mutations. For example, the Tg2576 mouse expresses APP 695 with the Swedish double mutation (Hsiao et al., 1996), the APP23 mouse expresses APP 751 with the Swedish double mutation (Sturchler-Pierrat et al., 1997), while the PDAPP mouse expresses the V717F APP mutation (Games et al., 1995). All three APP mouse models develop Aβ plaques, gliosis and dystrophic neurites. PS1 mutant mouse lines have been generated (Elder et al., 2010), but fail to develop plaque pathology. Only when crossed with an APP mutant line, do they develop plaques and the onset of plaque pathology is even accelerated (Holcomb et al., 1998).

Mouse models only recapitulate limited aspects of human AD patient pathology and symptoms and as such are incomplete models of AD (Radde et al., 2008). For example, neurofibrillary tangle pathology is only seen when an additional tau mutation (discovered in frontotemporal dementia patients) is expressed. Crossing the Tg2576 mouse with a mouse expressing Tau with the P301L mutation produced the same amount of plaques as Tg2576 mice, but the neurofibrillary tangle pathology was earlier and more extensive than the pure Tau P301L mouse (Lewis et al., 2001). Another model, the 3xTg mouse expresses APP, PS1

and tau mutations and develops plaques and neurofibrillary tangles (Oddo et al., 2003). Furthermore, the gross neuronal loss associated with AD (Figure 4) is strikingly absent from mouse models of AD (Radde et al., 2008). Nevertheless, incomplete mouse models are very useful to investigate certain aspects of the disease, for example amyloid plaque development, in isolation without the added complication of comorbid pathology.

1.5. Neuroinflammation in Alzheimer's Disease

As well summarised in a review entitled "Inflammation in Alzheimer disease: driving force, bystander or beneficial response?" (Wyss-Coray, 2006), there is no consensus as to the consequences of inflammation on the pathology of AD whether positive or detrimental. Inflammation is an important defence mechanism against invading pathogens and vital for the clearance of dead cell debris. In the central nervous system (CNS), neuroinflammation is mainly carried out by two glial cell types: microglia and astrocytes that appear to change during the course of AD. Microglia cluster around plaques in AD (Figure 4 (Itagaki et al., 1989)) and, in APP transgenic mice, are larger around plaques (Frautschy et al., 1998) and display an altered phenotype (Koenigsknecht-Talboo et al., 2008). Pharmacological suppression of microglial activation decreased the plaque deposition and hippocampal neuronal loss induced by $A\beta_{42}$ infusion (Craft et al., 2004). Microglia appear to regulate plaques as a study in APP transgenic mice revealed that microglia surrounding plaques internalise $A\beta$, removing it from the plaque (Bolmont et al., 2008). Yet a study that ablated 90% of the microglia in APP transgenic mice, did not show any alteration in plaque load or plaque size (Grathwohl et al., 2009). Therefore, the precise role microglia play in AD is still unclear.

Astrocytes are closely associated with synapses and play an active role in removing neurotransmitters from the synaptic cleft. This means that any perturbation in astrocyte functions could have damaging consequences for synaptic function and neuron viability. Plaques attract astrocytes which encircle the plaques (Figure 4 (Sofroniew & Vinters, 2010)) and astrocytes have also been shown to take up $A\beta$ for degradation and even clear tissue of plaques (Wyss-Coray et al., 2003). Whether this $A\beta$ clearing property could be harnessed to protect against AD or whether this would be detrimental to the synaptic functions of astrocytes remains unsolved.

A further component of neuroinflammation is the complement system. The complement system is made up of a number of complex molecular pathways that serve to 'complement' the cellular part of the immune system. It performs a number of tasks including stimulating inflammatory pathways, assisting phagocytosis and forming the membrane attack complex (MAC). The MAC is an assembly of complement proteins that inserts into membranes and induces membrane lysis. The complement system appears to be involved in the pathology of AD as complement proteins are found within plaques (Figure 4 (Eikelenboom et al., 1988)). MAC components are found within dystrophic neurites suggesting that the MAC may be active in these cells and contribute to the degeneration of these neurons by membrane lysis (Webster et al., 1997). Finally, in vitro aggregates of Aβ strongly activate the complement system showing that Aβ may trigger the complement system involvement in AD (Rogers et al., 1992).
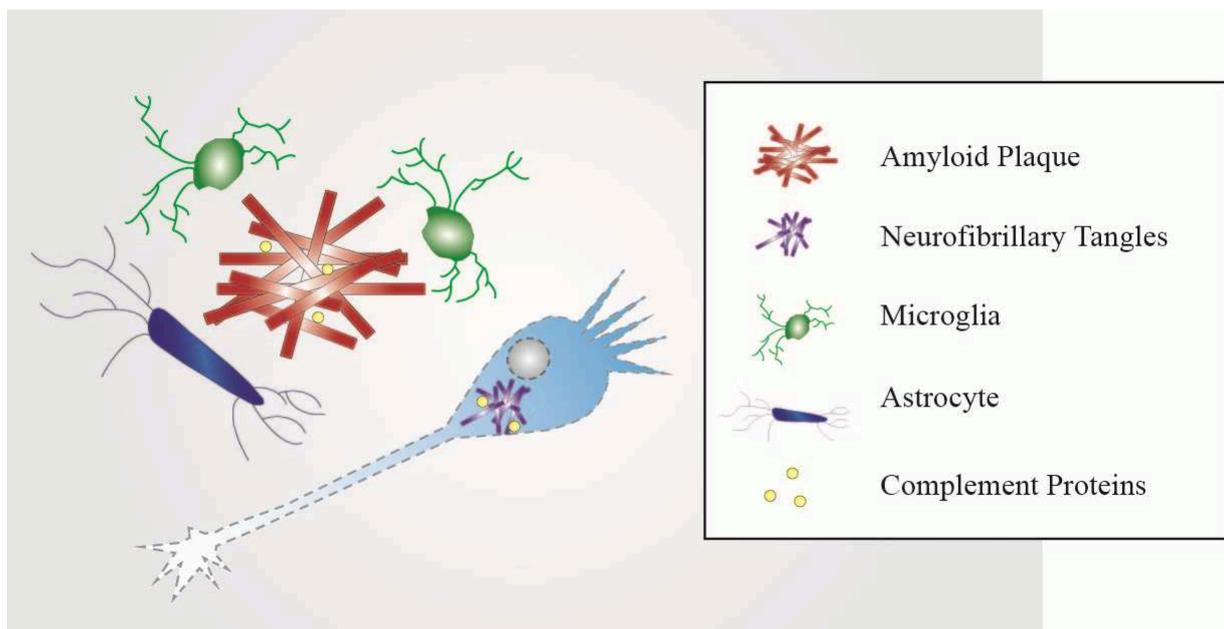

Figure 4: Neuroinflammation in Alzheimer's Disease. Microglia and astrocytes are recruited to amyloid plaques. Complement proteins associate with extracellular plaques and interneuronal neurofibrillary tangles.

Epidemiological studies found a link between long term NSAID (non-steroidal anti-inflammatory drugs) use, generally taken to reduce the symptoms of rheumatoid arthritis,

reduced the risk of AD (McGeer et al., 1990; Vlad et al., 2008). This link appeared to be a way of protecting against AD, indeed APP transgenic mice treated with Ibuprofen had fewer plaques and dystrophic neurites (Lim et al., 2000) and curcumin treatment reduced gliosis and plaque load (Lim et al., 2001). Despite these promising data, clinical trials of NSAID treatment in AD patients failed to show a beneficial effect (de Jong et al., 2008; Pasqualetti et al., 2009). Nevertheless, there seems to be an enigmatic link between inflammation and AD risk and pathology that warrants further exploration.

1.6. Neuronal and Synaptic Loss in Alzheimer's Disease

AD is characterised by a massive loss of neurons (Holtzman et al., 2011), most strikingly demonstrated by the gross loss of cortical grey matter that results in enlarged ventricles and severe brain shrinkage in post mortem samples of AD patients (Figure 5). Structural MRI (magnetic resonance imaging) studies have demonstrated a correlation between the extent of cortical atrophy and the severity of cognitive symptoms (Jack Jr et al., 2010). Moreover, functional imaging, e.g. FDG-PET (fluorodeoxyglucose - positron emission tomography), shows functional changes in the brain of AD patients. FDG-PET is a measure of net brain metabolism and indicates synaptic activity. AD patients have decreased FDG-PET uptake compared to control patients, implying a reduction in synaptic activity. This decreased uptake correlates well with the patients' cognitive decline (Minoshima et al., 1997) and correctly predicts post mortem AD diagnosis (Hoffman et al., 2000). Progressive neuronal and synaptic deficiency in AD is thought to underlie the cognitive decline observed throughout the disease and can be used to monitor disease progression.
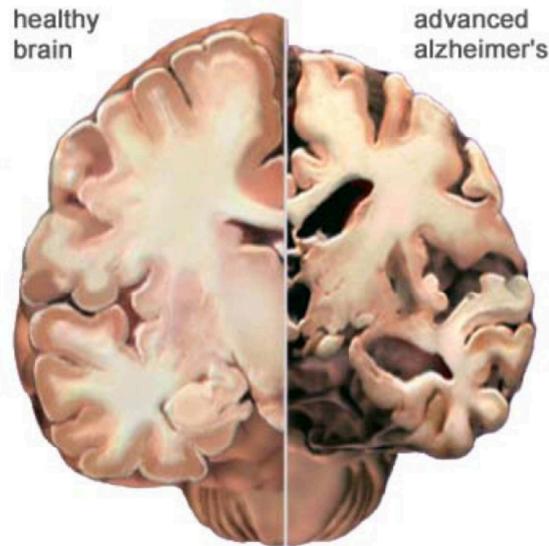
Figure 5: Cortical atrophy in advanced Alzheimer's disease. An Alzheimer's disease patient typically has substantial grey matter atrophy. From the Alzheimer's society (www.alz.org).

1.7. Lifestyle Risk Factors Associated with Alzheimer's Disease

Age is the most important risk factor for AD, but a number of lifestyle factors are associated with a modified risk of AD (Ballard et al., 2011). For example, obesity (Beydoun et al., 2008), regular smoking (Rusanen et al., 2011), and heavy alcohol consumption (Tyas, 2001) have all been linked to an increased risk of AD. Evidence has also come from animal studies for lifestyle risk factors for AD; APP transgenic mice fed a high-fat diet (Ho et al., 2004) or exposed to daily cigarette smoke (Moreno-Gonzalez et al., 2013) had exacerbated AD-related pathology. Regular physical exercise has a preventative effect in AD (Hamer & Chida, 2009) and numerous studies provide evidence that a high cognitive reserve – a measure of education, occupation and mental activities – delays the onset of AD symptoms in patients (Valenzuela & Sachdev, 2006). Supporting this correlation, mice expressing AD transgenes exposed to an enriched environment showed a decrease in AD pathology compared to mice housed in a standard environment (Lazarov et al., 2005).

AD develops over many decades and a human life is a complex mix of different lifestyle and environmental events. Even if these lifestyle factors only have a tiny influence on the progression of AD, this could have a substantial additive effect in promoting or delaying the progression of the disease over such a long time.

2. Amyloid- β peptide

2.1. Amyloid-β Aggregation

Aβ, especially Aβ$_{42}$, is prone to aggregation and forms plaques, a major neuropathological hallmark of AD. This aggregation is thought to follow a well-defined pathway to result in amyloid fibrils and plaques. It starts with Aβ monomers and they aggregate, via several intermediate steps, to form large fibrils with an amyloid structure. Amyloid is defined as "any proteinaceous polymer having a β-pleated sheet conformation" (Fiala, 2007).

The formation of amyloid fibrils from single Aβ peptide molecules is thought to follow a sequence of events that, at some stages, is reversible (Bitan et al., 2003; Cruz et al., 1997), but eventually becomes a self-propagating mechanism (Figure 6). Aβ monomers can reversibly form Aβ oligomers of various sizes and Aβ protofibrils (Grüning et al., 2013; Walsh et al., 1999). Protofibrils and oligomers further aggregate to form amyloid fibrils (Ahmed et al., 2010), the basic component of plaques (Martins et al., 2008).

Aβ Monomers   **Aβ Oligomers**   **Aβ Protofibrils**   **Amyloid fibrils**
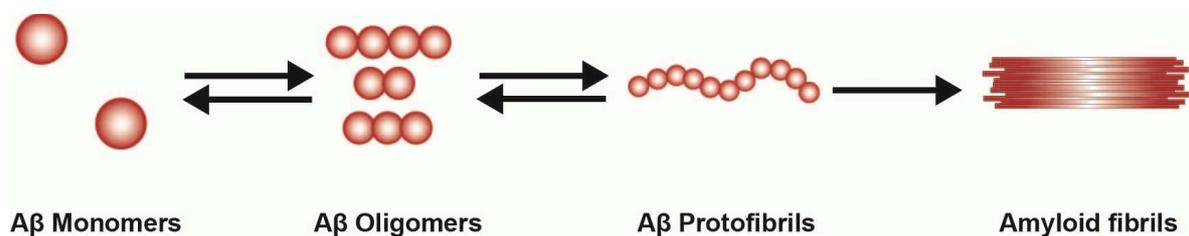
Figure 6: The Aβ aggregation process. Aβ is released as a monomer. Aβ momomers reversibly aggregate to form oligomers and protofibrils. Protofibrils aggregate irreversibly to form amyloid fibrils.

The Aβ aggregation process can be artificially accelerated by a process called seeding. Aβ may have to reach a certain state of aggregation before plaques can be seeded and by artificially providing Aβ in this state, the plaque deposition process is accelerated. This was first observed in in vitro experiments of Aβ aggregation. If pre-formed Aβ aggregates are added to a solution of Aβ monomers, the solution will form fibrils at a much higher rate than a pure Aβ monomer solution (Jarrett & Lansbury, 1992; Lomakin et al., 1997). Moreover, injecting brain homogenate from AD patients or aged APP transgenic mice into pre-

depositing mice produces plaques in these mice much earlier than if they had not been injected or had been injected with healthy control or wild-type brain homogenate (Kane et al., 2000; Meyer-Luehmann et al., 2006). This seeding process is dependent on both incubation time and injected material concentration (Harper & Lansbury, 1997; Meyer-Luehmann et al., 2006). The injected material is thought to contain a seeding factor that induces the aggregation of Aβ and the formation of plaques. This seeding factor has yet to be definitively identified, but there are some likely candidates. Aβ oligomers could be that 'seed' as synthetic Aβ oligomers injected into APP transgenic mice were found at the core of new plaques (Gaspar et al., 2010), implying the Aβ oligomers were involved in the initiation of plaque formation.

2.2. Amyloid-β Oligomers

Aβ oligomers may not only seed plaque formation, but may also contribute to neuronal toxicity in AD. The amyloid fibrils that make up plaques are large, compact and insoluble structures. Smaller, soluble forms of Aβ are thought to be the more likely mediators of cellular toxicity in AD (Haass & Selkoe, 2007). Aβ oligomers in particular have been put forwards as likely candidates for this toxic role (Larson & Lesné, 2012).

Aβ oligomers are a diverse group ranging from dimers to dodecamers and larger molecules. They have a clear opportunity to exert this toxic function as Aβ oligomers are found both intra- and extracellularly. (Benilova et al., 2012). Cell-derived Aβ oligomers, particularly Aβ trimers, decreased LTP (long term potentiation) in hippocampal slice culture preparations (Townsend et al., 2006) showing that they can perturb key brain functions. Moreover, Aβ oligomers derived from human cells and injected into rat ventricles reduced LTP in the nearby hippocampus (Walsh et al., 2002) and decreased the rats' cognitive ability (Cleary et al., 2005). A specific Aβ oligomer, Aβ*56, was discovered in older APP transgenic mice that disrupted memory when injected into young rats (Lesné et al., 2006) and is lowered in the CSF of AD patients (Lesné et al., 2013). Aβ oligomers isolated from AD patients also impaired LTP and altered neuronal morphology in hippocampal slice culture (Shankar et al., 2008) and induced neuritic dystrophies (Jin et al., 2011). In the brains of AD patients, there is evidence that Aβ oligomers interact with key synaptic components and oligomer levels are correlated to the loss of synaptic proteins (Pham et al., 2010). Taken together, these studies strongly implicate Aβ oligomers as a toxic species in AD, although the exact identity of the toxic oligomer(s) in question is still under debate.

3. The Amyloid Cascade Hypothesis

The amyloid cascade hypothesis is one of the best hypotheses that we have to model AD progression. It was first described by John Hardy and Gerald Higgins in 1992 (Hardy & Higgins, 1992). The hypothesis proposed that Aβ is the causative agent in AD and that neurofibrillary tangles, cell toxicity and neurodegeneration occur subsequent to Aβ pathology (Figure 7). According to the hypothesis, Aβ is the 'driver' of a cascade of down-stream events that ultimately leads to the death of neurons and the cognitive symptoms of AD. There are several lines of evidence to support this and others that cast some doubt on the simplicity of the hypothesis.

Aβ
-overproduction
-aggregation
-e.g. Aβ oligomers

Neuronal Dysfunction
-Tau
-oxidative stress
-synaptic toxicity

Neurodegeneration
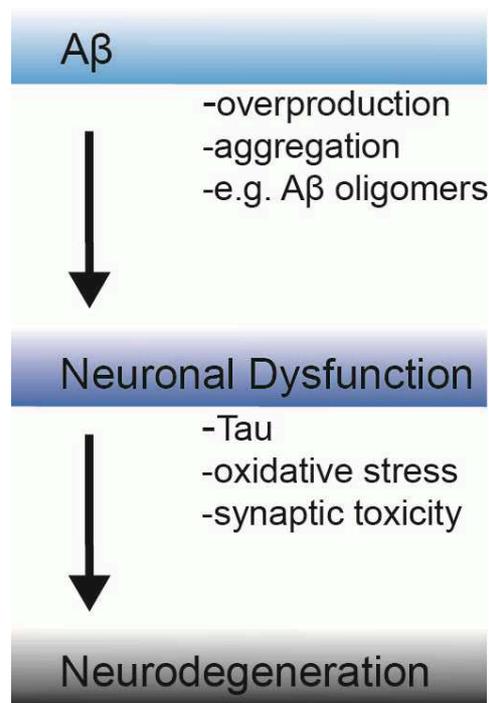
Figure 7: A simplified schematic of the amyloid cascade hypothesis. Aβ overproduction or aggregation is the trigger for downstream neuronal events and neurodegeneration in Alzheimer's disease.

In favour of this hypothesis are all the genetically forms of AD identified so far. Forms of FAD are very often associated with autosomal dominant mutations that universally implicate the production of Aβ in the etiology. There are mutations in APP itself or in the PS subunits

of the γ-secretase complex that releases Aβ from APP. These mutations often increase the amount of Aβ produced or modify the ratio of Aβ species cleaved from APP (Schellenberg & Montine, 2012), supporting the notion that Aβ is the initiator of the disease mechansim.

Further genetic support for Aβ as the initiator of the cascade is the cognitive deficit and AD-like pathology seen in Down's syndrome patients. Down's syndrome occurs when three copies of Chromosome 21 are inherited. The gene for APP lies in Chromosome 21 and so Down's syndrome patients have three copies of the APP gene and produce excess amounts of APP. These patients develop Aβ plaques by the age of 40 and subsequent dementia is common (Hof et al., 1995; O'Brien & Wong, 2011). This syndrome again implicates APP and Aβ as causes of neurodegeneration and dementia.

Further support for the amyloid cascade hypothesis comes from studies looking at the functional effect of Aβ. Aβ, when applied to neuronal cells or slice culture, is toxic to cells and detrimental to LTP. A 35 kDa fragment of APP was shown to bind to DR6 (death receptor 6) and trigger axonal degeneration and neuronal death (Nikolaev et al., 2009). Furthermore, transgenic mouse models expressing FAD mutations in APP and PSEN develop AD-like pathology and memory deficits (Hsiao et al., 1996; Radde et al., 2006), implying that these proteins do play a causative role in AD.

Aβ seems to require other proteins, namely Tau, to exert its neurotoxicity. If tau is knocked out, Aβ is no longer toxic to neurons and cognitive and behavioural deficits are rescued in a mouse model of AD (Roberson et al., 2007). Further evidence implicating Tau, not Aβ as the toxic factor in AD is a study correlating neurofibrillary tangle pathology with the neuron loss in AD (Giannakopoulos et al., 2003). However, mutations in Tau that increase tau aggregation lead to frontal temporal dementia, not AD (Mudher & Lovestone, 2002). Therefore, Tau may be the mediator by which Aβ exerts its toxic effect which does not rule out Aβ as the initial trigger that starts an independent chain of events leading to AD.

Critics of the amyloid cascade hypothesis commonly cite the fact that Aβ and plaques are found in cognitively normal aged people (Pimplikar, 2009) implying that Aβ and plaques do not necessarily spark a cascade of cerebral deterioration and cognitive decline. However, these people could simply be in the pre-cognitive phase of AD and their pathology may not be advanced enough to show any cognitive decline. Therefore, more in depth study about the

pre-cognitive phase of AD is required before this observation could definitively disprove the amyloid cascade hypothesis.

An alternative to the amyloid cascade hypothesis, the presenilin hypothesis of AD proposes that loss of PS function leads to the neuropathogenesis of AD (Shen & Kelleher, 2007). This hypothesis is supported by the fact that PS knockout mice had a severe loss of cortical neurons and cognitive defects (Saura et al., 2004). Nevertheless, it is still possible for PS dysfunction to be caused by Aβ overproduction, since Aβ may be upstream of a cascade that leads to a loss of PS function.

Therapies targeting Aβ plaques and Aβ oligomers have yet to be successful in human trials – indeed therapy patients have even declined faster than control patients. For example, in 2010, a high profile, stage 3 clinical trial of the γ-secretase inhibitor, Semagacestat, was halted early because patients treated with the highest dose of Semagacestat were deteriorating at a faster rate than patients treated with placebo (Doody et al., 2013). This failure could be attributed to the other, non-APP-shedding functions of γ-secretase or in not treating patients early enough in the disease (Karran et al., 2011). A modified version of the amyloid cascade hypothesis postulates that Aβ may just be the initial event that triggers a self-propagating cascade of adverse brain events that becomes independent of Aβ (Karran et al., 2011). If this is the case, then targeting Aβ once the disease has started would have little beneficial effect to the patient and this modified hypothesis would have strong implications for future therapeutic development.

A number of clinical studies in the pipeline aiming to slow or halt the progression of AD are based on the amyloid cascade hypothesis. A study by the Alzheimer Prevention Initiative will treat FAD cases from a Columbian town with a monoclonal antibody against Aβ (crenezumab) with the hope of preventing or delaying the certain onset of AD. The Dominantly Inherited Alzheimer Network (DIAN) is also running a trial to treat FAD cases with monoclonal antibodies against Aβ (gantenerumab and solanezumab) with the hope of altering pre-clinical biomarkers and, ultimately, the development of AD. In another study, mild to moderate AD patients actively immunised with a fragment of the Aβ peptide successfully developed an antibody response, although the efficacy of this strategy in improving symptoms has yet to be tested (Winblad et al., 2012). If either of these or other

anti-Aβ treatments prove beneficial to AD patients, then this would add strong support to the amyloid cascade hypothesis.

Taken together, this genetic and experimental data does seem to support the amyloid cascade hypothesis that Aβ is the primary cause of AD and the amyloid cascade hypothesis remains the dominant theory of AD etiology over two decades after it was originally formulated.

4. Amyloid-β Plaques

Aβ plaques are one of the two major pathological hallmarks of AD. Plaques are extracellular deposits of aggregated Aβ, typically within a spherical region (Fiala, 2007). This thesis investigates the growth and development of plaques and this section will examine their role in AD.

4.1. Origin of Amyloid-β Plaques

The main component of plaques is aggregated Aβ. However, the origin of the Aβ used to create plaques and where the aggregation takes places is under debate. There are many different hypotheses which are highlighted in the following paragraphs (Figure 8).

Firstly, there is a theory that Aβ is secreted from blood vessels into the perineuronal space where it aggregates and forms amyloid deposits (Figure 8a). This theory is supported by the fact that AD patients often display extensive amyloid deposition within the walls of the cerebral blood vessels, a phenomenon called cerebral amyloid angiopathy (CAA). CAA is frequently associated with intense surrounding plaque pathology in the parenchyma (Kumar-Singh et al., 2005) showing that cerebral blood vessels and their surroundings are a site for Aβ aggregation and a possible source of Aβ. Moreover, cerebral microstrokes in APP transgenic mice caused a local spike in plaque number (Garcia-Alloza et al., 2011). An intriguing study injected brain homogenate into the peritoneal cavity of APP transgenic mice and saw cerebral amyloid deposits predominantly in the vicinity of blood vessels (Eisele et al., 2010) showing that Aβ 'seeds' may travel in the blood stream and trigger plaque deposits to form in the brain.

Secondly, there is a theory that neurons secrete Aβ for plaque formation, either from cell bodies, or from axon terminals (Figure 8b). A cell culture study discovered that Aβ can be released into the extracellular space via exosomes at the cell membrane (Rajendran et al., 2006). The specific synaptic release of Aβ is supported by data that Aβ levels in the brain seem to correlate with local neuronal activity (Bero et al., 2011) and if synaptic transmission is blocked, Aβ levels decrease in the parenchyma (Cirrito et al., 2005). Once released in to the extracellular space, secreted Aβ could then follow the aggregation pathway to form plaques.

Thirdly, there is a hypothesis that Aβ monomers aggregate intraneuronally to form Aβ oligomers or fibrils (Takahashi et al., 2004; Walsh et al., 2000) and are then secreted into the extracellular space to induce plaque formation (Figure 8c). Immunohistochemical analysis of neuronal cultures showed that Aβ oligomers are found in multivesicular bodies in the synapses and along microtubules in neural processes (Takahashi et al., 2004). Further validating the idea of intracellular Aβ aggregation, physiological concentrations of Aβ do not aggregate to form fibrils in vitro (Parbhu et al., 2002), indicating that other co-factors may be needed for aggregation and a study demonstrated that Aβ oligomers were unable to form extracellularly and required cells to be produced (Walsh et al., 2000).

All these theories have considerable experimental support and so it is perhaps probable that they all contribute to plaque formation. Aβ originates from many sources and therefore it is possible that multiple, diverse mechanisms contribute to the formation of amyloid plaques.
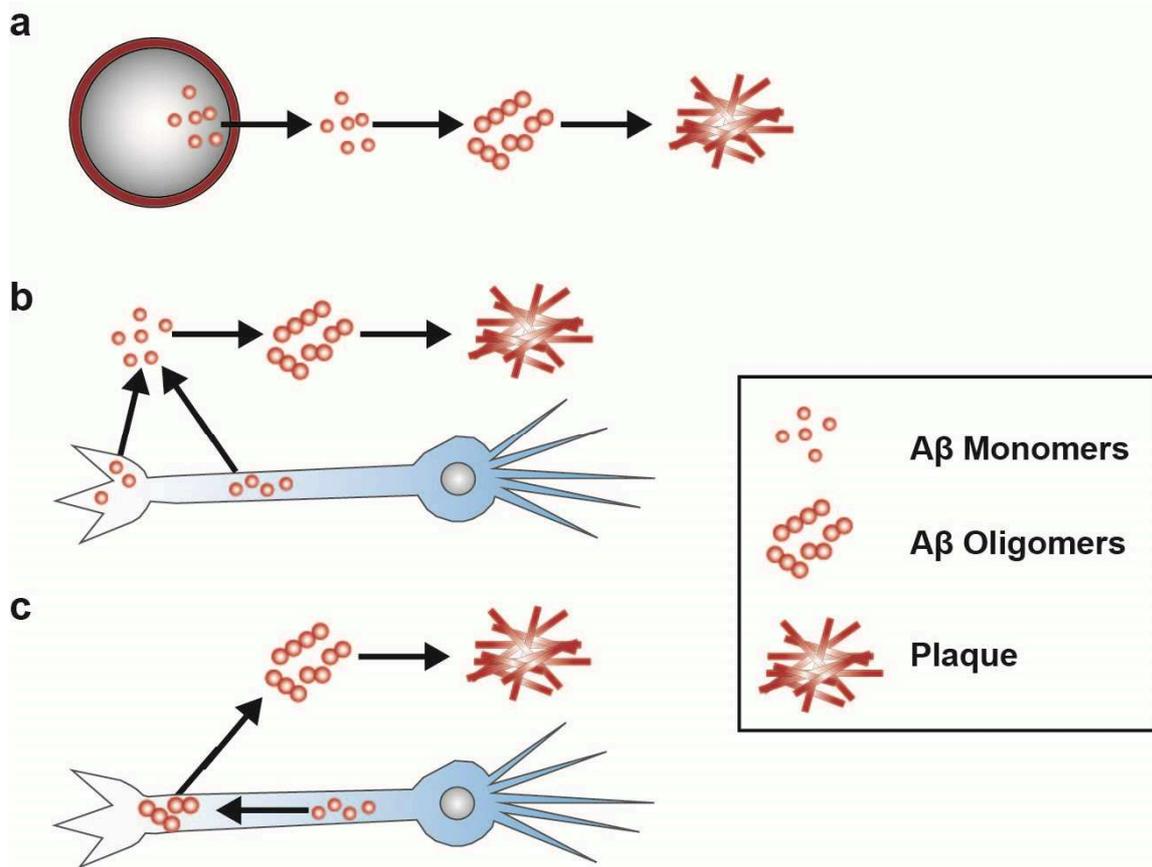
Figure 8: Origin of plaques. In (a), Aβ monomers diffuse out of blood vessels into the extracellular spaces in the brain, aggregate and deposit as plaques. Alternatively, Aβ monomers may originate from neurons, be secreted and thereby form plaques (b). Finally, Aβ could form oligomeric aggregates intraneuronally, then be secreted and form plaques (c).

4.2. Diffuse and Dense-cored Plaques

There are two main types of plaques found in AD: diffuse and dense-cored plaques (Figure 9; (Rak et al., 2007)). Diffuse plaques consist of amorphous Aβ (without a β-sheet structure) (Tagliavini et al., 1988) and are proposed to be the precursors of dense-cored plaques (Armstrong, 1998). Dense-cored plaques are, in contrast, amyloid (β-sheet) rich and are typically well stained by amyloid-specific dyes such as Congo Red and Thiaflavin S. Dense-cored plaques are often surrounded by diffuse Aβ material (Rak et al., 2007). The two parts of the plaque – diffuse and dense-core – are very different structures as demonstrated by an anti-Aβ antibody therapy study in APP transgenic mice; treatment with the antibody for 12 weeks stripped the diffuse material from the plaques, but left the dense-core unaltered (Wang et al., 2011).
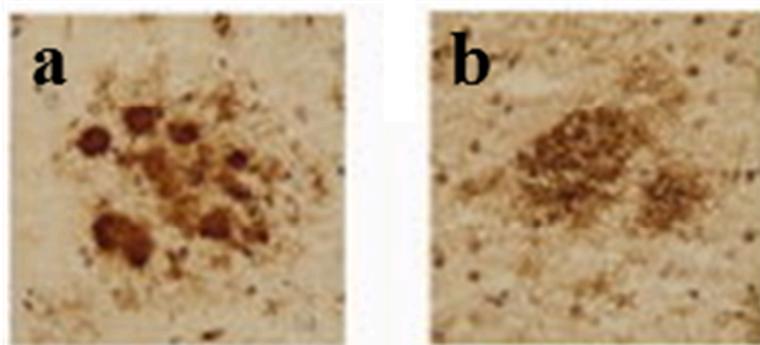
Figure 9: The two types of Amyloid plaque. Examples of a dense-cored plaque (a) and a diffuse plaque (b) from an 11 month old APP transgenic mouse brain immunostained with anti-Aβ antibody 4G8. Adapted from (Rak et al., 2007)

In FAD, the predominant plaque type seems to be determined by the mutation that triggered the disease. For example, some forms of FAD with PS1 mutations develop so called 'cotton wool' plaques (Snider et al., 2005; Steiner et al., 2001; Takao et al., 2002) characterised by their large size and limited Thioflavin S staining (Schellenberg & Montine, 2012). Mouse models expressing FAD mutations also develop different plaque types based on the transgenes they express; APP23 mice develop both Congo Red positive dense-core plaques and diffuse plaques (Sturchler-Pierrat et al., 1997) while APPPS1 mice develop mainly dense-core plaques (Radde et al., 2006).

Why these different types of plaque develop and whether the distinctions are important for AD progression are still open questions. Understanding more about how the different plaques arise may shed some light on the etiology of AD.

4.3. Amyloid-β Plaque Spreading

In 1991, a pivotal study of AD patients' brains obtained at autopsy led to the staging of AD severity based on neuropathological changes (Braak & Braak, 1991). Plaque pathology was staged based on location and density of deposits and was further refined in a later study (Thal et al., 2002). This staging shows that plaques first appear in the neocortex, then in the allocortex and diencephalon and finally invade the brain stem and cerebellum (Figure 10). This characteristic spatial march of plaque pathology appears to follow the path of

31

anterograde neural connections; once an area displays plaque pathology, the areas synaptically connected with that area are subsequently affected (Thal et al., 2002). This has lent support to the idea that Aβ pathology is relayed between neurons by synaptic connections and spreads throughout the brain along neural networks.
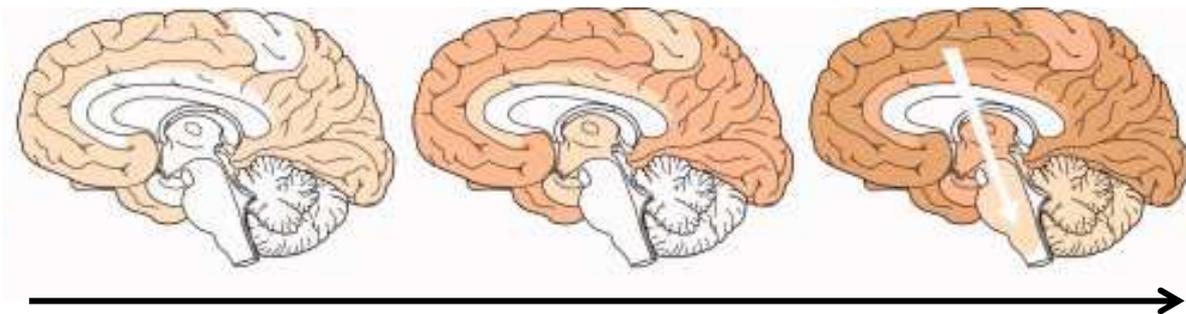
Figure 10: Spread of Aβ plaque pathology in AD patients. Plaques first appear in the neocortex, then allocortex, then diencephalon and cerebellum. Image adapted from (Jucker & Walker, 2011).

Synaptic transmission of Aβ is validated by *in vitro* experiments that showed that neurons in culture can directly transfer soluble Aβ from neuron to neuron via direct cellular connections (Nath et al., 2012). An electron microscopy study of an AD mouse model showed that Aβ is indeed present in synapses and accumulates in vesicles in the pre- and post-synaptic compartments of neurons (Takahashi et al., 2002). These data indicate that Aβ is, most likely, both released by axonal terminals and taken up by post-synaptic compartments thereby travelling along neuronal connections.

Data obtained from mouse models have also provided support for the spreading hypothesis. When APP is expressed exclusively in one region of a mouse brain, the entorhinal cortex, plaques are first seen only in this small area, but are later observed in the dentate gyrus, specifically at the synaptic terminals of the perforant path that connect the two areas (Harris et al., 2010). In the reverse of this study, injection of brain homogenate into the hippocampus showed plaque formation in the retrograde entorhinal cortex (Walker et al., 2002). Furthermore, severing the axons of the perforant path in APP transgenic mice, reduced plaque pathology in the dentate gyrus (Lazarov et al., 2002; Sheng et al., 2002). These studies

imply that Aβ is transported bi-directionally along the perforant path to induce pathologic changes in the dentate gyrus and entorhinal cortex supporting the notion of Aβ travelling through the brain along neuronal connections.

Taken together, the anatomical and experimental data strongly suggest that Aβ can spread intracellularly and trans-synaptically along neuronal connections and, in this manner, plaque pathology expands throughout the brain.

4.4. Amyloid Plaque Toxicity

Despite being a major pathological hallmark of AD, the amount of plaques in the brains of AD patients does not correlate with the severity of the disease symptoms (Terry et al., 1991). Therefore, it was thought that plaques could merely be by-products of the AD process, and even that they have a protective function in AD (Lee et al., 2004). However, there are several hints that plaques may be detrimental to brain tissue, most notably that the cerebral area immediately surrounding plaques is differentially disturbed in AD. Synapses are reduced in AD (Masliah et al., 2001) and are particularly reduced in the vicinity of plaques (Bittner et al., 2012; Spires et al., 2005; Tsai et al., 2004), suggesting that plaques, or some molecules associated with plaques, are toxic to neurons.

Further support for the toxicity of plaques is the morphology of neurites in the vicinity of plaques. Neurites normally display very straight trajectory, but near to plaques they appear curved and distorted (Knowles et al., 1999; Wu et al., 2010). These distorted neurites often have fewer spines. Neighbouring neurites also display signs of oxidative stress in the vicinity of plaques (Hensley et al., 1995; McLellan et al., 2003) and antioxidant treatment seems to reverse these abnormalities (Garcia-Alloza et al., 2010). This oxidative stress is most likely mitigated via mitochondrial damage as mitochondria are less numerous and more fragmented in cells nearby plaques (Xie et al., 2013). Moreover, APP transgenic mice treated with anti-Aβ-antibody to clear plaques showed a marked recovery in plaque-associated neuritic dystrophy (Brendza et al., 2005) implying that removing the plaques removed their toxic influence on neurites. Neuronal morphological changes also resulted in functional changes, since neuronal activity was shown to be decreased near to plaques (Meyer-Luehmann et al., 2009) and in vivo imaging studies showed that plaques are surrounded by hyperactive neurons with more spontaneous firing and higher Ca^{2+} load which led to altered neuritic morphology (Busche et al., 2008; Kuchibhotla et al., 2008). Plaques have also been shown to

exert more long-distant detrimental effects on the brain; inter-hemisphere functional connectivity was reduced in areas associated with the degree of plaque deposition in a mouse model of AD (Bero et al., 2012).

An in vivo imaging study in APP transgenic mice revealed a halo of oligomeric Aβ surrounding plaques in AD transgenic mice (Koffie et al., 2009). This suggests that perhaps the amyloid fibres in plaques are not toxic per se, but that plaques contain soluble Aβ oligomers that can diffuse into the surrounding tissue and damage neurons.

These observations hint that plaques are not mere benign by-products of AD, but their presence is detrimental to brain tissue and that they therefore warrant further study.

5. Investigating Amyloid-β Plaques in APP transgenic mice

This thesis investigates the development of plaques using the APPPS1 transgenic mouse as a model of the cerebral amyloidosis seen in AD patients.

5.1. The APPPS1 Mouse Model

The APPPS1 mouse model of AD (Radde et al., 2006) expresses two transgenes: human APP with the Swedish mutation (Mullan et al., 1992) and human PS1 with the L166P mutation. The Swedish APP mutation causes production of Aβ to increase 6-8 fold (Citron et al., 1992) due to a different cellular location of β-secretase APP cleavage (Haass et al., 1995). In human patients, this leads to FAD with average age of symptom onset 55 and average disease duration 7 years (Mullan et al., 1992). The L166P PS1 mutation is very aggressive, with AD symptoms beginning in patients as early as 24 years of age (Moehlmann et al., 2002). This PS mutation alters the γ-secretase complex to increase the ratio of $A\beta_{40}/A\beta_{42}$ cleaved from APP (Bentahir et al., 2006) and produce mainly the aggregation-prone species $A\beta_{42}$.

The APPPS1 mouse develops plaques characteristic of human AD patients. Moreover, the plaques develop in a relatively short space of time –they begin to appear in the neocortex at 2 months of age and by 8 months of age, there is substantial plaque load in these mice (Figure 11). Plaques are seen in the dentate gyrus at 3 months of age and in the CA1 region by 5 months of age in female mice. The deposits are over 95% dense cored with plaques in older

mice often displaying a diffuse Aβ surround. At 8 months old, APP PS1 mice have dystrophic neurites in the vicinity of plaques and show slight neuronal loss. These APP PS1 mice also develop cognitive deficits: at 8 months of age; they have more difficulty learning a maze task than their wild-type littermates (Radde et al., 2006), imitating the loss of spatial memory seen in human AD patients.

This AD mouse model is ideal to study plaque development over time because this is a rapid model with plaques at an early age. These plaques have a very similar molecular structure and recapitulate some neuronal and cognitive deficits of AD, which makes it a good model in which to study plaque development.
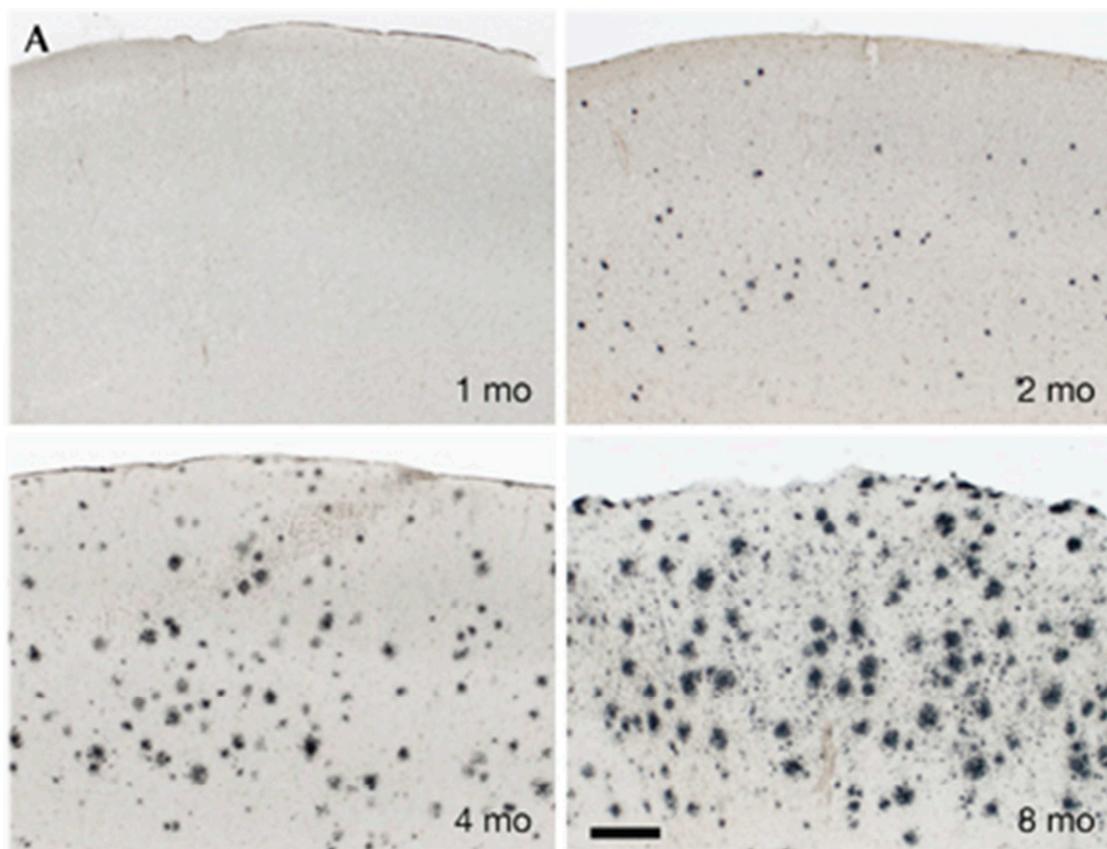

Figure 11: Plaque load increases with age in APPPS1 mice. No plaques observed at 1 month of age advancing to substantial plaque load at 8 months of age. Anti-Aβ antibody NT12 immunostaining of the neocortex. 'mo' indicates months of age. Scale bar: 200µm Adapted from (Radde et al., 2006)

5.2. In vivo 2-photon Imaging in Mouse Models of Alzheimer's Disease

This thesis uses acute 2-photon microscopy to image plaque development in APPPS1 mice. Conventional assessment of AD brains is carried out on post mortem tissue and only allows for a snap-shot/static view of the pathology. With development of 2-photon microscopy and cranial window implantation techniques (Holtmaat et al., 2009), the dynamics of cerebral pathology in multiple cortical layers of mouse models can be imaged over time, at a far greater depth than is possible with confocal microscopy.

2-photon microscopy uses pulsed infrared light with a long wavelength to prevent light scattering at greater depths in the tissue. The fluorophores absorb 2 photons simultaneously, instead of the one in conventional microscopy. The 2 photons absorbed each have approximately half the energy needed to excite the fluorophore. Because of this dual photon mechanism, the area of excitement is much smaller than normal microscopy, therefore reducing out of focus excitation and photobleaching.

Fluorescent dyes such as Methoxy-X04 label amyloid fibres and allow plaques to be visualised (Klunk et al., 2002). Methoxy-X04 crosses the blood brain barrier and so can be administered peripherally. This means that it can be administered repeatedly which can reveal changes in the plaque population over time (Liebscher & Meyer-Luehmann, 2012). Methoxy-X04 also binds stably to plaques for several months (Condello et al., 2011). Fluorescently-labelled Pittsburgh compound B (PIB) can also be used to image plaques and binds to plaques for up to 3 days (Bacskai et al., 2003). With these staining techniques, combined with 2-photon microscopy, individual plaques can be followed over time (Hefendehl et al., 2011) and the appearance and location of new plaques can be precisely monitored (Meyer-Luehmann et al., 2008).

Transgenic technology has been applied to great effect to generate fluorescent-labelled brain cells. Green fluorescent protein (GFP) expressing neurons allow for neurites and dendritic spines to be visualised with 2-photon microscopy. Studies with labelled neurons have shown the temporal relationship between plaques and neuronal abnormalities (Bittner et al., 2012; Dong et al., 2010; Meyer-Luehmann et al., 2008) and GFP-labelled microglia were used to demonstrate, that microglia can phagocytose Aβ *in vivo* (Bolmont et al., 2008).

Despite the limited imageable volume and several other technical limitations, 2-photon microscopy is a powerful technique. It is an invaluable tool to image the dynamics and kinetic of Aβ plaques over time in the same model animal.

5.3. Growth and Development of Amyloid-β Plaques in Alzheimer's Disease

This thesis specifically studies the growth and development of plaques. Plaques are one of the major hallmarks of AD and they are accompanied by neuronal and glial changes and oxidative stress in the surrounding neuronal tissue. However, little is known about how they form and develop over time. Studies in APP transgenic mice have shown that initial plaques are quite small, but as the pathology progresses, larger plaques are apparent (Figure 11, (Radde et al., 2006)). How these large plaques form is still under debate and is the central question of this thesis. An attractive hypothesis that large plaques are simply smaller plaques that have grown over time (Figure 12a) has garnered some experimental support (Burgold et al., 2011; Condello et al., 2011; Hefendehl et al., 2011). However, an alternative, most likely complimentary, hypothesis that small plaques form clusters and fuse together over time to give rise to large plaques (Figure 12b), has yet to be thoroughly investigated in vivo.
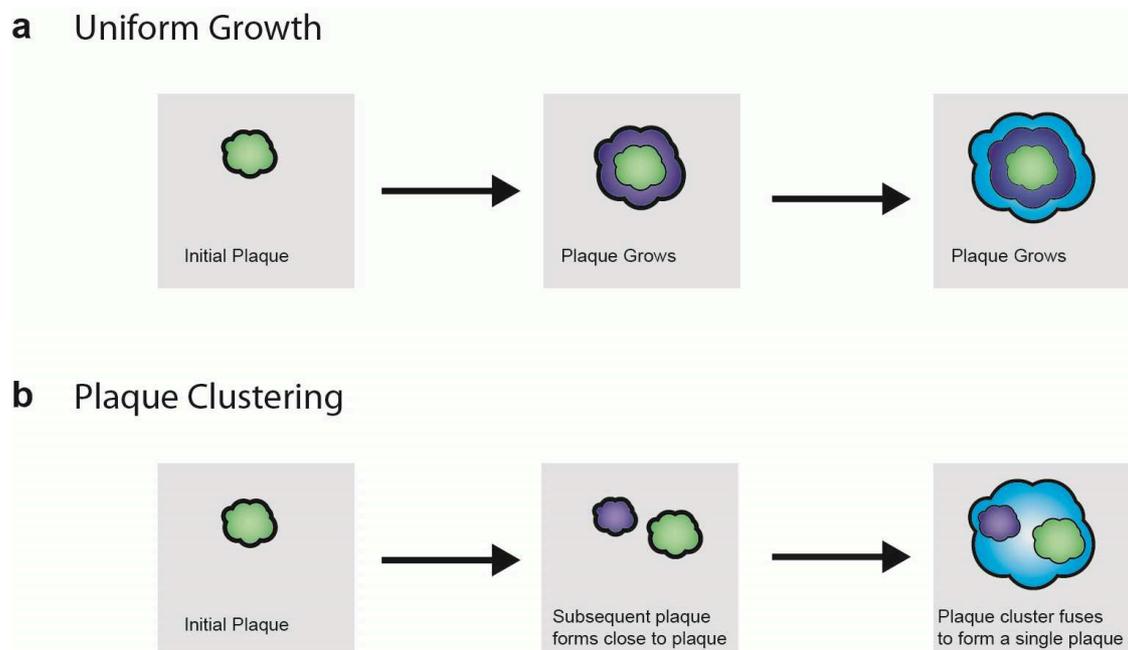

Figure 12: Two Hypotheses of Plaque Development. The uniform growth theory (a) says that an initial plaque uniformly grows over time to become a larger plaque. The plaque clustering theory (b) says that clusters of plaques form and grow together over time to form a large plaque.

A previous study using 2-photon imaging over time in APP transgenic mice showed that new plaques can appear very rapidly, within 24 hours. These new-born plaques remained the same size for up to two weeks following initial appearance (Meyer-Luehmann et al., 2008). Two studies applying 2-photon imaging to AD mice over longer periods have shown that plaques grow uniformly over extended periods of time from a single, smaller plaque. The first study followed new plaques over 6 weeks in Tg2576 mice and observed a significant increase in plaque volume 16 days after the plaque first appeared. Plaque growth was fairly uniform throughout the 6 week period, although there was considerable variation (Burgold et al., 2011). The second study gained very similar results in the APP PS1 mouse model of AD. The mice were imaged for up to 6 months and new plaques in this study also showed a uniform growth from an initially small plaque (Hefendehl et al., 2011). A study using a very different, post mortem 'time-stamp' technique also discovered that new plaques are initially small and grow gradually over 90 days. This study used Methoxy-X04 to label plaques at one time point and then left the mice to develop normally. At various time points afterwards, the mice were sacrificed and Methoxy-X04 staining was compared to post mortem staining to denote how much the plaques had grown over the intervening time (Condello et al., 2011). Taken together, these studies give a picture of plaques that form very rapidly to reach an initial size, but then continue to gradually grow uniformly over time.

Conceivably, this gradual uniform growth is not the only mechanism of plaque growth. Analysis of plaque deposition in sections from APP transgenic mice revealed that plaques cluster together in small areas. Modelling this with a computer simulation showed that newly formed in silico plaques had to form preferentially in the vicinity of a pre-existing plaque to create a representative model of in vivo plaque distribution (Urbanc et al., 1999). Plaque clustering was also observed in a study of AD patient pathology (Armstrong et al., 1993). The clustering hypothesis of plaque growth (Figure 12b) builds on this idea to postulate that these clusters of plaques fuse together over time to form single plaques. Furthermore, large plaques can be composed of multiple, smaller, precursor plaques. However, detailed in vivo experimental evidence is still missing to provide support for this hypothesis.

6. Aims of This Study

By establishing a method to follow plaque development over time, this study thoroughly investigated the mechanism and possible mode of plaque development in AD.

The overall objective of this study was to explore the clustering hypothesis of plaque development with three specific aims:

1) To establish a two-stage staining technique to investigate plaques at multiple time points.

2) To identify the comparative location of new to pre-existing plaques.

3) To classify and characterise any large plaques that might have formed from clusters of pre-existing plaques.

The successful completion of these aims would provide novel support for the clustering mechanism of plaque growth and shed light on the development of a key neuropathological hallmark of AD.

Materials and Methods

1. Materials

Standard laboratory materials were purchased from Sigma Aldrich (MO, USA), Merck (NJ, USA) or Roth (Germany). Other materials and their manufacturers are listed in Table 1.

Table 1: Non-Standard Materials

Material (trade name)	Manufacturer
6E10 Antibody	Sigma Aldrich, MO, USA
APEX^{TM} AlexaFlor ® 594 Antibody Labelling Kit	Invitrogen, CA, USA
Cremophore EL	Sigma Aldrich, MO, USA
Dental Cement (Paladur)	Heraeus, IN, USA
DNA polymerase (GoTaq®)	Promega, WI, USA
Eye Cream (Bepanthen)	Bayer Vital, Germany
Glue (Pattex Ultra)	Henkel, Germany
Ketamine (Ketavet)	Pharmacia, Pfizer, Germany
Methoxy-X04	Neuroptix, MA, USA
Mounting Media (Aqua-Polymount)	PolySciences, Germany
PCR reaction buffer (GoTaq®)	Promega, WI, USA
Sterile Sponges (Gelaspon)	Cauvin Ankerpharm, Germany
Thiazin Red	Sigma Aldrich, MO, USA
Xylazine (Rompun)	Bayer Vital, Germany

2. Equipment

All laboratory equipment used and their manufacturers are listed below in table 2.

Table 2: Equipment

Equipment (trade name)	Manufacturer
2-photon microscope (FV1000)	Olympus, Japan
Centrifuge (Fresco17)	Thermo Scientific, MA, USA
Drill (Microdrill)	Stoelting, IL, USA
Electrophoresis power supply (PowerPac™)	Bio-Rad, CA, USA
Fluorescence microscope (BX61)	Olympus, Japan
Metal head bar	Custom-made
Microtome (SM200R)	Leica Biosystems, Germany
Scissors	Fine Science Tools, Canada
Sections slides (Superfrost)	Thermo Scientific, MA, USA
Shaker (KM-2)	Edmund Bühler GmbH, Germany
Syringes (Omnican®)	B. Braun, Germany
Thermocyler (Mastercycler Gradient)	Eppendorf, Germany
Thermoshaker (Thermomixer Compact)	Eppendorf, Germany
Tweezers	Fine Science Tools, Canada
Vortex (Vortex-Genie 2)	Scientific Industries, NY, USA

3. Buffers

The buffers used for all experiments are listed below in table 3 along with their composition.

Table 3: Buffers

Buffers	Composition
PBS	14mM NaCl, 10mM $Na_2HPO4.2H_2O$, 2mM KH_2PO_4, 3mM KCl, pH 7.4
TAE	40mM Tris, 20mM Ascorbic Acid, 1mM EDTA
Lysis buffer	1M Tris-HCl, 0.5M EDTA, 10% SDS, 2.5M NaCl, 1:1000 Proteinase K
TBS	600mM Tris, 2.6M NaCl. pH 7.8
TBST	TBS with 0.3% Triton-X 100

4. Animals

Male heterozygous APPPS1 mice expressing human $APP_{KM670/671NL}$ and $PS1_{L166P}$ under the control of the neuron-specific Thy-1 promoter (Radde et al., 2006) were used for all analyses. Mice were housed in specific pathogen free conditions with a maximum group size of six. Mice were kept in a 12/12 hour light/dark cycle and had access to food and water ad libitum. All animal procedures were carried out in accordance with animal protocols approved by the government of Upper Bavaria, Germany (licence numbers 55.2-1-54-2531.3-13-10 and 55.2-1-54-2532-152-11).

4.1. Genotyping

A small section of tail was removed from each mouse for genotyping. First, the DNA was extracted: the tissue was incubated in 500µl lysis buffer overnight at 55°C and agitated at 750 rpm. 400µl Isopropanol was added and the solution thoroughly vortexed followed by 20 minutes centrifugation at 17,000 x g. The supernatant was removed and the pellet washed with 500µl 70% ethanol. The pellet was air dried and then re-suspended in 150µl distilled water and incubated for 5 minutes at room temperature followed by an hour in the thermoshaker at 55°C and 750 rpm.

The extracted DNA was subjected to a polymerase chain reaction (PCR) to amplify the human APP gene - if present. The PCR solution consisted of; 4µl reaction buffer, 0.5µl deoxynucleotide triphosphate mix, 1µl forward primer (5'-ATG GAT GTA TTC ATG AAA GG-3'), 1µl reverse primer (5'-TTA GGC TTC AGG TTC GTA G-3'), 0.2µl DNA polymerase, 11.3µl distilled water and 2 µl DNA. This solution was placed in a thermocycler and the following cycle run: 1) 5 minutes at 95°C, 2) 30 seconds at 95°C, 3) 1 minute at 38°C, 4) 1 minute at 72°C, 5) steps 2) to 4) repeated 30 times, 6) 5 minutes at 72°C and then held at 4°C.

The PCR samples were separated by gel electrophoresis using a 1% agarose TAE gel containing 1:2500 ethyl bromide using TAE buffer as the running buffer. 90V of voltage was applied for approximately 20 minutes and the gel imaged with a UV light source. A photograph was taken for documentation.

4.2. Two-Stage Staining Technique

Cerebral plaques were stained pre mortem with Methoxy-X04 on day 0 of the experiment to label all plaques at that time (Figure 13a). After an incubation time of 1 day, 1 month or 4 months, one of two protocols were carried out (Figure 13 b). Either an anti-Aβ antibody was topically applied to the brain, followed by acute in vivo imaging, or, the mouse was sacrificed for post mortem Aβ staining. The number of mice in each group is listed in table 4.
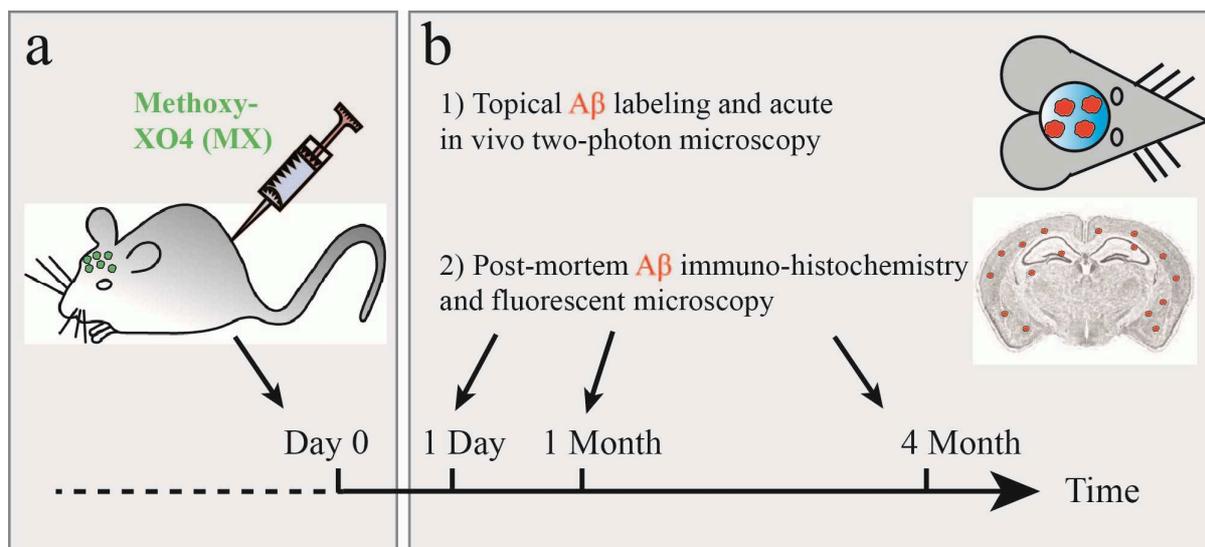
Figure 13: Schematic of dual staining technique. First, the mouse is injected with Methoxy-X04 (a). After 1day, 1 month or 4 months, the mouse was either imaged *in vivo*, or sacrificed for post mortem analysis (b).

Table 4: The Number of Animals Used in Each Experimental Group.

Group name	Age of animal at Methoxy-X04 injection	Post injection interval	Number of animals
Early	2 months	2 weeks	4
1 Day	3 months	1 day	5
1 Month	3 months	1 month	6
4 Months	3 months	4 months	5
Acute *in vivo* imaging	3 months	4 months	3

4.3. Pre Mortem Amyloid-β Plaque Staining

Methoxy-X04 was injected intraperitoneally into 2 or 3 months old mice (apart from one group of mice that were injected at 2 months of age – see table 4). The Methoxy-XO4 solution consisted of 33.3% 10mg/ml Methoxy-X04 in DMSO and 66.6% volume Cremophore EL in PBS and was applied at a dose of 3.33 µg/kg body weight.

5. Acute In Vivo Imaging

5.1. Antibody Labelling

To directly image an antibody applied directly to the surface of the brain without the need for a secondary antibody, the anti-Aβ antibody 6E10 was covalently bound to the fluorophore Alexa 594. To label the antibody, an antibody labelling kit was used according to the manufacturer's instructions. Briefly, the provided column was hydrated and the 6E10 antibody and dye mix applied to the column. The column was incubated at room temperature for 2 hours and then washed twice before the labelled antibody was eluted with neutralisation buffer. The labelled antibody was stored at 4°C until further use.

5.2. Cranial Window Implantation

Mice were anaesthetised with a mixture of Ketamine (10 µg/kg) and Xylacine (20 µg/kg) administered intraperitoneally. The eyes were covered with eye cream to prevent harm. The fur was sterilised with ethanol and a circular piece of skin removed from the top of the head with small scissors. The skull was cleaned with cotton buds and a circle, approximately 6 mm in diameter, lightly drilled into the bone with a micro drill. The anterior of the circle was approximately 1 µm above bregma, the posterior of the circle just above lambda and the circle was equally positioned over the parietal cortex of both hemispheres. Using the tip of a syringe, the skull outside the circle was treated to create a mesh of light scratches to give the glue a rougher surface to adhere to. The circle was drilled more deeply until tweezers could be inserted under the bottom of the circle and the entire circle of bone easily removed. Small pieces of sterile PBS-soaked sponges were gently placed on top of the exposed dura mater to absorb any blood.

Once the bleeding had stopped, the dura mater was removed from the visible brain with fine tweezers. Sponges were applied again to absorb any blood. Once the bleeding had stopped, 20 µl of Alexa 594-labelled 6E10 was applied to the cerebral cortex for 30 minutes. Plastic film was used to keep the antibody in place and prevent evaporation and the mouse's head was covered in aluminium foil to avoid fluorophore bleaching. After 30 minutes, the antibody was removed and the brain surface washed 2 x 30 minutes with sterile PBS. The head was also covered with foil during these washing steps. An 8 mm circle of glass was placed on top of the exposed brain. Any excess liquid was removed from underneath the glass with small, absorbent sponges. Glue was applied between glass and the bone surrounding the exposed

brain. Care was taken that no glue leaked onto the brain itself. Once the glue was dry, a raised circle of dental cement was applied to fix the window in place and to create a well to contain the microscope objective immersion water. A small metal head bar with two holes drilled in was placed into the cement to attach the mouse to the microscope apparatus.

5.3. In vivo 2-photon Microscopy

The mouse was secured, using the head bar, in a custom-built frame with three-dimensional adjustability. The frame was positioned under the 2-photon microscope. Surface blood vessels were imaged with the fluorescence lamp and used for gross orientation.

The Mai Tai Deep See Laser (Spectra Physics, Newport Corporation, MA, USA) at 850 nm was used to excite the two dyes. A 420-500 nm emission filter was used to image the pre-mortem injected Methoxy-XO4 and a 590-650 nm emission filter used to image the topically applied Alexa 594-labelled 6E10 antibody. 634 x 634 x 150 µm (xyz dimensions) volumes of cortex were imaged with a resolution of 512 x 512 pixels and 5µm z axis increments. Images were collected and processed using the Olympus FV10-ASW 3.1 software.

6. Post Mortem Imaging

6.1. Section Preparation

The mice were sacrificed and the brains removed. The brains were fixed in 4% PFA for 48 hours followed by 48 hour in 30% sucrose in PBS. The tissue was then flash frozen on dry ice and stored at -20°C until further use. Brains were sliced into 25 µm thick sections with a microtome cooled with dry ice. Sections were collected in 10 1.5 ml centrifuge tubes so that each tube contained every 10th section. Sections were stored in a solution of 15% glycerol in PBS at -20°C until further use.

6.2. Antibody Staining

Sections were washed 3 x 10 minutes in TBS to remove any glycerol and blocked in a solution of 5% NGS (normal goat serum) in TBST for 60 minutes. This was carried out at room temperature and sections were gently agitated on a shaker during incubation steps. The

sections were incubated overnight at 4°C with gentle agitation in primary antibody (see table 5) diluted in 5% NGS in TBST.

Table 5: Primary Antibodies Used for Section Staining

Antibody	Antibody Conditions	Manufacturer
3552	1:3000, overnight, 4°C	Non-commercial (Page et al., 2010)
4G8	1:150, overnight, 4°C	Covance, NJ, USA

The primary antibody was removed and the sections washed 3 x 10 minute with TBST. The sections were incubated in secondary antibody (see table 6) diluted in 5% NGS in TBST for one hour. This was followed by 3 x 10 minute TBST washes and a final, 10 minute wash in TBS.

Table 6: Secondary Antibodies Used for Section Staining

Antibody	Antibody Conditions	Manufacturer
Alexa 488	1:1000, 1 hour, room temperature	Invitrogen, Life Technologies, UK
Alexa 555	1:250, 1 hour, room temperature	Invitrogen, Life Technologies, UK

6.3. Thiazin Red Staining

Sections were thawed and washed 3 x 10 minutes in PBS to clean the sections of any glycerol. Sections were incubated for 20 minutes in a 2 µM solution of Thiazin Red diluted in PBS. The sections were then washed 3 x 5 minutes in PBS.

6.4. Section Mounting

The stained sections were mounted onto coated glass slides, dried and covered with mounting media and a glass coverslip.

6.5. Post Mortem Microscopy

Mounted sections were imaged with a multi-channel fluorescent microscope with an EXFO-Xcite Laser. A 20x UPLSAPO air objective was used. The filters used for each dye are listed in Table 7.

Table 7: Fluorescence Filters used for Imaging

Dye	Filter	Excitation (nm)	Emission (nm)
Methoxy-X04	U-MNUA	345	455
Alexa 488	U-MNIBA	495	519
Alexa 555/Thiazin Red	Cy3 filter	550	565

Images were taken using an F-view 11FW camera (Olympus) and were 688 x 512 µm in size. Images were taken of the dorsal, lateral and ventral cortical regions of both hemispheres. Each image was defined as a region of interest (ROI). Therefore 6 ROIs were imaged per brain section. This resulted in a total of 89 ± 10.3 (mean ± standard deviation) ROIs imaged per animal.

6.6. Post mortem Methoxy-X04 Staining

Sections were thawed and washed 3 x 10 minutes in PBS to clean the sections of any glycerol. Sections were mounted and covered as above and images of the pre-mortem Methoxy-X04 were taken as above. Slides were soaked in distilled water for 2 to 3 minutes to remove the cover slip. Care was taken not to dislodge any mounted sections. The slides were incubated for 10 minutes in a 100 µM solution of Methoxy-X04 diluted in 40% ethanol, pH 10 and then briefly dipped in distilled water five times. The slides were then incubated in a solution of 0.2% NaOH in 80% ethanol for 2 minutes and then washed in water for 10 minutes. A coverslip was attached with mounting media and the section re-imaged at the same locations as the pre mortem Methoxy-X04 images.

7. Image Analysis

Images were analysed using Photoshop CS5 (Adobe Systems Inc. CA, USA). Background signal was manually subtracted using the linear histogram tool. Pre and post mortem plaque staining were compared with each other and a new plaque defined as any structure positive for post mortem dye, but Methoxy-X04 negative. The distance between plaque cores was measured in ImageJ (National Institute of Health freeware). New plaques $< 40\,\mu m$ from a pre-existing plaque as measured from core to core were categorised as close or 'in the vicinity' of the pre-existing plaque.

Flower plaques were defined as a cluster of plaques with two or more new plaques in the vicinity ($< 40\,\mu m$) of a common pre-existing plaque. They were called 'flower plaques' due to their resemblance to petals around a central core. Multicore plaques were defined as plaques that were a single structure in the post mortem staining, but had two or more distinct Methoxy-X04 cores. All the plaque categories are summarised in Table 8.

Table 8: Description of Plaque Categories

Plaque Category	Description
Pre-existing	Methoxy-X04 and anti-Aβ antibody positive
New	Methoxy-X04 negative, anti-Aβ antibody positive
New in vicinity	A 'new' plaque $< 40\,\mu m$ from a 'pre-existing' plaque
Flower	≥ 2 'new' plaques $< 40\,\mu m$ from the same 'pre-existing' plaque
Multicore	≥ 2 distinct Methoxy-X04 positive cores within a single antibody positive plaque

Plaque size distribution was computed in ImageJ. Smoothing, thresholding and background subtraction steps were carried out before an 'analyse particles' command was run. The lower size limit for a plaque was set as ≥ 30 pixels ($\geq 5.5\,\mu m^2$) of anti-Aβ antibody positive area. Autofluorescent signal from particles or section edges was manually removed from the data set.

To mimic a chance level of plaque deposition in close vicinity of a pre-existing plaque, a rotation analysis was performed (Keck et al., 2011). A mask containing marks for the location of newly developed plaques was rotated by 180° and superimposed onto the pre-existing plaque image. The distance between these rotated 'new plaques' and original pre-existing plaques was measured and the proportion of new close plaques ($< 40\,\mu m$) occurring by chance was compared to the original fraction of new plaques.

To quantify the areal fraction of each ROI that was in the vicinity ($< 40\,\mu m$) of a new plaque, ImageJ software was used to superimpose circles with a radius of $40\,\mu m$ centred over every new plaque. The software was used to combine any overlapping circles and quantified the area covered by the combined circles. The proportion of ROI covered by the circle area was calculated gave me the fraction of ROI area within $40\,\mu m$ of a new plaque.

8. Graphs and Statistics

Data was collected in Microsoft excel and graphics generated with GraphPad prism 5.04. All data was tested for normality with the D'Agostino-Pearson omnibus K2 normality test with the significance level set to $p < 0.05$. The appropriate parametric or non-parametric test was then carried out in GraphPad prism 5.04.

Results

1. Two-stage post mortem imaging technique

To follow the single plaques over their development, a two-stage staining technique was developed that allowed for two snap-shots of the plaque development to be imaged simultaneously. Methoxy-X04 was injected intraperitoneally at Day 0 to label the plaques at this time point. Methoxy-X04 crosses the blood-brain-barrier, stably binds to dense core plaques and remains bound and fluorescent for several months (Condello et al., 2011). Following a subsequent post-injection time of 1 day, 1 month or 4 months, an anti-Aβ antibody was applied to post mortem sections to label the plaques in their current state. Thus, how the plaque looked at day 0 was labelled with Methoxy-X04 and how it looked, e.g. after 4 months was labelled with the anti-Aβ antibody. Comparing the two stainings made new plaques and changes to plaques in the period between the two label applications visible (Figure 14). It is important to note that the longer incubation time also equates to older animals.
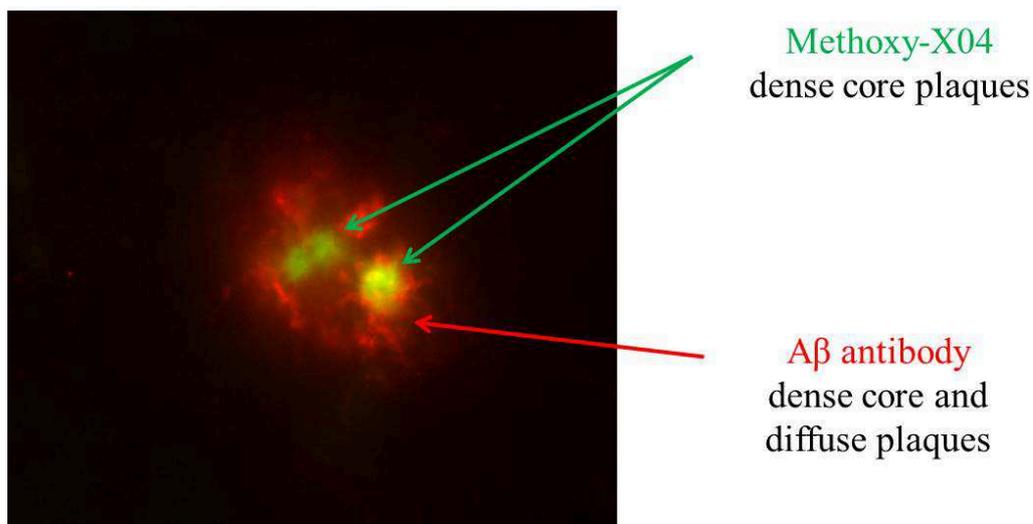

Figure 14: Example of dual staining. The core of the plaque is stained with Methoxy-X04 (green) and the Aβ antibody (red) stains the diffuse surrounding as well as the dense core.

The vast majoriy, 96.2%, of all plaques counted were double stained after 1 day with only a negliable amount of Methoxy-X04-negative plaques. This confirms an earlier study of this mouse model which showed that these mice almost exclusively develop dense core plaques (Radde et al., 2006)

The post mortem anti-Aβ antibody 3552 applied to sections (Figure 15) after 1 day (Figure 15 a-c), 1 month (Figure 15 d-f) and 4 months (Figure 15 g-i) after Methoxy-X04 injection at day 0 revealed that after 1 day of incubation, almost all plaques were double labelled (Figure 15 c). However, after 1 and 4 months, some new plaques in the anti-Aβ antibody staining were clearly identifiable due to their lack of Methoxy-X04 staining (white arrow heads, Figure 15 f, i). Additionally, some new plaques appeared very close to pre-existing plaques (< 40 µm, yellow arrow heads, Figure 15 f, i).
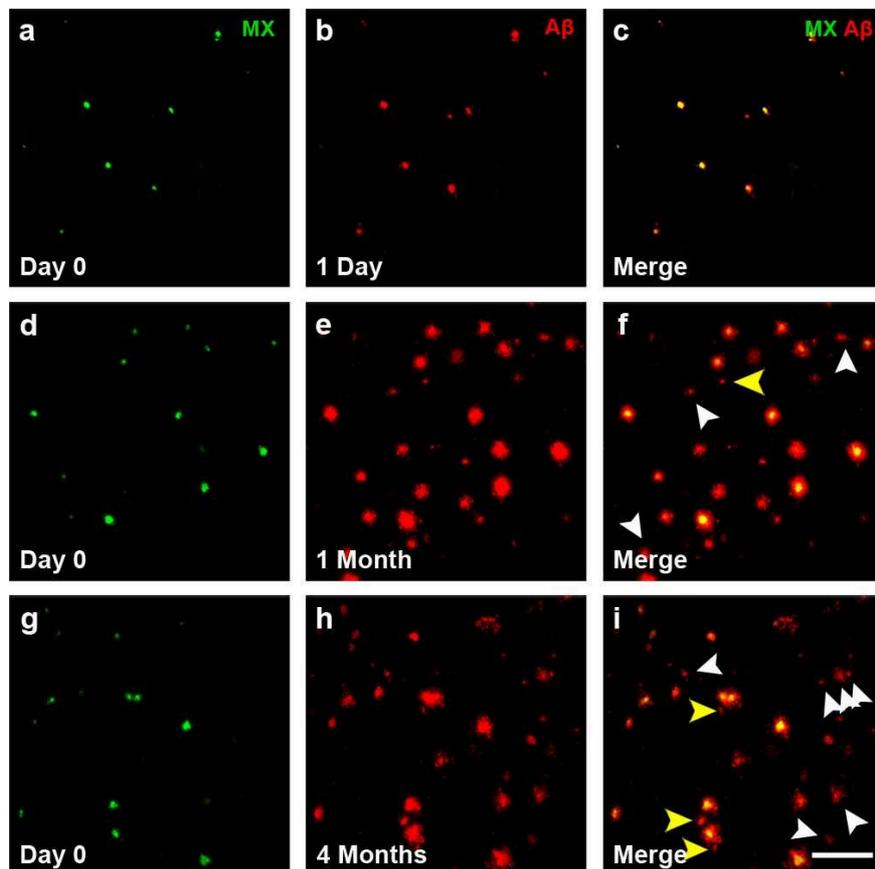
Figure 15: Two-stage staining technique allows for new plaques to be distinguished from pre-existing plaques. Methoxy-X04 (MX) was applied at day 0 (a, d, g) and post mortem anti-Aβ antibody 3552 (Aβ) applied 1 day (b), 1 month (e) or 4 months (h) after day 0. After 1 day, almost all plaques were double-stained (c). After 1 month (f) or 4 months (i), new plaques (white arrow heads) and close new plaques (yellow arrowheads) could be distinguished by comparing the two stainings. Scale bar: 100 µm

To further characterise the end point of the three incubation time groups, the size of all the anti-Aβ antibody positive plaques at the three time points were quantified (Figure 16). The plaques were separated by size into small ($< 50\,\mu m^2$), medium ($50\text{-}300\mu m^2$) and large ($> 300\mu m^2$) plaques. There were more plaques in general in the longer incubation time groups and, notably, many more medium and large plaques.
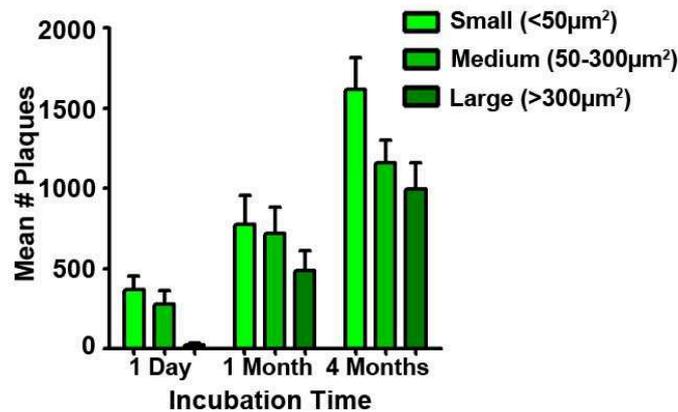
Figure 16: Size distribution of plaques. The number of plaques increases with increasing incubation time in all 3 categories of plaque size – small ($< 50\,\mu m^2$), medium ($50\text{-}300\,\mu m^2$) and large ($> 300\,\mu m^2$) plaques. Mean ± SEM. n = 5-6 per group.

2. Two-stage in vivo Imaging

Acute 2-photon in vivo imaging also used a two-stage staining technique to visualise new plaques. An anti-Aβ antibody was applied directly to the brain surface of a mouse that had received Methoxy-X04 4 months earlier. A cranial window was then implanted and the cerebral cortex of the anaesthetized mouse was imaged. New plaques that were just antibody stained could be distinguished from pre-existing plaques (Figure 17 c, white arrowheads point to new plaques). However, as this technique has a very low penetrance of the antibody ($\sim$200 μm deep into the tissue) and the volume of tissue that can be analysed is much smaller than *post mortem* preparation (Spires et al., 2005), this study investigated plaque development primarily with post mortem tissue analysis.
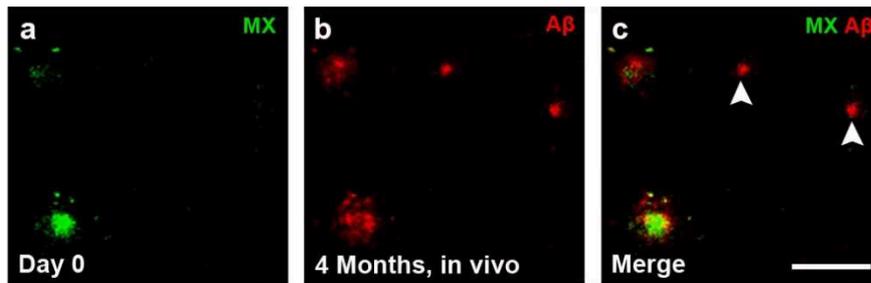
Figure 17: In vivo 2 photon imaging of new plaques 4 months after Methoxy-X04 injection. Methoxy-X04 (MX) was applied 4 months before imaging session (a) and Alexa 594 labelled anti-Aβ antibody 6E10 (Aβ, b) topically to the brain before cranial window attachment. The merged image (c) allows for newly formed plaques (white arrowheads) to be distinguished from pre-existing plaques. Scale bar: 50 µm.

3. Detailed Images of Plaque Categories

High magnification images of double-stained plaques allowed for a more detailed view of the two-staining technique. If plaques were stained with both Methoxy-X04 and anti-Aβ antibody 3552, then they were categorised as pre-existing plaques, but plaques without Methoxy-X04 staining must have developed over the incubation time and are therefore new plaques. New plaques could be identified very close (< 40 µm) to pre-existing plaques after all time points investigated (Figure 18, yellow arrowheads in c, f, i).
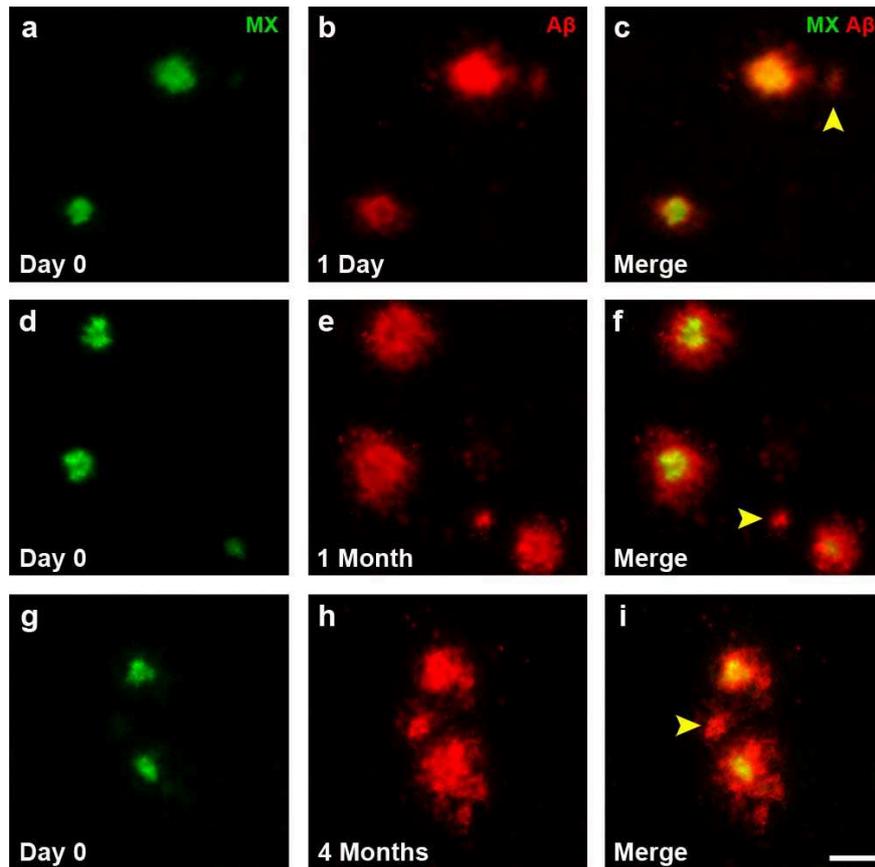
Figure 18: High magnification images of close new plaques. Comparison of the Methoxy-X04 staining (MX, a, d, g) and the anti-Aβ antibody 3552 (Aβ, b, e, h) showed close new plaques (yellow arrowheads) 1 day, (c), 1 month (f) and 4 months (i) after Methoxy-X04 injection. Scale bar: 25 µm

4. Staining Validation

To ensure that the 3552 anti-Aβ antibody staining was representative of Aβ, a second slightly different Aβ antibody, 4G8 was used and compared with the 3552 antibody. 4G8 was chosen for comparison due to its frequent use in AD patient data and it was shown to be the best antibody at labelling diffuse amyloid in human sections (Alafuzoff et al., 2008). The 4G8 plaque staining (Figure 19) compared very well with the 3552 staining. For example, the 4G8 antibody stained plaques at 3 time points (Figure 19 d, h, l), are very comparable to those seen with the 3552 anti-Aβ antibody, especially the appearance of the staining and the size of the antibody halo around the Methoxy-X04 positive core (Figure 18 c, f, i). Comparing the 4G8 staining to Thiazin Red (a post-mortem dye for dense core plaques) (Bacskai et al., 2003) confirmed that 4G8 stains not only the dense core of the plaque, but also the diffuse

surround. This confirms the reliability of the 3552 anti-Aβ antibody as it compares favourably to another, well used, anti-Aβ antibody.
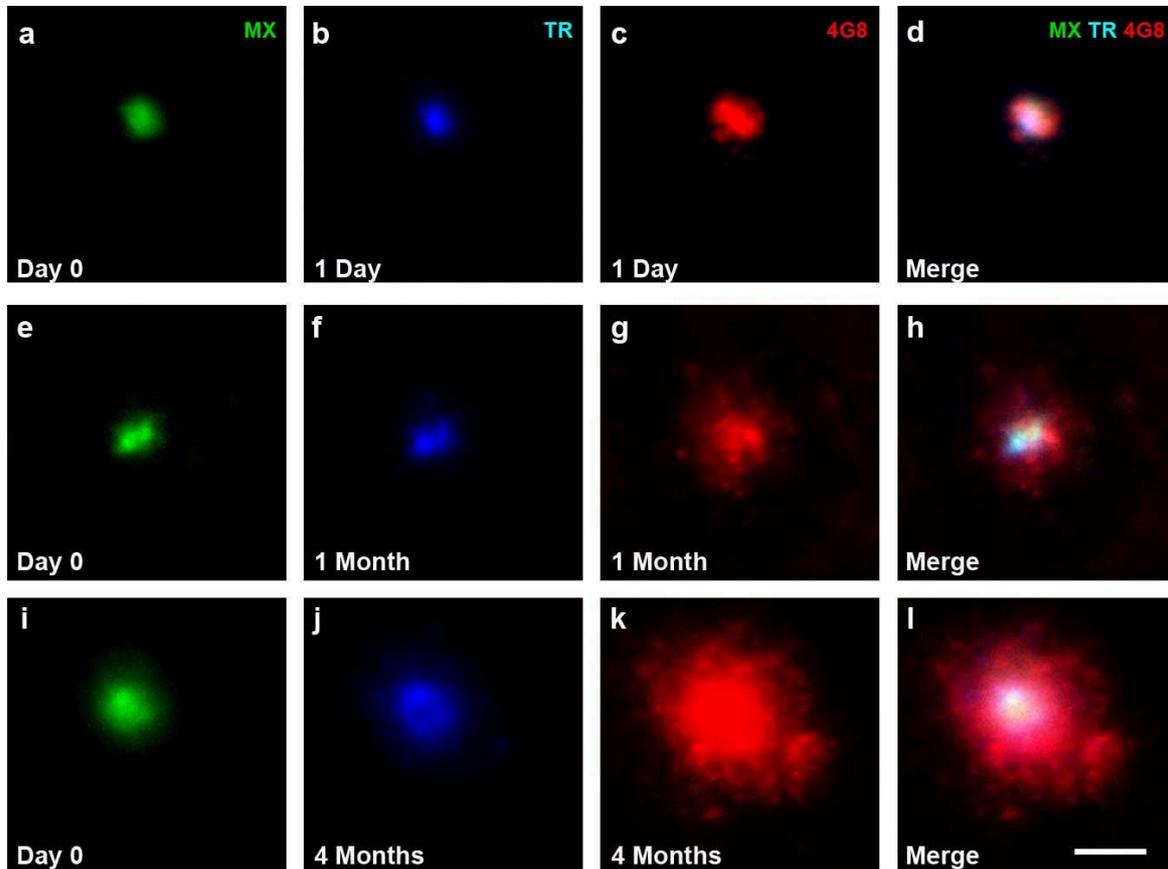
Figure 19: Staining with another anti-Aβ antibody, 4G8, showed staining of surrounding plaque halo 1 day (a-d), 1 month (e-h) and 4 months (i-l) after Methoxy-X04 injection. Thiazin Red (TR) shown for comparison (b, f, j). The plaque halo increased with increasing post injection time (d, h, l). Scale bar: 50 µm

To ensure that the 'new' plaques detected had genuinely appeared after the initial Methoxy-X04 injection and were not simply a different category of plaque, some sections were re-stained with Methoxy-X04 post mortem. This involved imaging the slices with their pre-mortem Methoxy-X04 staining, removing the cover slip and re-staining the slice with Methoxy-X04. The slice was then re-imaged and this image was manually overlaid onto the previous image of the initial Methoxy-X04 staining. The two images were then compared to find newly appeared plaques that were present in the overlay, but not in the original image.

New plaques were identified that were not visible with the Methoxy-X04 injected at Day 0, but were visible in the post-mortem Methoxy-X04 applied 4 months after injection (white arrowheads, Figure 20 c), confirming that newly appeared plaques can be Methoxy-X04 positive and therefore have the same structural characteristics as the pre-existing plaques.

Similar results were obtained with post mortem Thiazin Red staining. Sections were taken from an animal that had Methoxy-X04 4 months prior to sacrifice and were stained with Thiazin Red. This Thiazin Red staining also confirmed the dense core nature of new plaques as plaques were visible in the Thiazin Red channel that were not seen in the Methoxy-X04 channel (white arrow heads, Figure 20 f). Analysis of Thiazin Red staining compared to the anti-Aβ antibody 3552 affirmed that only 0.8% of plaques were not dense core positive, further validating the antibody staining technique.
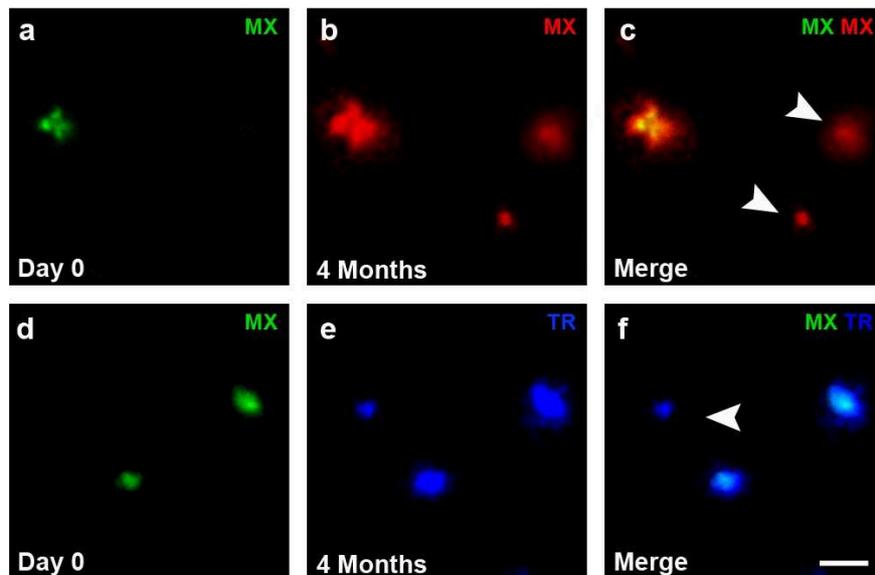
Figure 20: Post mortem dense core staining. (a-c) Comparison between pre-mortem Day 0 and (b) post mortem 4 months Methoxy-X04 (MX) staining showed that new plaques were Methoxy-X04 positive (white arrowheads, c). (d-f) Post mortem 4 months Thiazin Red (TR) staining (e) compared to pre-mortem Day 0 Methoxy-X04 (d) also revealed new dense core plaques (white arrowhead, f). Scale bar: 25 µm

In this study, the Methoxy-X04 is in the brain for up to 4 months and could well be degraded over that time. Although Methoxy-X04 has been shown to be stable in vivo over long periods

(Condello et al., 2011), it was important to ensure that Methoxy-X04 did not fade over time in this experiment, under these particular conditions. If Methoxy-X04 did fade, then there is the possibility that the Methoxy-X04 staining could be lost over time and that plaques that were classified as new due to their lack of Methoxy-X04 could therefore not really be new, but pre-existing plaques that have lost their Methoxy-X04 staining. If this happens, then a decrease in Methoxy-X04 positive plaques over time would be expected as the dye faded. However, quantification of the amount of Methoxy-X04 in the different time points, did not reveal a decline, but rather even a slight, but non-significant, increase in the amount of positive plaques over time (Figure 21). These data indicate that plaques did not lose their Methoxy-X04 staining over the 4 months of this study.
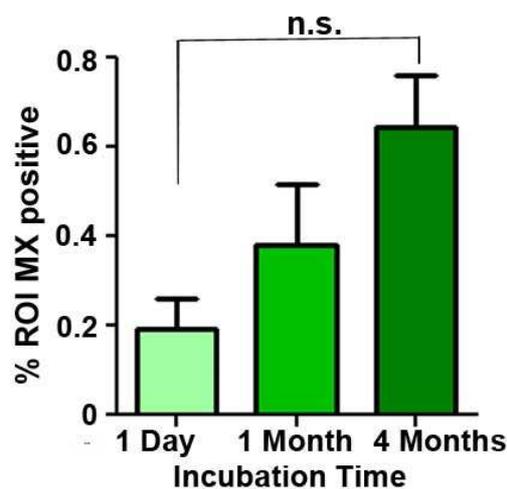
Figure 21: Percentage of ROI Methoxy-X04 positive. The proportion of ROI covered with Methoxy-X04 positive signal increased with increasing incubation time, but not significantly. Mean ± SEM, n = 5-6 per group. Kruskal-Wallis with Dunn's post hoc test. n.s. p>0.05.

5. Investigation of New Plaques

To quantify how the new plaques had developed over time, all plaques were classified into new and pre-existing plaques. To study where the new plaques formed, the new plaque category was further sub-divided and the distance between new plaques and their closest pre-existing neighbour determined the categorisation. The two groups were < 40 µm and > 40 µm from a pre-existing plaque. For each ROI, the number of plaques belonging to each of the

three plaque categories were quantified (Figure 22 a). This quantification showed that the total amount of plaques goes up with increasing incubation time (as would be expected – these mice are also older) and that the amount of new and close ($< 40\,\mu m$) new plaques also increases. The proportion of new plaques that were found in the close vicinity of a pre-existing plaque was, however, consistent over all incubation times; around 22% of all new plaques were found in the vicinity of a pre-existing plaque, regardless of incubation time (Figure 22 b).
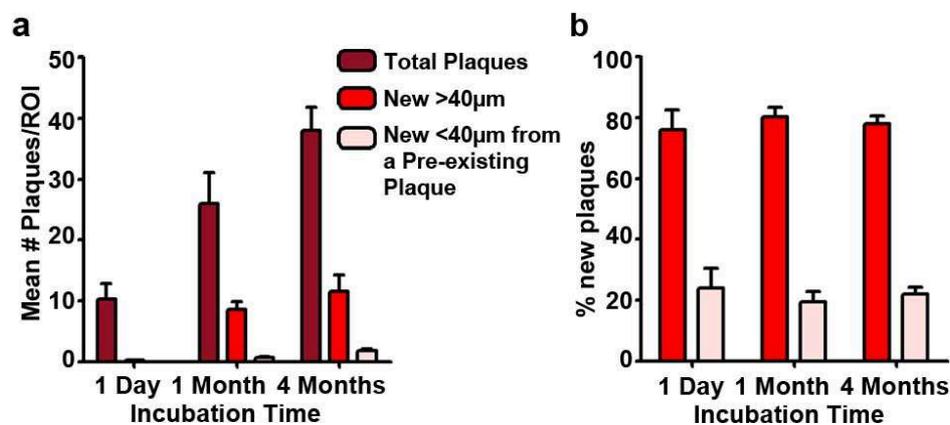
Figure 22: Proportion of plaques by classification. (a) Number of total plaques, new plaques and close new plaques increased with increasing incubation time. Mean ± SEM, n = 5-6 per group. (b) The proportion of the new plaque population that was close to a pre-existing plaque was fairly constant across all 3 incubation times. Mean ± SEM, n = 5-6 per group.

Next, the close ($< 40\,\mu m$ from a pre-existing plaque) new plaque population was explored in more detail. Was it just chance that this 22% of all new plaques occurred in the vicinity ($< 40\,\mu m$) of a pre-existing plaque? Did the plaques randomly deposit there, or was the vicinity of a plaque more conducive than other areas of the brain for a new plaque to form? To answer these questions, the original data set was compared to a set of data generated to represent the chance deposition of plaques.

To generate the chance data set, the location of the new plaques were marked on an overlay of the original image, rotated this overlay by 180° and then measured the distance of these rotated 'plaques' on the overlay and the nearest pre-existing plaque on the original image.

This 'rotated 180°' data set had a significantly lower average of new plaques close (< 40 µm) to a pre-existing plaque than the original dataset, but only in the younger animals group (Figure 23 a); the younger animals group is made up by combining the early and 1 day groups (see Table 4 for details.). This implies that in the original dataset, plaques formed close to pre-existing plaque at a higher than chance level thereby forming clusters of multiple plaques. However, in the longer incubation (1 and 4 months) time points, there was no difference between the original and 'chance' rotated 180° data sets (Figure 23 b).
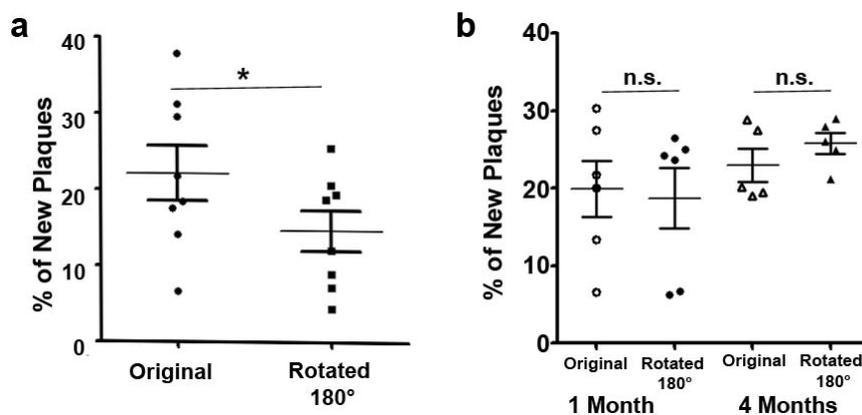
Figure 23: Likelihood of plaque appearing in the vicinity of a pre-existing plaque. Close new plaques in original and chance data sets. Y axes display the % of new plaques that are in the vicinity of a pre-existing plaque. (a) Likelihood of plaque appearing in the vicinity (< 40 µm) of pre-existing plaque is higher than chance (represented by the rotated 180° data set) in younger animals. (b) In the 1 month and 4 month incubation time points, the likelihood was no higher than chance. Mean ± SEM, n = 5-8 per group. Symbols represent individual animals. Two-tailed paired T-test. * $p < 0.05$, n.s. $p > 0.05$.

This apparent discrepancy between incubation time groups could be due to the increase in plaque density over time (Figure 24 a). As the incubation time increased, the pathology worsened and the plaque load increased. There was a negative correlation between the number of plaques per regions of interest (ROI) and the difference in the original and rotated 180° data sets (Figure 24 b). With a lower plaque density, the difference was positive – implying that the original data was more than chance, but at a higher number of plaques/ROI, the difference was gone – implying that the original data was no more than chance level and the likelihood of a new plaque appearing close to a pre-existing plaque was no more than chance level.

The high density of plaques at longer incubation times indicates that the proportion of ROI area $< 40\,\mu m$ from a new plaque is quite large. This was quantified by laying circles with a radius of $40\,\mu m$ on top of all new plaques and determining what proportion of the ROI was obscured by these circles (Figure 24 c). The proportion of a ROI $< 40\,\mu m$ from a new plaque was dramatically larger in the longer incubation times leading to an increased chance of randomly being close to a pre-existing plaque.
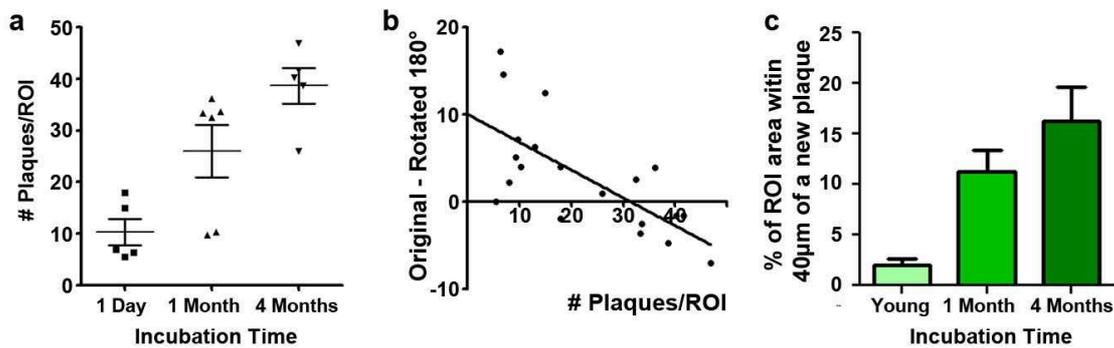
Figure 24: Plaque density over time. Longer incubation time increased the number of plaques per ROI (a). Mean $\pm$ SEM. n = 5-6 per group. The graph in (b) shows the difference between the original and rotated values plotted against the total numbers of plaques per ROI for each animal as determined by Aβ antibody staining. A value of zero indicates that the original and rotated values were the same and therefore chance level. n=20, various ages and incubation times; negative linear regression (R^2=0.4915) line significantly different from zero (F test, p = 0.0006). Graph (c) shows the proportion of ROI area that was $< 40\,\mu m$ from a new plaque. Mean $\pm$ SEM. n = 5-6 per group.

Some very close new plaques cluster around the same pre-existing plaque – this constellation was named a 'flower plaque' due to their resemblance to petals around a common central plaque (Figure 25). Flower plaques were defined as any Methoxy-X04 positive plaque with ≥ 2 new plaques $< 40\,\mu m$ away. Acute in vivo imaging first revealed a flower plaque (Figure 25 a-c) as shown by the new plaques (yellow arrowheads) clustered around a common Methoxy-X04 positive plaque. In the post-mortem 3552 anti-Aβ antibody analysis, several flower plaques were found with an example shown in Figure 25 d-f, yellow arrowheads point to new, 'petal' plaques. A quantification of the post mortem analysis revealed that 10.5% of all close new plaques contribute to flower plaque clusters (Figure 25 j). Post mortem Thiazin

red staining showed that the flower plaque petals can also be of dense core nature (Figure 25 g-i). These flower plaques are examples of plaques forming a cluster of multiple plaques.
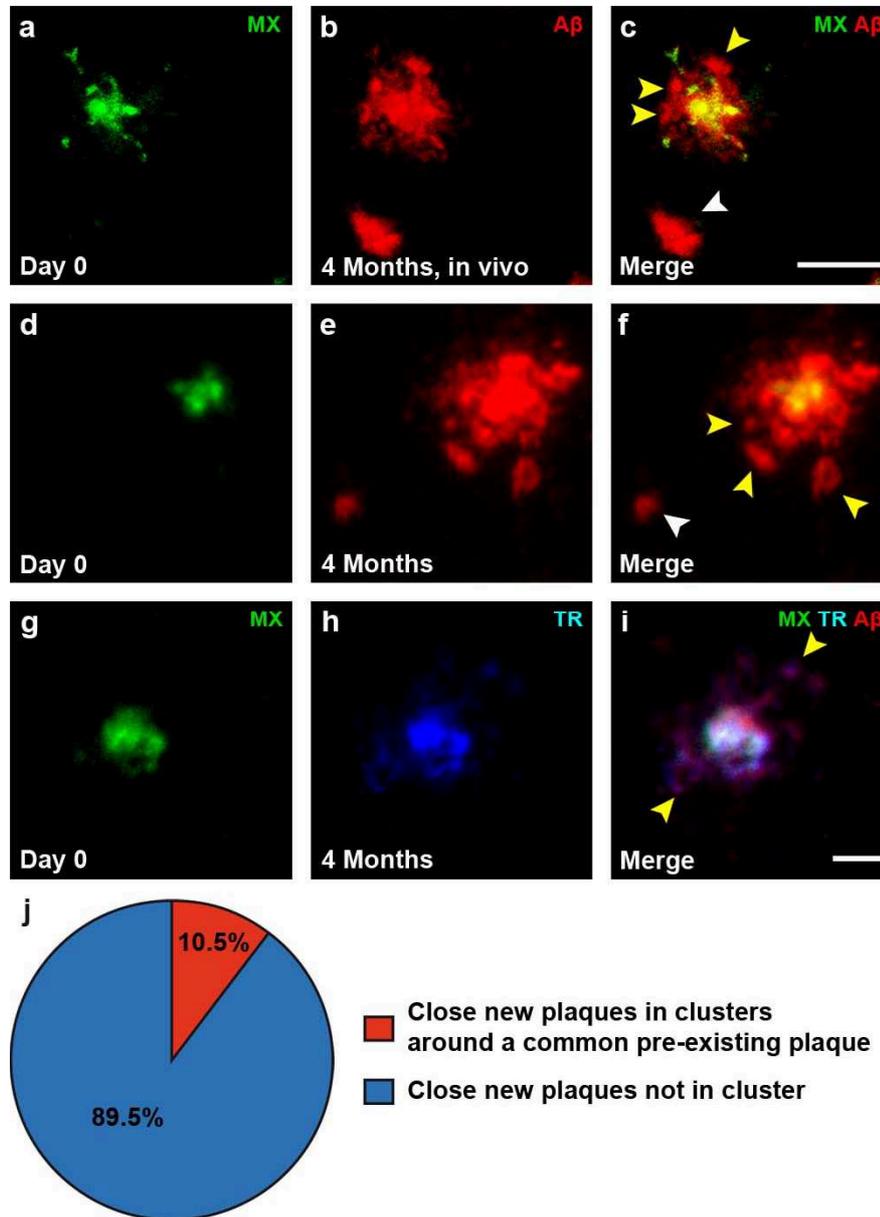
Figure 25: Multiple new plaques cluster around pre-existing plaque to form 'flower plaques'. (a-c) Flower plaques were seen during in vivo imaging and distinguished by multiple new plaques around a pre-existing Methoxy-X04 (MX) positive core (yellow arrowheads in c). (d-f) Post mortem analysis also revealed flower plaques with anti-Aβ antibody 3552 (Aβ) and in (g-i) with Thiazin Red (TR) staining. White arrow heads point to new plaques > 40µm from the pre-existing plaque. (j) Quantification of post mortem anti-Aβ antibody flower plaques showed that 10.5% of all close new plaques were petals of a flower plaque. Scale bars: 25 µm

To determine whether there was any particular 'preferred' distance for the close new plaques within this 40 µm range, the exact distances between the close new plaques and their nearest pre-existing neighbour was measured. Figure 26 shows the results of this analysis for each of the 3 incubation time points. The 1 and 4 month time points have a small proportion of very close plaques (closer than 15 µm from nearest pre-existing plaque), but a plateau at the farther distances. In contrast, the 1 day time point had most close plaques within 15 µm and a smaller proportion at further distances (20 – 40 µm). Therefore there did not appear to be any preferred distance for the close new plaques, but the discrepancy between the 1 day and the two later time points may be a technical artefact which will be discussed later.
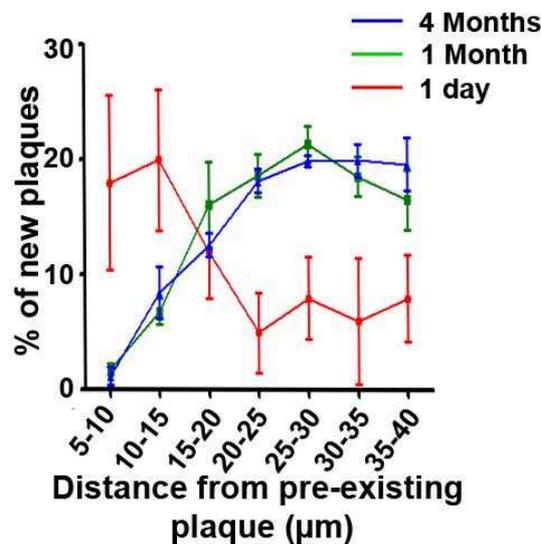
Figure 26: Distance of new plaques from nearest pre-existing plaque. Data plotted for three incubation times: 1 day, 1 month and 4 months. Mean ± SEM. n = 5-6 per group.

6. Multicored Plaques Show Merger of Plaques over Time

Detailed analysis of high resolution pictures revealed an interesting class of plaques that were named 'multicore plaques'. These plaques are characterised by multiple, separate Methoxy-X04 cores within a larger plaque stained with the anti-Aβ antibody 3552 (Figure 27). Multicore plaques were evident after just 1 day (Figure 27 a-c) as well as in the 1 month (Figure 27 d-e) and 4 months (Figure 27 g-i) incubation time. This characteristic staining strongly implies that these plaques were originally two separate plaques (in the Methoxy-X04

staining), but then merged over time to ultimately form one, larger plaque (in the anti-Aβ antibody staining).
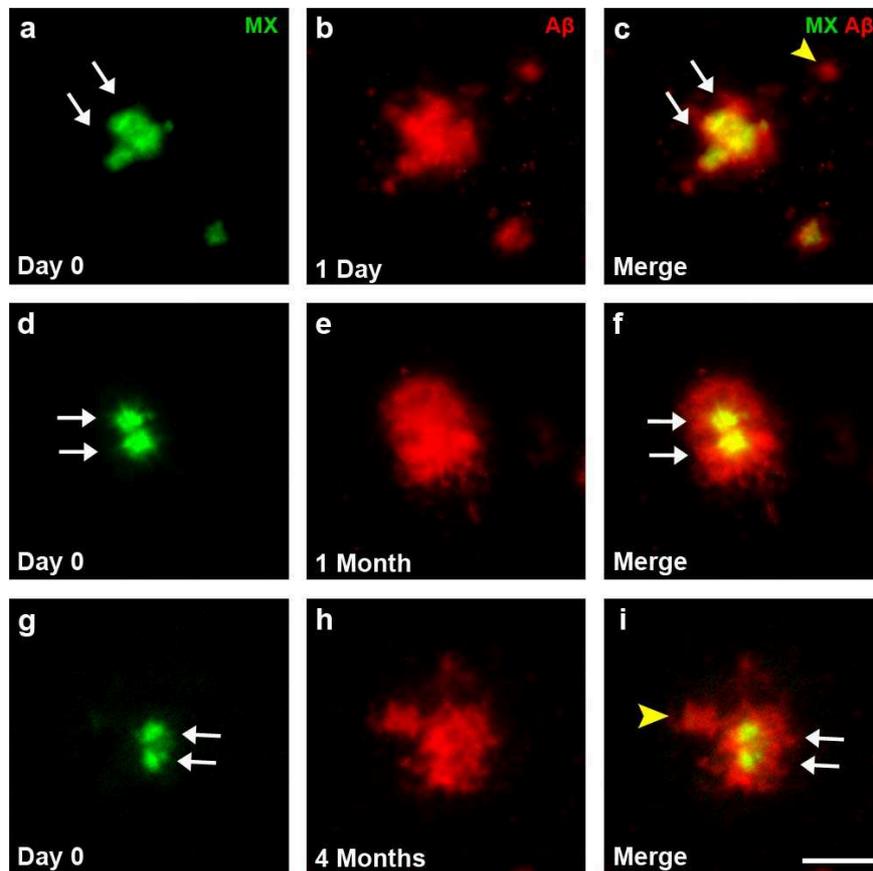
Figure 27: Large, multicored plaques formed from multiple pre-existing plaques. Multicored plaques have more than one Methoxy-X04 (MX) positive core (a, d, g) within a single anti-Aβ antibody 3552 (Aβ) positive area (b, e, h). Multicored plaques were found after 1 day (c), 1 month (f) and 4 months (i) of incubation time. Scale bar: 25 µm.

The occurrence of these multicored plaques were quantified and the number of multicored plaques increased significantly with increasing post-Methoxy-X04-injection incubation time (Figure 28 a), showing that multicored plaques were more numerous with more advanced pathology. The size of multicored plaques was also examined and, interestingly, the size of multicored plaques was correlated with the number of cores the multicored plaque contained (Figure 28 b); a larger multicore plaque had more precursor plaques. Multicore plaques

appear to be a very consistent phenomenon as they contribute ~13% of all large ($>300\,\mu m^2$) plaques, regardless of incubation time (Figure 28 c).
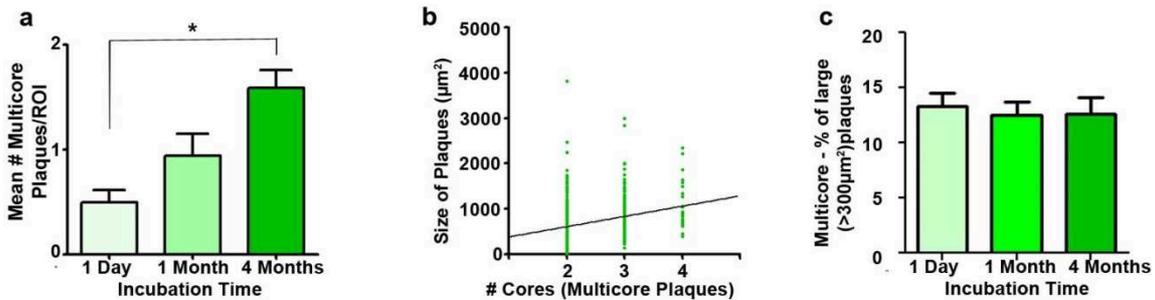
Figure 28: Multicored plaques. The number of multicored plaques per ROI increases with incubation time (a). Mean ± SEM. n = 5-6 per group. Kruskal-Wallis test with Dunn's post hoc text. * $p<0.05$. The number of cores per multicored plaque is positively correlated to the size of the plaque (b). Linear regression, $R^2=0.07474$; $p<0.0001$, n=687 plaques from 5 mice. The proportion of large ($>300\mu m^2$) plaques that were multicored plaques was fairly constant over incubation time (c). Mean ± SEM. n = 5-6 per group.

To examine the fate of the cores of these multicored plaques, brain sections were stained with Thiazin Red, a post mortem stain for dense-cored plaques. Thus, the core at day 0 was stained with Methoxy-X04, but how the dense material looked at the end of the incubation time was shown with the Thiazin Red staining. A triple staining method allowed for the initial dense core state to be labelled with Methoxy-X04, the ultimate dense core state to be labelled with Thiazin Red and the ultimate diffuse state labelled with anti-Aβ antibody 3552 (Figure 29).

Comparison of these three stainings revealed two fates for the dense cores of multicored plaques as defined by multiple Methoxy-X04 positive cores within an anti-Aβ antibody positive plaque. Firstly, the multiple cores can merge together over time to create a single, dense cored plaque (Figure 29 e-h), showing that dense core material can fuse over time. Secondly, the multiple cores can remain separate within the antibody labelled material Figure 29 a-d), despite the cores being very close together. Approximately 25% Figure 29 i) of all multicored plaques cores fused over the 4 month incubation period. The rest, 75%, still had multiple Thiazin Red positive cores, showing that they had remained multicored over this period. These data show that dense cores can merge over time.
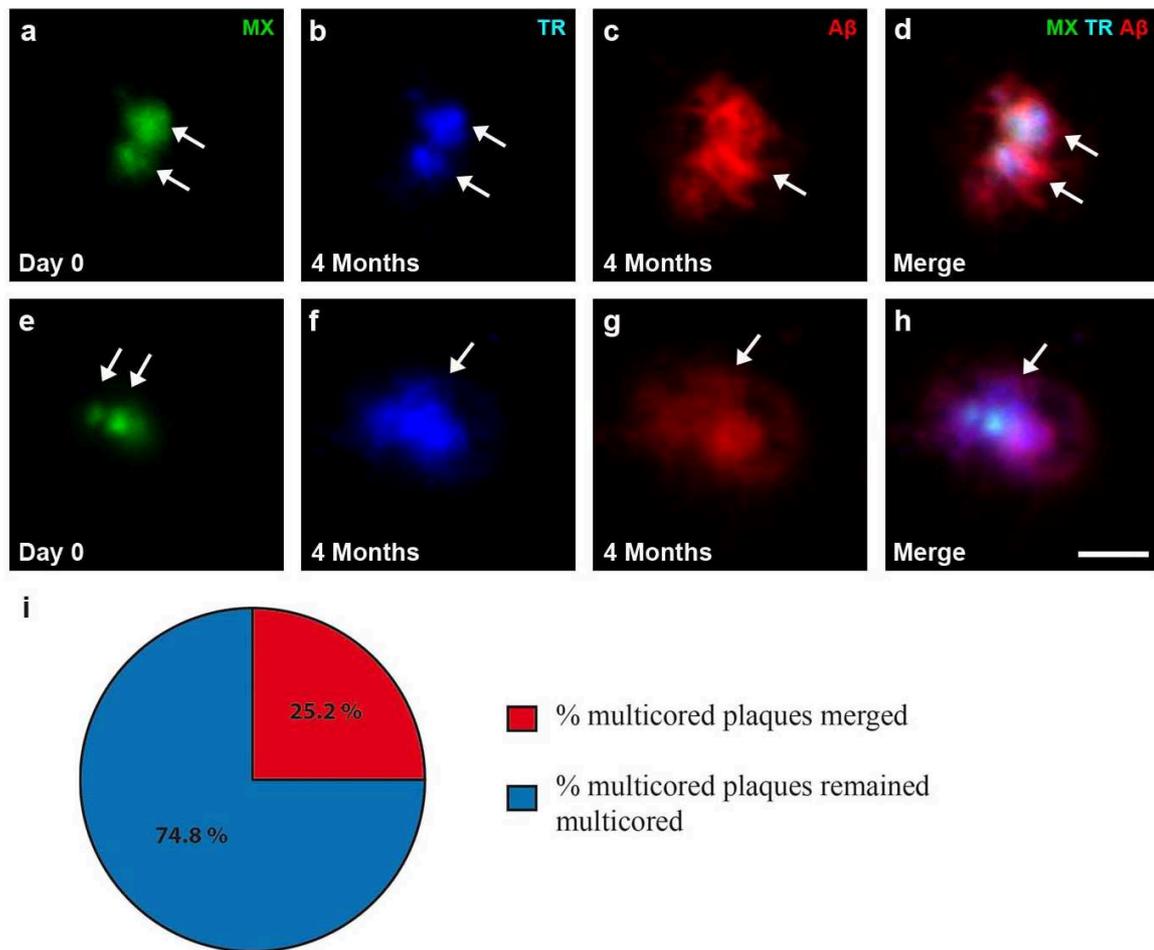
Figure 29: Fate of multicored plaques. Thiazin Red (TR) post mortem staining was used to examine the fate of multicore plaques defined by their multiple Methoxy-X04 (MX) cores. In (a-d), the cores remain separate (white arrows) within the anti-Aβ antibody 3552 (Aβ) staining and the plaque is still multicored at the 4 month time point. In (e-h) the two MX cores have merged into one TR core by the 4 month time point (white arrows). (i) Proportion of multicored plaques that merge or remain multicored over 4 months incubation time. n=5. Scale bar: 25 µm.

When these triple stained images were examined for examples of newly emerging multicored plaques, plaques were found that would not be classified as multicored from the Methoxy-X04, day 0 staining, but that would be 4 month later by the Thiazin Red staining (Figure 30). These plaques had developed into multicore plaques over the 4 month incubation time showing that a new close plaque had developed over the 4 months. This phenomenon demonstrates that the multiple dense cores of multicored plaques can form sequentially.
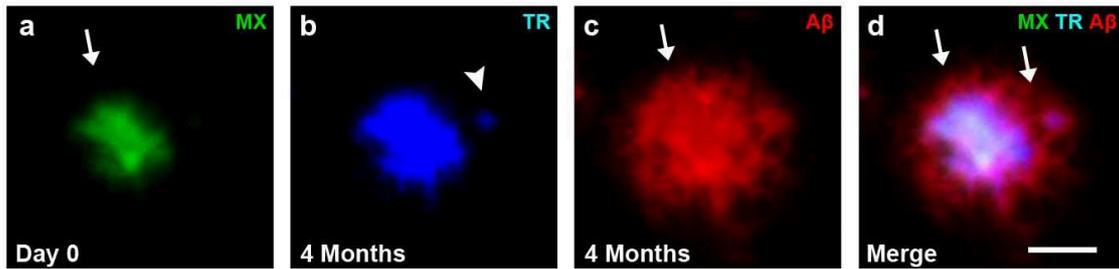
Figure 30: Multicored plaques can form at different times. A single plaque (a) is joined by a newly formed dense cored plaque (b, white arrowhead) within the anti-Aβ antibody positive halo (c, d). Scale bar: 25 µm.

This study has identified three interesting plaque categories of plaques: flower plaques, clusters of plaques and merging plaques. In a control experiment, the post-mortem Methoxy-X04 images were re-examined to find examples of these categories to rule out any confounding effect of the multiple staining techniques. Indeed, examples of all three plaque categories could be found in these images: flower plaques (Figure 31a), plaque clusters (Figure 31b) and merging plaques (Figure 31c).
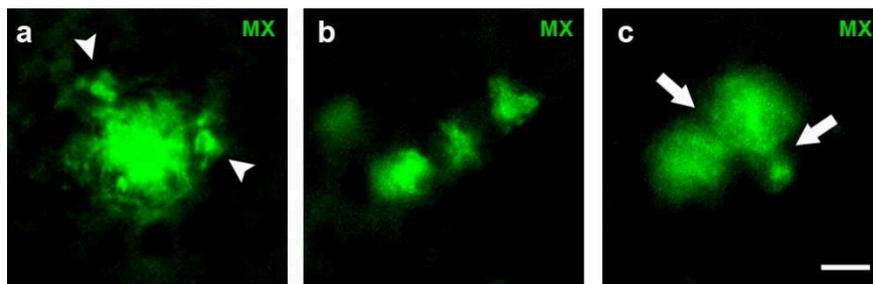
Figure 31: Post mortem Methoxy-X04 staining of plaque development categories. A flower plaque (a, white arrowheads are 'petal' plaques), a plaque cluster (b) and merging plaques (c, white arrows).Scale bar: 25 µm

Discussion

Clustering Hypothesis of Amyloid Plaque Development

Plaques are one of the hallmarks of AD and are associated with toxicity of the surrounding tissue. This study, using a two-stage plaque staining technique, examined plaques over time and generated two important conclusions:

1) New plaques are more likely to form in the vicinity of a pre-existing plaque thereby forming clusters of plaques

2) Large plaques can have grown from several precursors showing that plaque clusters can fuse over time

Together, these results built a new hypothesis of plaque development to compliment the uniform growth theory, namely the clustering hypothesis of plaque development. This new hypothesis, as illustrated by the schematic in Figure 32 explains how large plaques arise from clusters of multiple smaller plaques. The presented data support three different scenarios whereby this could happen and these are illustrated in Figure 32. In the first scenario, a new plaque deposits in the vicinity of the initial plaque and these two plaques grow and merge together over time, eventually forming a large plaque with a single core. Alternatively, those two neighbouring plaque cores can remain separate and the diffuse material grows around to create a large plaque with multiple, separate cores. In a third scenario, the initial plaque develops multiple neighbouring plaques (a flower plaque) and then, hypothetically, grows a diffuse halo and ultimately becomes a multicored plaque. By this, the presented data provide evidence for a clustering hypothesis of large plaque development. The clustering hypothesis is an alternative theory of how plaques can grow, and complements the uniform growth theory of plaque development (Figure 12 a).
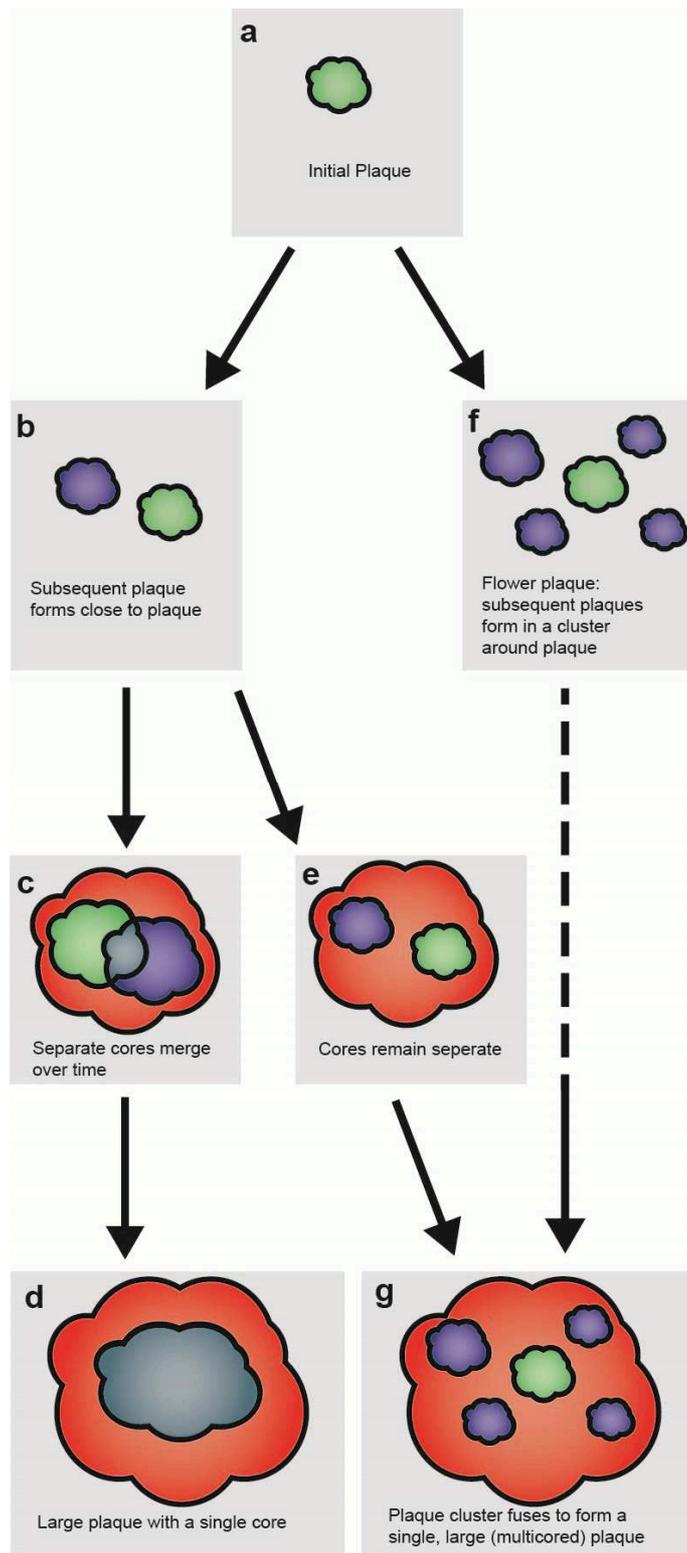
Figure 32: Schematic figure of the clustering hypothesis of plaque growth. An initial single plaque (a) is joined by a new, very close plaque (b). These two plaques fuse over time (c) to produce a larger plaque with a single core (d) or remain separate (e) and grow to be a large, multicored plaque (g). Alternatively, the initial plaque (a) can be joined by multiple new neighbour plaques (f) and grow to be a large, multicored plaque (g). Solid arrows represent events supported by the presented data; the dashed arrow represents hypothetical plaque development.

Non-Random Location of Plaque Deposition

The first major conclusion, that new plaques deposit close to pre-existing plaques, can be interpreted as evidence for the non-random location of plaque deposition. This project was inspired by the finding that, plaques in brain sections from APP transgenic mice showed non-random clustering of plaques (Urbanc et al., 1999). The presented data confirmed this result experimentally in a mouse model of AD; new plaques deposited $< 40\,\mu m$ from a pre-existing plaque at higher than chance level. This could be because of one of two reasons: either the microenvironment in which the first plaque appeared is conducive to plaque development, hence subsequent plaques also appear there, or, the first plaque itself somehow induces further plaques to develop in the vicinity. Each possibility will be discussed in turn.

As mentioned in the introduction, the precise origin of Aβ for plaque development is currently under debate and many factors may influence the location of plaque formation. These factors may well make it more likely that a first plaque, and subsequent plaques, develop in a particular location of the cerebral cortex rather than even a relatively short distance away. For example, if the Aβ for plaques originates from the blood vessels (Fiala, 2007), then the tissue close to blood vessels maybe particularly favourable for plaque development. Or, if highly active neurons promote plaque development (Bero et al., 2011), then the environment around highly active axon terminals may be a source of multiple plaques. Studies of plaque deposition in AD patients (Beach & McGeer, 1992) and transgenic mice (Beker et al., 2012) showed that cortical structure influences plaque deposition. This could also mean that some cortical areas are chemically or structurally more conducive to plaque deposition. These areas may secrete more Aβ than other areas, or have reduced Aβ clearance, leading to a build-up of Aβ and triggering plaque formation. Taken together, these factors show that plaque deposition occurs more favourably in certain microenvironments meaning that many plaques would form close to each other.

The second reason, that plaques can encourage the further deposition of plaques, is also supported by a body of experimental data. Pre-existing plaques may harbour the seeding material to seed new plaques – be it oligomers or some other Aβ aggregates. Plaques have been shown to co-localise with and be surrounded by soluble Aβ oligomers (Koffie et al., 2009), which may be the seed plaques (Langer et al., 2011). Therefore, it is possible that

plaques harbour the material necessary to seed new plaques and would seed new plaques in their direct vicinity.

Alternatively, plaque seeding material may develop intracellularly, e.g. there is a theory that Aβ fibrilises intracellularly and is then released via cell lysis to form a plaque (D'Andrea et al., 2001). As reviewed in the introduction, plaques are toxic to neurons in the near vicinity (Bittner et al., 2012; McLellan et al., 2003) and can damage local cell membranes (Praprotnik et al., 1995). This being true, the presence of a pre-existing plaque could damage the local neurons, releasing intracellular plaque seeding material. Thereby a new plaque would be more likely to form in the vicinity of a pre-existing plaque.

Taken together, there is a lot of evidence for the non-random deposition of new plaques. It is therefore possible that both factors are involved in this phenomenon, but more research is needed to fully elucidate the many influences on localisation of plaque deposition.

Merger of Plaques over Time

The second major conclusion of this study is that clusters of plaques can merge over time to form a single, large plaque. This is supported by previous studies that also found examples of multicored plaques (Condello et al., 2011; Rak et al., 2007). However, this thesis provided a detailed quantification of this plaque population and mapped their fate over time. Plaques that merged over time made up a sizable proportion (13%) of all large ($> 300 \, \mu m^2$) plaques and ~25% of these multicores merged over a four month period. It would be interesting to conduct a longer study to determine if more cores would merge over a longer period, or if some cores remain separate for very long periods, and whether there is a particular point in the pathological progression of plaques where cluster fusion happens.

How and why would neighbouring plaques merge over time? Three different possible scenarios could be envisioned. In the first scenario, the two plaques simply grow uniformly and the space between them slowly decreases so that they automatically gradually merge together. This scenario is certainly attractively simple, but a second scenario, whereby the space in between two close plaques is preferential for Aβ deposition is also intriguing. The surfaces of the two close plaques presumably offers lots of fibril ends to which Aβ molecules

can bind and elongate the fibres (Jucker & Walker, 2011). But in the space between the two plaques, the density of fibril ends is higher and so the probability of a 'passing' Aβ molecule to bind to a fibril within this space is higher than for it to bind to the rest of the plaques' surfaces. Thereby, the amount of Aβ deposition in between the two close plaques may be higher than other places on the spherical plaques favouring the fusion of the two plaques.

The third scenario is that the diffuse Aβ halo surrounding the dense cores of the two plaques can change conformation over time to a dense core conformation and thereby the cores merge over time. In fact, new dense core material was observed developing nearby and seemingly within diffuse Aβ material (Figure 30). It is tempting to speculate that the new cores emerging in the halo of diffuse Aβ had developed directly from the diffuse Aβ and that diffuse Aβ can change conformation into an amyloid structure. One theory, still widely debated, suggests that dense core plaques develop out of diffuse plaques (Fiala, 2007) and that diffuse Aβ deposits are the precursors to cored plaques. One study examined the conformation of plaques in young and aged mice using fluorescent probes and showed that Aβ likely changes conformation within plaques as plaques in older animals had less immature fibrils and more mature filaments than plaques in younger animals (Nyström et al., 2013). Indeed, this is discussed in (Meyer-Luehmann et al., 2008) as a reason they saw such a rapid formation of dense core plaques: that pre-amyloid Aβ was already present at that location and rapidly changed to a visible amyloid structure. The method employed in this thesis does not, unfortunately, have the temporal resolution to explore this possibility. It is nevertheless a compelling notion, and with advances in in vivo imaging techniques, this issue can hopefully be further investigated in the near future.

The three scenarios discussed are all possible ways how multiple close plaques could merge over time, but to fully understand the precise mechanism behind merging plaques more experiments are needed.

Data with Differences between Young and Older Mice

There were two sets of data in this thesis where there were clear differences in shorter and longer incubation time groups. However, the differences in the plaque development between these groups are most likely due to technical artefacts as discussed below.

The first data set was the rotation analysis that compared data from this study to chance levels (Figure 23). This comparison only showed a significant result in the younger animals group. The two older groups – 1 month and 4 months - were not significantly different from chance levels. To explain this, it is important to keep in mind that the older groups have a higher plaque density than the younger group and this even has a significant negative correlation to the chance of a new plaque being close to a pre-existing plaque. This seems a plausible explanation for the disparity between groups – a higher plaque density makes it more likely that plaques will deposit by chance in the vicinity of a pre-existing plaque. Moreover, if there are more plaques in the cortex, then the deposition becomes more 'general' and more random as the niches that were particularly conducive to plaque development are saturated.

Another explanation for the discrepancy between the groups in the rotation data could be that in the older groups, the analysis underestimates the amount of close new plaques. This underestimation could occur because of three reasons. Firstly, clusters of new plaques within the new plaque population were observed. Over the longer incubation time points, many new plaques are deposited. If several new plaques formed over the longer time point, some of the later new plaques probably formed nearby the earlier new plaques. Therefore, the method used here, with only two 'snap-shots' of plaque development, would not discern all the plaques that developed close to a pre-existing plaque and thereby underestimating the amount of close new plaques. Secondly, the older groups have larger plaques than the younger groups (Figure 16). The large plaques often had large diffuse halos surrounding the initial Methoxy-X04 positive core. This could mean that subsequent plaques that formed very close to pre-existing plaques would have been engulfed by the large plaque and would be counted as a single, multicored plaque (Figure 30). Thus, these new close plaques would not be counted as new and therefore the real amount of close new plaques in the longer time point groups was underestimated. Thirdly, we cannot rule out the possibility that Methoxy-X04 continues to label plaques after the injection and binds to new plaques, which would then not count as new plaques. This would also lead to an underestimation of the amount of new plaques.

Any, or a mixture of all three explanations would lead to an underestimation of new plaques in later time points and therefore a bias in the rotation data for the older groups.

The second data set with discrepancies between age groups was the analysis of the exact distances between new plaques and their close pre-existing plaque neighbours (Figure 26). In

this data set, the data from the younger animals behaving differently from the two older groups: the younger animals show a peak between 5 and 15 µm, followed by a drop to a steady plateau at 20-25 µm, whereas the two older groups show most of their new plaques 20-25 µm away (Figure 26). Again, because of the increase in larger plaques in the older animals, this could obscure any very close new plaques, and therefore the older groups show very few very close (5-15 µm) new plaques. The younger animals have very few large plaques and so very close new plaques are not obscured and are still apparent. If one were to take out the very close distance groups, the plateau phases look very similar. Therefore, there doesn't appear to be any preferred location once more than 20 µm away.

The staining artefacts discussed are likely explanations for the discrepancies seen in the two data sets. Further analysis with shorter incubation times might definitively address these issues.

Aβ-plaque Associated Therapeutic Strategies

The study of plaque formation and development is important for the advance of new, disease-modifying treatment strategies; many therapeutics in development are based on preventing the formation of plaques, or removing the aggregated Aβ that has already deposited (Citron, 2010). Therefore the results of this study and the clustering hypothesis of plaque development could have important implications for future AD therapeutics.

One strategy for combating AD is to prevent aggregation of Aβ and plaque deposition. Many molecules that interfere with Aβ aggregation have been suggested as therapy for AD (Selkoe, 2001). Aggregation inhibitors, such as cyclohexanehexol inhibitors (McLaurin et al., 2006), keep Aβ in monomeric form, rather than forming toxic oligomeric aggregates. Whether this would prevent further plaque formation once the disease has started and rescue the disease pathology requires detailed knowledge of the influences on Aβ deposition. Another strategy is to promote aggregation, so that Aβ quickly aggregates to amyloid fibrils and thereby also avoids the toxic oligomer stage – this would create more plaques, and so knowledge of how they form would be very useful for this line of therapy. However, as postulated by (Selkoe, 2011), plaques may only 'trap' oligomeric Aβ up to a certain saturation level. Thereafter, once the brain is full of plaques, they may actually act as reservoirs to store Aβ oligomers and

increase toxicity. Detailed knowledge of plaque deposition and deposition niches could help develop focused therapy to prevent the formation of plaques and protect the brain from AD.

Immunotherapy is another strategy to clear plaques from the brain parenchyma. By targeting Aβ, antibodies reduce the amount of Aβ available and thereby reduce the formation of plaques. Immunotherapy against Aβ is thought to reduce plaques by one or more of three mechanisms (Citron, 2010). Firstly, by activating nearby microglia to clear the plaque material (Bard et al., 2000). Secondly, the antibodies themselves may directly resolve the plaque material, but due to the low penetrance of antibodies (just 0.1% of serum level) into the brain (Bard et al., 2000), this mechanism seems unlikely. Thirdly, peripheral antibodies could capture Aβ, thereby acting as a 'peripheral sink' and reducing the Aβ concentration in the brain parenchyma and clearing plaques in that way (DeMattos et al., 2002; Dodart et al., 2002; Marques et al., 2009). Active immunisation with aggregated $Aβ_{42}$ reduced cerebral plaques and neuritic dystrophies in APP transgenic mice (Schenk et al., 1999), but clinical trials in AD patients have led to mixed results. Passive immunisation with pre-made antibodies is a prominent option as a cure for AD, however, this treatment has been marred by the side effect of micro-haemorrhages (Meyer-Luehmann et al., 2011; Pfeifer et al., 2002). This thesis expands knowledge of plaque deposition and formation and may help understand plaque clearing strategies better and target them more effectively to plaque-forming niches.

The clustering hypothesis describes how large plaques in particular can arise and the formation of large plaque is particularly interesting as they have been shown to have different properties compared with smaller plaques. An in vivo study in mice investigating oxidative stress in the neurons surrounding plaques found more oxidised neurites in the vicinity of larger plaques (Xie et al., 2013). Assuming that plaques do host molecules that are toxic to neurons, then it could be argued that larger plaques are logically more toxic than smaller plaques. However, another study that quantified the neuritic damage surrounding plaques observed, that smaller, faster growing plaques are surrounded by more dystrophic neurites than larger plaques (Condello et al., 2011). Either way, large plaques seem to have different effects on the surrounding tissue to smaller plaques, and therefore knowing specifically how they form and grow is an important topic and may be useful in developing novel therapeutic strategies.

Concluding Remarks

In conclusion, the presented data provide a detailed description of plaque development over time and gave strong in vivo support for a clustering mechanism of large plaque growth. This clustering hypothesis complements a uniform growth hypothesis and gives another dimension to our knowledge of plaque development. The data also give interesting hints that plaques deposit in a non-random manner and that multiple plaques do fuse over time to give rise to large plaques. Both are interesting phenomena and could warrant study.

Why plaques form in clusters and how new plaques are seeded are still open questions. The answers to these questions and an increasing understanding of plaque formation and development will hopefully lead to greater understanding of the AD etiology and finally, in the future, to disease modifying therapies.

Acknowledgments

Firstly, I would like to thank my supervisor Melanie Meyer-Luehmann. She conceived this project and was incredibly supportive throughout. She inspired me with her enthusiasm and motivation for the project and was involved at every step. Secondly, I would like to thank Christian Haass for his keen interest for the project, innovative suggestions and unfailing support for its completion. The other members of my thesis advisory committee, Magdalena Götz and Swasti Raychaudhuri, were also always full of helpful comments and constructive advice for these experiments.

Big thanks go to Teresa Bachhuber, who was always willing to discuss results, strategy and hand out well-reasoned advice. I thank Sabine Liebscher for helping me think through some analytical issues that came up in this project. I also thank Claudia Abou-Abrams for her consistently excellent technical advice and for teaching me several of the techniques I employed for this thesis.

I would also like to thank everyone in the Haass department at the Adolf-Butenandt Institute for being so welcoming and friendly and proving to be such brilliant colleagues. And the GSN and IMPRS graduate schools for all their support and advice throughout the PhD process.

Thanks for the support and distraction of my family and friends that have made this time much easier and pleasanter than otherwise.

And finally, thanks to Jonny. For everything.

References

Ahmed, M., Davis, J., Aucoin, D., Sato, T., Ahuja, S., Aimoto, S., Elliott, J. I., Van Nostrand, W. E. & Smith, S. O. (**2010**). Structural conversion of neurotoxic amyloid-[beta]1-42 oligomers to fibrils. *Nat Struct Mol Biol*, 17 (5), 561-567

Alafuzoff, I., Pikkarainen, M., Arzberger, T., Thal, D., Al-Sarraj, S., Bell, J., Bodi, I., Budka, H., Capetillo-Zarate, E., Ferrer, I., Gelpi, E., Gentleman, S., Giaccone, G., Kavantzas, N., King, A., Korkolopoulou, P., Kovács, G., Meyronet, D., Monoranu, C., Parchi, P., Patsouris, E., Roggendorf, W., Stadelmann, C., Streichenberger, N., Tagliavini, F. & Kretzschmar, H. (**2008**). Inter-laboratory comparison of neuropathological assessments of β-amyloid protein: a study of the BrainNet Europe consortium. *Acta Neuropathologica*, 115 (5), 533-546

Alzheimer, A. (**1907**). Über eine eigenartige Erkrankung der Hirnrinde. *Allgemeine Zeitschrift für Psychiatrie und phychish-Gerichtliche Medizin*, 64 146-148

Armstrong, R. A. (**1998**). β-Amyloid Plaques: Stages in Life History or Independent Origin? *Dementia and Geriatric Cognitive Disorders*, 9 (4), 227-238

Armstrong, R. A., Myers, D. & Smith, C. U. M. (**1993**). The spatial patterns of β/A4 deposit subtypes in Alzheimer's disease. *Acta Neuropathologica*, 86 (1), 36-41

Attems, J., Yamaguchi, H., Saido, T. C. & Thal, D. R. (**2010**). Capillary CAA and perivascular Aβ-deposition: Two distinct features of Alzheimer's disease pathology. *Journal of the Neurological Sciences*, 299 (1–2), 155-162

Bacskai, B. J., Hickey, G. A., Skoch, J., Kajdasz, S. T., Wang, Y., Huang, G.-f., Mathis, C. A., Klunk, W. E. & Hyman, B. T. (**2003**). Four-dimensional multiphoton imaging of brain entry, amyloid binding, and clearance of an amyloid-β ligand in transgenic mice. *Proceedings of the National Academy of Sciences*, 100 (21), 12462-12467

Ballard, C., Gauthier, S., Corbett, A., Brayne, C., Aarsland, D. & Jones, E. (**2011**). Alzheimer's disease. *The Lancet*, 377 (9770), 1019-1031

Bard, F., Cannon, C., Barbour, R., Burke, R.-L., Games, D., Grajeda, H., Guido, T., Hu, K., Huang, J., Johnson-Wood, K., Khan, K., Kholodenko, D., Lee, M., Lieberburg, I., Motter, R., Nguyen, M., Soriano, F., Vasquez, N., Weiss, K., Welch, B., Seubert, P., Schenk, D. & Yednock, T. (**2000**). Peripherally administered antibodies against amyloid [beta]-peptide enter the central nervous system and reduce pathology in a mouse model of Alzheimer disease. *Nature Medicine*, 6 (8), 916-919

Beach, T. G. & McGeer, E. G. (**1992**). Senile plaques, amyloid β-protein, and acetylcholinesterase fibres: laminar distributions in Alzheimer's disease striate cortex. *Acta Neuropathologica*, 83 (3), 292-299

Beker, S., Kellner, V., Kerti, L. & Stern, E. A. (**2012**). Interaction between Amyloid-β Pathology and Cortical Functional Columnar Organization. *The Journal of Neuroscience*, 32 (33), 11241-11249

Benilova, I., Karran, E. & De Strooper, B. (**2012**). The toxic A[beta] oligomer and Alzheimer's disease: an emperor in need of clothes. *Nature Neuroscience*, 15 (3), 349-357

Bentahir, M., Nyabi, O., Verhamme, J., Tolia, A., Horré, K., Wiltfang, J., Esselmann, H. & De Strooper, B. (**2006**). Presenilin clinical mutations can affect γ-secretase activity by different mechanisms. *The Journal of Neurochemistry*, 96 (3), 732-742

Bero, A. W., Bauer, A. Q., Stewart, F. R., White, B. R., Cirrito, J. R., Raichle, M. E., Culver, J. P. & Holtzman, D. M. (**2012**). Bidirectional Relationship between Functional Connectivity and Amyloid-β Deposition in Mouse Brain. *The Journal of Neuroscience*, 32 (13), 4334-4340

Bero, A. W., Yan, P., Roh, J. H., Cirrito, J. R., Stewart, F. R., Raichle, M. E., Lee, J. M. & Holtzman, D. M. (**2011**). Neuronal activity regulates the regional vulnerability to amyloid-beta deposition. *Nature Neuroscience*, 14 (6), 750-6

Beydoun, M. A., Beydoun, H. A. & Wang, Y. (**2008**). Obesity and central obesity as risk factors for incident dementia and its subtypes: a systematic review and meta-analysis. *Obesity Reviews*, 9 (3), 204-218

Bitan, G., Kirkitadze, M. D., Lomakin, A., Vollers, S. S., Benedek, G. B. & Teplow, D. B. (**2003**). Amyloid β-protein (Aβ) assembly: Aβ40 and Aβ42 oligomerize through distinct pathways. *Proceedings of the National Academy of Sciences*, 100 (1), 330-335

Bittner, T., Burgold, S., Dorostkar, M., Fuhrmann, M., Wegenast-Braun, B., Schmidt, B., Kretzschmar, H. & Herms, J. (**2012**). Amyloid plaque formation precedes dendritic spine loss. *Acta Neuropathologica*, 124 (6), 797-807

Bolmont, T., Haiss, F., Eicke, D., Radde, R., Mathis, C. A., Klunk, W. E., Kohsaka, S., Jucker, M. & Calhoun, M. E. (**2008**). Dynamics of the Microglial/Amyloid Interaction Indicate a Role in Plaque Maintenance. *The Journal of Neuroscience*, 28 (16), 4283-4292

Braak, H. & Braak, E. (**1991**). Neuropathological stageing of Alzheimer-related changes. *Acta Neuropathologica*, 82 (4), 239-259

Brendza, R. P., Bacskai, B. J., Cirrito, J. R., Simmons, K. A., Skoch, J. M., Klunk, W. E., Mathis, C. A., Bales, K. R., Paul, S. M., Hyman, B. T. & Holtzman, D. M. (**2005**). Anti-Aβ antibody treatment promotes the rapid recovery of amyloid-associated neuritic dystrophy in PDAPP transgenic mice. *The Journal of Clinical Investigation*, 115 (2), 428-433

Brookmeyer, R., Evans, D. A., Hebert, L., Langa, K. M., Heeringa, S. G., Plassman, B. L. & Kukull, W. A. (**2011**). National estimates of the prevalence of Alzheimer's disease in the United States. *Alzheimer's & Dementia*, 7 (1), 61-73

Burgold, S., Bittner, T., Dorostkar, M., Kieser, D., Fuhrmann, M., Mitteregger, G., Kretzschmar, H., Schmidt, B. & Herms, J. (**2011**). In vivo multiphoton imaging reveals gradual growth of newborn amyloid plaques over weeks. *Acta Neuropathologica*, 121 (3), 327-335

Busche, M. A., Eichhoff, G., Adelsberger, H., Abramowski, D., Wiederhold, K.-H., Haass, C., Staufenbiel, M., Konnerth, A. & Garaschuk, O. (**2008**). Clusters of Hyperactive Neurons Near Amyloid Plaques in a Mouse Model of Alzheimer's Disease. *Science*, 321 (5896), 1686-1689

Chow, V., Mattson, M., Wong, P. & Gleichmann, M. (**2010**). An Overview of APP Processing Enzymes and Products. *NeuroMolecular Medicine*, 12 (1), 1-12

Cirrito, J. R., Yamada, K. A., Finn, M. B., Sloviter, R. S., Bales, K. R., May, P. C., Schoepp, D. D., Paul, S. M., Mennerick, S. & Holtzman, D. M. (**2005**). Synaptic Activity Regulates Interstitial Fluid Amyloid-β Levels In Vivo. *Neuron*, 48 (6), 913-922

Citron, M. (**2010**). Alzheimer's disease: strategies for disease modification. *Nature Reviews Drug Discovery*, 9 (5), 387-398

Citron, M., Oltersdorf, T., Haass, C., McConlogue, L., Hung, A. Y., Seubert, P., Vigo-Pelfrey, C., Lieberburg, I. & Selkoe, D. J. (**1992**). Mutation of the [beta]-amyloid precursor protein in familial Alzheimer's disease increases [beta]-protein production. *Nature*, 360 (6405), 672-674

Cleary, J. P., Walsh, D. M., Hofmeister, J. J., Shankar, G. M., Kuskowski, M. A., Selkoe, D. J. & Ashe, K. H. (**2005**). Natural oligomers of the amyloid-[beta] protein specifically disrupt cognitive function. *Nat Neurosci*, 8 (1), 79-84

Condello, C., Schain, A. & Grutzendler, J. (**2011**). Multicolor time-stamp reveals the dynamics and toxicity of amyloid deposition. *Sci Rep*, 1

Craft, J. M., Watterson, D. M., Frautschy, S. A. & Eldik, L. J. V. (**2004**). Aminopyridazines inhibit β-amyloid-induced glial activation and neuronal damage in vivo. *Neurobiology of Aging*, 25 (10), 1283-1292

Cruz, L., Urbanc, B., Buldyrev, S. V., Christie, R., Gómez-Isla, T., Havlin, S., McNamara, M., Stanley, H. E. & Hyman, B. T. (**1997**). Aggregation and disaggregation of senile plaques in Alzheimer disease. *Proceedings of the National Academy of Sciences*, 94 (14), 7612-7616

D'Andrea, M. R., Nagele, R. G., Wang, H. Y., Peterson, P. A. & Lee, D. H. S. (**2001**). Evidence that neurones accumulating amyloid can undergo lysis to form amyloid plaques in Alzheimer's disease. *Histopathology*, 38 (2), 120-134

de Jong, D., Jansen, R., Hoefnagels, W., Jellesma-Eggenkamp, M., Verbeek, M., Borm, G. & Kremer, B. (**2008**). No Effect of One-Year Treatment with Indomethacin on Alzheimer's Disease Progression: A Randomized Controlled Trial. *PLoS One*, 3 (1), e1475

DeMattos, R. B., Bales, K. R., Cummins, D. J., Paul, S. M. & Holtzman, D. M. (**2002**). Brain to Plasma Amyloid-β Efflux: a Measure of Brain Amyloid Burden in a Mouse Model of Alzheimer's Disease. *Science*, 295 (5563), 2264-2267

Dodart, J.-C., Bales, K. R., Gannon, K. S., Greene, S. J., DeMattos, R. B., Mathis, C., DeLong, C. A., Wu, S., Wu, X., Holtzman, D. M. & Paul, S. M. (**2002**). Immunization reverses memory deficits without reducing brain A[beta] burden in Alzheimer's disease model. *Nature Neuroscience*, 5 (5), 452-457

Dong, J., Revilla-Sanchez, R., Moss, S. & Haydon, P. G. (**2010**). Multiphoton in vivo imaging of amyloid in animal models of Alzheimer's disease. *Neuropharmacology*, 59 (4-5), 268-275

Doody, R. S., Raman, R., Farlow, M., Iwatsubo, T., Vellas, B., Joffe, S., Kieburtz, K., He, F., Sun, X., Thomas, R. G., Aisen, P. S., Siemers, E., Sethuraman, G. & Mohs, R. (**2013**). A Phase 3 Trial of Semagacestat for Treatment of Alzheimer's Disease. *New England Journal of Medicine*, 369 (4), 341-350

Drechsel, D. N., Hyman, A. A., Cobb, M. H. & Kirschner, M. W. (**1992**). Modulation of the dynamic instability of tubulin assembly by the microtubule-associated protein tau. *Molecular Biology of the Cell*, 3 (10), 1141-1154

Edbauer, D., Winkler, E., Regula, J. T., Pesold, B., Steiner, H. & Haass, C. (**2003**). Reconstitution of [gamma]-secretase activity. *Nature Cell Biology*, 5 (5), 486-488

Eikelenboom, P., Hack, C. E., Rozemuller, J. M. & Stam, F. C. (**1988**). Complement activation in amyloid plaques in Alzheimer's dementia. *Virchows Archiv B*, 56 (1), 259-262

Eisele, Y. S., Obermüller, U., Heilbronner, G., Baumann, F., Kaeser, S. A., Wolburg, H., Walker, L. C., Staufenbiel, M., Heikenwalder, M. & Jucker, M. (**2010**). Peripherally Applied Aβ-Containing Inoculates Induce Cerebral β-Amyloidosis. *Science*, 330 (6006), 980-982

Elder, G. A., Gama Sosa, M. A. & De Gasperi, R. (**2010**). Transgenic Mouse Models of Alzheimer's Disease. *Mount Sinai Journal of Medicine: A Journal of Translational and Personalized Medicine*, 77 (1), 69-81

Fiala, J. C. (**2007**). Mechanisms of amyloid plaque pathogenesis. *Acta Neuropathologica*, 114 (6), 551-571

Frautschy, S. A., Yang, F., Irrizarry, M., Hyman, B., Saido, T. C., Hsiao, K. & Cole, G. M. (**1998**). Microglial response to amyloid plaques in APPsw transgenic mice. *Am J Pathol*, 152 (1), 307-317

Games, D., Adams, D., Alessandrini, R., Barbour, R., Borthelette, P., Blackwell, C., Carr, T., Clemens, J., Donaldson, T., Gillespie, F., Guido, T., Hagopian, S., Johnson-Wood, K., Khan, K., Lee, M., Leibowitz, P., Lieberburg, I., Little, S., Masliah, E., McConlogue, L., Montoya-Zavala, M., Mucke, L., Paganini, L., Penniman, E., Power, M., Schenk, D., Seubert, P., Snyder, B., Soriano, F., Tan, H., Vitale, J., Wadsworth, S., Wolozin, B. & Zhao, J. (**1995**). Alzheimer-type neuropathology in transgenic mice overexpressing V717F [beta]-amyloid precursor protein. *Nature*, 373 (6514), 523-527

Garcia-Alloza, M., Borrelli, L. A., Hyman, B. T. & Bacskai, B. J. (**2010**). Antioxidants have a rapid and long-lasting effect on neuritic abnormalities in APP:PS1 mice. *Neurobiology of Aging*, 31 (12), 2058-2068

Garcia-Alloza, M., Gregory, J., Kuchibhotla, K. V., Fine, S., Wei, Y., Ayata, C., Frosch, M. P., Greenberg, S. M. & Bacskai, B. J. (**2011**). Cerebrovascular lesions induce transient β-amyloid deposition. *Brain*,

Gaspar, R. C., Villarreal, S. A., Bowles, N., Hepler, R. W., Joyce, J. G. & Shughrue, P. J. (**2010**). Oligomers of β-amyloid are sequestered into and seed new plaques in the brains of an AD mouse model. *Experimental Neurology*, 223 (2), 394-400

Gendreau, K. & Hall, G. F. (**2013**). Tangles, toxicity, and tau secretion in AD – new approaches to a vexing problem. *Frontiers in Neurology*, 4

Giannakopoulos, P., Herrmann, F. R., Bussière, T., Bouras, C., Kövari, E., Perl, D. P., Morrison, J. H., Gold, G. & Hof, P. R. (**2003**). Tangle and neuron numbers, but not amyloid load, predict cognitive status in Alzheimer's disease. *Neurology*, 60 (9), 1495-1500

Golde, T. E., Schneider, L. S. & Koo, E. H. (**2011**). Anti-Aβ Therapeutics in Alzheimer's Disease: The Need for a Paradigm Shift. *Neuron*, 69 (2), 203-213

Grathwohl, S. A., Kalin, R. E., Bolmont, T., Prokop, S., Winkelmann, G., Kaeser, S. A., Odenthal, J., Radde, R., Eldh, T., Gandy, S., Aguzzi, A., Staufenbiel, M., Mathews, P. M., Wolburg, H., Heppner, F. L. & Jucker, M. (**2009**). Formation and maintenance of Alzheimer's disease [beta]-amyloid plaques in the absence of microglia. *Nature Neuroscience*, 12 (11), 1361-1363

Grundke-Iqbal, I., Iqbal, K., Tung, Y. C., Quinlan, M., Wisniewski, H. M. & Binder, L. I. (**1986**). Abnormal phosphorylation of the microtubule-associated protein tau (tau) in Alzheimer cytoskeletal pathology. *Proceedings of the National Academy of Sciences*, 83 (13), 4913-4917

Grüning, C. S. R., Klinker, S., Wolff, M., Schneider, M., Toksöz, K., Klein, A. N., Nagel-Steger, L., Willbold, D. & Hoyer, W. (**2013**). The Off-Rate of Monomers Dissociating from Amyloid-β Protofibrils. *Journal of Biological Chemistry*,

Guerreiro, R., Wojtas, A., Bras, J., Carrasquillo, M., Rogaeva, E., Majounie, E., Cruchaga, C., Sassi, C., Kauwe, J. S. K., Younkin, S., Hazrati, L., Collinge, J., Pocock, J., Lashley, T., Williams, J., Lambert, J.-C., Amouyel, P., Goate, A., Rademakers, R., Morgan, K., Powell, J., St. George-Hyslop, P., Singleton, A. & Hardy, J. (**2013**). TREM2 Variants in Alzheimer's Disease. *New England Journal of Medicine*, 368 (2), 117-127

Haass, C., Hung, A. Y., Selkoe, D. J. & Teplow, D. B. (**1994**). Mutations associated with a locus for familial Alzheimer's disease result in alternative processing of amyloid beta-protein precursor. *Journal of Biological Chemistry*, 269 (26), 17741-8

Haass, C., Lemere, C. A., Capell, A., Citron, M., Seubert, P., Schenk, D., Lannfelt, L. & Selkoe, D. J. (**1995**). The Swedish mutation causes early-onset Alzheimer's disease by [beta]-secretase cleavage within the secretory pathway. *Nature Medicine*, 1 (12), 1291-1296

Haass, C. & Selkoe, D. J. (**2007**). Soluble protein oligomers in neurodegeneration: lessons from the Alzheimer's amyloid [beta]-peptide. *Nat Rev Mol Cell Biol*, 8 (2), 101-112

Hamer, M. & Chida, Y. (**2009**). Physical activity and risk of neurodegenerative disease: a systematic review of prospective evidence. *Psychological Medicine*, 39 (01), 3-11

Hardy, J. & Higgins, G. (**1992**). Alzheimer's disease: the amyloid cascade hypothesis. *Science*, 256 (5054), 184-185

Harper, J. D. & Lansbury, P. T. (**1997**). MODELS OF AMYLOID SEEDING IN ALZHEIMER'S DISEASE AND SCRAPIE:Mechanistic Truths and Physiological Consequences of the Time-Dependent Solubility of Amyloid Proteins. *Annual Review of Biochemistry*, 66 (1), 385-407

Harris, J. A., Devidze, N., Verret, L., Ho, K., Halabisky, B., Thwin, M. T., Kim, D., Hamto, P., Lo, I., Yu, G.-Q., Palop, J. J., Masliah, E. & Mucke, L. (**2010**). Transsynaptic Progression of Amyloid-β-Induced Neuronal Dysfunction within the Entorhinal-Hippocampal Network. *Neuron*, 68 (3), 428-441

Hefendehl, J. K., Wegenast-Braun, B. M., Liebig, C., Eicke, D., Milford, D., Calhoun, M. E., Kohsaka, S., Eichner, M. & Jucker, M. (**2011**). Long-Term In Vivo Imaging of {beta}-Amyloid Plaque Appearance and Growth in a Mouse Model of Cerebral {beta}-Amyloidosis. *The Journal of Neuroscience*, 31 (2), 624-629

Hensley, K., Hall, N., Subramaniam, R., Cole, P., Harris, M., Aksenov, M., Aksenova, M., Gabbita, S. P., Wu, J. F., Carney, J. M., Lovell, M., Markesbery, W. R. & Butterfield, D. A. (**1995**). Brain Regional Correspondence Between Alzheimer's Disease Histopathology and Biomarkers of Protein Oxidation. *The Journal of Neurochemistry*, 65 (5), 2146-2156

Ho, L., Qin, W., Pompl, P. N., Xiang, Z., Wang, J., Zhao, Z., Peng, Y., Cambareri, G., Rocher, A., Mobbs, C. V., Hof, P. R. & Pasinetti, G. M. (**2004**). Diet-induced insulin resistance promotes amyloidosis in a transgenic mouse model of Alzheimer's disease. *The FASEB Journal*,

Hof, P. R., Bouras, C., Perl, D. P., Sparks, D., Mehta, N. & Morrison, J. H. (**1995**). Age-related distribution of neuropathologic changes in the cerebral cortex of patients with down's syndrome: Quantitative regional analysis and comparison with alzheime's disease. *Archives of Neurology*, 52 (4), 379-391

Hoffman, J. M., Welsh-Bohmer, K. A., Hanson, M., Crain, B., Hulette, C., Earl, N. & Coleman, R. E. (**2000**). FDG PET Imaging in Patients with Pathologically Verified Dementia. *Journal of Nuclear Medicine*, 41 (11), 1920-1928

Holcomb, L., Gordon, M. N., McGowan, E., Yu, X., Benkovic, S., Jantzen, P., Wright, K., Saad, I., Mueller, R., Morgan, D., Sanders, S., Zehr, C., O'Campo, K., Hardy, J., Prada, C.-M., Eckman, C., Younkin, S., Hsiao, K. & Duff, K. (**1998**). Accelerated Alzheimer-type phenotype in transgenic mice carrying both mutant amyloid precursor protein and presenilin 1 transgenes. *Nature Medicine*, 4 (1), 97-100

Holtmaat, A., Bonhoeffer, T., Chow, D. K., Chuckowree, J., De Paola, V., Hofer, S. B., Hubener, M., Keck, T., Knott, G., Lee, W.-C. A., Mostany, R., Mrsic-Flogel, T. D., Nedivi, E., Portera-Cailliau, C., Svoboda, K., Trachtenberg, J. T. & Wilbrecht, L. (**2009**). Long-term, high-resolution imaging in the mouse neocortex through a chronic cranial window. *Nature Protocols*, 4 (8), 1128-1144

Holtzman, D. M., Morris, J. C. & Goate, A. M. (**2011**). Alzheimer's Disease: The Challenge of the Second Century. *Science Translational Medicine*, 3 (77), 77sr1

Hsiao, K., Chapman, P., Nilsen, S., Eckman, C., Harigaya, Y., Younkin, S., Yang, F. & Cole, G. (**1996**). Correlative Memory Deficits, Aβ Elevation, and Amyloid Plaques in Transgenic Mice. *Science*, 274 (5284), 99-103

Hudry, E., Dashkoff, J., Roe, A. D., Takeda, S., Koffie, R. M., Hashimoto, T., Scheel, M., Spires-Jones, T., Arbel-Ornath, M., Betensky, R., Davidson, B. L. & Hyman, B. T. (**2013**). Gene Transfer of Human Apoe Isoforms Results in Differential Modulation of Amyloid Deposition and Neurotoxicity in Mouse Brain. *Science Translational Medicine*, 5 (212), 212ra161

Ishii, K., Lippa, C., Tomiyama, T., Miyatake, F., Ozawa, K., Tamaoka, A., Hasegawa, T., Fraser, P. E., Shoji, S. i., Nee, L. E., Pollen, D. A., St. George-Hyslop, P. H., Ii, K., Ohtake, T., Kalaria, R. N., Rossor, M. N., Lantos, P. L., Cairns, N. J., Farrer, L. A. & Mori, H. (**2001**). Distinguishable effects of Presenilin-1 and APP717 mutations on amyloid plaque deposition. *Neurobiology of Aging*, 22 (3), 367-376

Itagaki, S., McGeer, P. L., Akiyama, H., Zhu, S. & Selkoe, D. (**1989**). Relationship of microglia and astrocytes to amyloid deposits of Alzheimer disease. *Journal of Neuroimmunology*, 24 (3), 173-182

Jack Jr, C. R., Knopman, D. S., Jagust, W. J., Shaw, L. M., Aisen, P. S., Weiner, M. W., Petersen, R. C. & Trojanowski, J. Q. (**2010**). Hypothetical model of dynamic biomarkers of the Alzheimer's pathological cascade. *The Lancet Neurology*, 9 (1), 119-128

Jarrett, J. T. & Lansbury, P. T. (**1992**). Amyloid fibril formation requires a chemically discriminating nucleation event: studies of an amyloidogenic sequence from the bacterial protein OsmB. *Biochemistry*, 31 (49), 12345-12352

Jin, M., Shepardson, N., Yang, T., Chen, G., Walsh, D. & Selkoe, D. J. (**2011**). Soluble amyloid β-protein dimers isolated from Alzheimer cortex directly induce Tau hyperphosphorylation and neuritic degeneration. *Proceedings of the National Academy of Sciences*, 108 (14), 5819-5824

Jonsson, T., Atwal, J. K., Steinberg, S., Snaedal, J., Jonsson, P. V., Bjornsson, S., Stefansson, H., Sulem, P., Gudbjartsson, D., Maloney, J., Hoyte, K., Gustafson, A., Liu, Y., Lu, Y., Bhangale, T., Graham, R. R., Huttenlocher, J., Bjornsdottir, G., Andreassen, O. A., Jonsson, E. G., Palotie, A., Behrens, T. W., Magnusson, O. T., Kong, A., Thorsteinsdottir, U., Watts, R. J. & Stefansson, K. (**2012**). A mutation in APP protects against Alzheimer/'s disease and age-related cognitive decline. *Nature*, 488 (7409), 96-99

Jonsson, T., Stefansson, H., Steinberg, S., Jonsdottir, I., Jonsson, P. V., Snaedal, J., Bjornsson, S., Huttenlocher, J., Levey, A. I., Lah, J. J., Rujescu, D., Hampel, H., Giegling, I., Andreassen, O. A., Engedal, K., Ulstein, I., Djurovic, S., Ibrahim-Verbaas, C., Hofman, A., Ikram, M. A., van Duijn, C. M., Thorsteinsdottir, U., Kong, A. & Stefansson, K. (**2013**). Variant of TREM2 Associated with the Risk of Alzheimer's Disease. *New England Journal of Medicine*, 368 (2), 107-116

Jucker, M. & Walker, L. C. (**2011**). Pathogenic protein seeding in alzheimer disease and other neurodegenerative disorders. *Annals of Neurology*, 70 (4), 532-540

Kane, M. D., Lipinski, W. J., Callahan, M. J., Bian, F., Durham, R. A., Schwarz, R. D., Roher, A. E. & Walker, L. C. (**2000**). Evidence for Seeding of β-Amyloid by Intracerebral Infusion of Alzheimer Brain Extracts in β-Amyloid Precursor Protein-Transgenic Mice. *The Journal of Neuroscience*, 20 (10), 3606-3611

Karran, E., Mercken, M. & Strooper, B. D. (**2011**). The amyloid cascade hypothesis for Alzheimer's disease: an appraisal for the development of therapeutics. *Nat Rev Drug Discov*, 10 (9), 698-712

Keck, T., Scheuss, V., Jacobsen, R. I., Wierenga, Corette J., Eysel, Ulf T., Bonhoeffer, T. & Hübener, M. (**2011**). Loss of Sensory Input Causes Rapid Structural Changes of Inhibitory Neurons in Adult Mouse Visual Cortex. *Neuron*, 71 (5), 869-882

Kim, J., Basak, J. M. & Holtzman, D. M. (**2009**). The Role of Apolipoprotein E in Alzheimer's Disease. *Neuron*, 63 (3), 287-303

Klunk, W. E., Bacskai, B. J., Mathis, C. A., Kajkasz, S. T., McLellan, M. E., Frosch, M. P., Debnath, M. L., Holt, D. P., Wang, Y. & Hyman, B. T. (**2002**). Imaging A[beta] Plaques in Living Transgenic Mice with Multiphoton Microscopy and Methoxy-X04, a Systemically Administered Congo Red Derivative. *Journal of Neuropathology & Experimental Neurology*, 61 (9), 797-805

Knowles, R. B., Wyart, C., Buldyrev, S. V., Cruz, L., Urbanc, B., Hasselmo, M. E., Stanley, H. E. & Hyman, B. T. (**1999**). Plaque-induced neurite abnormalities: Implications for disruption of neural networks in Alzheimer's disease. *Proceedings of the National Academy of Sciences*, 96 (9), 5274-5279

Koenigsknecht-Talboo, J., Meyer-Luehmann, M., Parsadanian, M., Garcia-Alloza, M., Finn, M. B., Hyman, B. T., Bacskai, B. J. & Holtzman, D. M. (**2008**). Rapid Microglial Response Around Amyloid Pathology after Systemic Anti-Aβ Antibody Administration in PDAPP Mice. *The Journal of Neuroscience*, 28 (52), 14156-14164

Koffie, R. M., Meyer-Luehmann, M., Hashimoto, T., Adams, K. W., Mielke, M. L., Garcia-Alloza, M., Micheva, K. D., Smith, S. J., Kim, M. L., Lee, V. M., Hyman, B. T. & Spires-Jones, T. L. (**2009**). Oligomeric amyloid β associates with postsynaptic densities and correlates with excitatory synapse loss near senile plaques. *PNAS*, 106 (10), 4012-4017

Kuchibhotla, K. V., Goldman, S. T., Lattarulo, C. R., Wu, H.-Y., Hyman, B. T. & Bacskai, B. J. (**2008**). Aβ Plaques Lead to Aberrant Regulation of Calcium Homeostasis In Vivo Resulting in Structural and Functional Disruption of Neuronal Networks. *Neuron*, 59 (2), 214-225

Kuhn, P.-H., Wang, H., Dislich, B., Colombo, A., Zeitschel, U., Ellwart, J. W., Kremmer, E., Roszner, S. & Lichtenthaler, S. F. (**2010**). ADAM10 is the physiologically relevant, constitutive [alpha]-secretase of the amyloid precursor protein in primary neurons. *EMBO Journal*, 29 (17), 3020-3032

Kumar-Singh, S., Pirici, D., McGowan, E., Serneels, S., Ceuterick, C., Hardy, J., Duff, K., Dickson, D. & Van Broeckhoven, C. (**2005**). Dense-Core Plaques in Tg2576 and PSAPP Mouse Models of Alzheimer's Disease Are Centered on Vessel Walls. *The American journal of pathology*, 167 (2), 527-543

Lambert, J.-C., Ibrahim-Verbaas, C. A., Harold, D., Naj, A. C., Sims, R., Bellenguez, C., Jun, G., DeStefano, A. L., Bis, J. C., Beecham, G. W., Grenier-Boley, B., Russo, G., Thornton-Wells, T. A., Jones, N., Smith, A. V., Chouraki, V., Thomas, C., Ikram, M. A., Zelenika, D., Vardarajan, B. N., Kamatani, Y., Lin, C.-F., Gerrish, A., Schmidt, H., Kunkle, B., Dunstan, M. L., Ruiz, A., Bihoreau, M.-T., Choi, S.-H., Reitz, C., Pasquier, F., Hollingworth, P., Ramirez, A., Hanon, O., Fitzpatrick, A. L., Buxbaum, J. D., Campion, D., Crane, P. K., Baldwin, C., Becker, T., Gudnason, V., Cruchaga, C., Craig, D., Amin, N., Berr, C., Lopez, O. L., De Jager, P. L., Deramecourt, V., Johnston, J. A., Evans, D., Lovestone, S., Letenneur, L., Moron, F. J., Rubinsztein, D. C., Eiriksdottir, G., Sleegers, K., Goate, A. M., Fievet, N., Huentelman, M. J., Gill, M., Brown, K., Kamboh, M. I., Keller, L., Barberger-Gateau, P., McGuinness, B., Larson, E. B., Green, R., Myers, A. J., Dufouil, C., Todd, S., Wallon, D., Love, S., Rogaeva, E., Gallacher, J., St George-Hyslop, P., Clarimon, J., Lleo, A., Bayer, A., Tsuang, D. W., Yu, L., Tsolaki, M., Bossu, P., Spalletta, G., Proitsi, P., Collinge, J., Sorbi, S., Sanchez-Garcia, F., Fox, N. C., Hardy, J., Naranjo, M. C. D., Bosco, P., Clarke, R., Brayne, C., Galimberti, D., Mancuso, M., Matthews, F., European Alzheimer's Disease, I., Genetic,

Environmental Risk in Alzheimer's, D., Alzheimer's Disease Genetic, C., Cohorts for, H., Aging Research in Genomic, E., Moebus, S., Mecocci, P., Del Zompo, M., Maier, W., Hampel, H., Pilotto, A., Bullido, M., Panza, F., Caffarra, P., Nacmias, B., Gilbert, J. R., Mayhaus, M., Lannfelt, L., Hakonarson, H., Pichler, S., Carrasquillo, M. M., Ingelsson, M., Beekly, D., Alvarez, V., Zou, F., Valladares, O., Younkin, S. G., Coto, E., Hamilton-Nelson, K. L., Gu, W., Razquin, C., Pastor, P., Mateo, I., Owen, M. J., Faber, K. M., Jonsson, P. V., Combarros, O., O'Donovan, M. C., Cantwell, L. B., Soininen, H., Blacker, D., Mead, S., Mosley Jr, T. H., Bennett, D. A., Harris, T. B., Fratiglioni, L., Holmes, C., de Bruijn, R. F. A. G., Passmore, P., Montine, T. J., Bettens, K., Rotter, J. I., Brice, A., Morgan, K., Foroud, T. M., Kukull, W. A., Hannequin, D., Powell, J. F., Nalls, M. A., Ritchie, K., Lunetta, K. L., Kauwe, J. S. K., Boerwinkle, E., Riemenschneider, M., Boada, M., Hiltunen, M., Martin, E. R., Schmidt, R., Rujescu, D., Wang, L.-S., Dartigues, J.-F., Mayeux, R., Tzourio, C., Hofman, A., Nothen, M. M., Graff, C., Psaty, B. M., Jones, L., Haines, J. L., Holmans, P. A., Lathrop, M., Pericak-Vance, M. A., Launer, L. J., Farrer, L. A., van Duijn, C. M., Van Broeckhoven, C., Moskvina, V., Seshadri, S., Williams, J., Schellenberg, G. D. & Amouyel, P. (**2013**). Meta-analysis of 74,046 individuals identifies 11 new susceptibility loci for Alzheimer's disease. *Nature Genetics*, 45 (12), 1452-1458

Lammich, S., Kojro, E., Postina, R., Gilbert, S., Pfeiffer, R., Jasionowski, M., Haass, C. & Fahrenholz, F. (**1999**). Constitutive and regulated α-secretase cleavage of Alzheimer's amyloid precursor protein by a disintegrin metalloprotease. *Proceedings of the National Academy of Sciences*, 96 (7), 3922-3927

Lane, R. F., Raines, S. M., Steele, J. W., Ehrlich, M. E., Lah, J. A., Small, S. A., Tanzi, R. E., Attie, A. D. & Gandy, S. (**2010**). Diabetes-Associated SorCS1 Regulates Alzheimer's Amyloid-β Metabolism: Evidence for Involvement of SorL1 and the Retromer Complex. *The Journal of Neuroscience*, 30 (39), 13110-13115

Langer, F., Eisele, Y. S., Fritschi, S. K., Staufenbiel, M., Walker, L. C. & Jucker, M. (**2011**). Soluble Aβ Seeds Are Potent Inducers of Cerebral β-Amyloid Deposition. *The Journal of Neuroscience*, 31 (41), 14488-14495

Larson, M. E. & Lesné, S. E. (**2012**). Soluble Aβ oligomer production and toxicity. *J Neurochem*, 120 125-139

Lazarov, O., Lee, M., Peterson, D. A. & Sisodia, S. S. (**2002**). Evidence That Synaptically Released β-Amyloid Accumulates as Extracellular Deposits in the Hippocampus of Transgenic Mice. *The Journal of Neuroscience*, 22 (22), 9785-9793

Lazarov, O., Robinson, J., Tang, Y.-P., Hairston, I. S., Korade-Mirnics, Z., Lee, V. M. Y., Hersh, L. B., Sapolsky, R. M., Mirnics, K. & Sisodia, S. S. (**2005**). Environmental Enrichment Reduces Aβ Levels and Amyloid Deposition in Transgenic Mice. *Cell*, 120 (5), 701-713

Lee, H.-G., Casadesus, G., Zhu, X., Takeda, A., Perry, G. & Smith, M. A. (**2004**). Challenging the Amyloid Cascade Hypothesis: Senile Plaques and Amyloid-β as Protective Adaptations to Alzheimer Disease. *Annals of the New York Academy of Sciences*, 1019 (1), 1-4

Lesné, S., Koh, M. T., Kotilinek, L., Kayed, R., Glabe, C. G., Yang, A., Gallagher, M. & Ashe, K. H. (**2006**). A specific amyloid-[beta] protein assembly in the brain impairs memory. *Nature*, 440 (7082), 352-357

Lesné, S. E., Sherman, M. A., Grant, M., Kuskowski, M., Schneider, J. A., Bennett, D. A. & Ashe, K. H. (**2013**). Brain amyloid-β oligomers in ageing and Alzheimer's disease. *Brain*,

Lewis, J., Dickson, D. W., Lin, W.-L., Chisholm, L., Corral, A., Jones, G., Yen, S.-H., Sahara, N., Skipper, L., Yager, D., Eckman, C., Hardy, J., Hutton, M. & McGowan, E. (**2001**). Enhanced Neurofibrillary Degeneration in Transgenic Mice Expressing Mutant Tau and APP. *Science*, 293 (5534), 1487-1491

Liebscher, S. & Meyer-Luehmann, M. (**2012**). A peephole into the brain: Neuropathological features of Alzheimer's Disease revealed by in vivo two-photon imaging. *Frontiers in Psychiatry*, 3

Lim, G. P., Chu, T., Yang, F., Beech, W., Frautschy, S. A. & Cole, G. M. (**2001**). The Curry Spice Curcumin Reduces Oxidative Damage and Amyloid Pathology in an Alzheimer Transgenic Mouse. *The Journal of Neuroscience*, 21 (21), 8370-8377

Lim, G. P., Yang, F., Chu, T., Chen, P., Beech, W., Teter, B., Tran, T., Ubeda, O., Ashe, K. H., Frautschy, S. A. & Cole, G. M. (**2000**). Ibuprofen Suppresses Plaque Pathology and Inflammation in a Mouse Model for Alzheimer's Disease. *The Journal of Neuroscience*, 20 (15), 5709-5714

Lomakin, A., Teplow, D. B., Kirschner, D. A. & Benedek, G. B. (**1997**). Kinetic theory of fibrillogenesis of amyloid β-protein. *Proceedings of the National Academy of Sciences*, 94 (15), 7942-7947

Luo, Y., Bolon, B., Damore, M. A., Fitzpatrick, D., Liu, H., Zhang, J., Yan, Q., Vassar, R. & Citron, M. (**2003**). BACE1 (β-secretase) knockout mice do not acquire compensatory gene expression changes or develop neural lesions over time. *Neurobiology of Disease*, 14 (1), 81-88

Marques, M. A., Kulstad, J. J., Savard, C. E., Green, P. S., Lee, S. P., Craft, S., Watson, G. S. & Cook, D. G. (**2009**). Peripheral Amyloid-β Levels Regulate Amyloid-β Clearance from the Central Nervous System. *Journal of Alzheimer's Disease*, 16 (2), 325-329

Martins, I. C., Kuperstein, I., Wilkinson, H., Maes, E., Vanbrabant, M., Jonckheere, W., Van Gelder, P., Hartmann, D., D'Hooge, R., De Strooper, B., Schymkowitz, J. & Rousseau, F. (**2008**). Lipids revert inert A[beta] amyloid fibrils to neurotoxic protofibrils that affect learning in mice. *EMBO J*, 27 (1), 224-233

Masliah, E., Mallory, M., Alford, M., DeTeresa, R., Hansen, L. A., McKeel, D. W. & Morris, J. C. (**2001**). Altered expression of synaptic proteins occurs early during progression of Alzheimer's disease. *Neurology*, 56 (1), 127-129

Mattson, M. P., Cheng, B., Culwell, A. R., Esch, F. S., Lieberburg, I. & Rydel, R. E. (**1993**). Evidence for excitoprotective and intraneuronal calcium-regulating roles for secreted forms of the β-amyloid precursor protein. *Neuron*, 10 (2), 243-254

McGeer, P., McGeer, E., Rogers, J. & Sibley, J. (**1990**). Anti-inflammatory drugs and Alzheimer disease. *The Lancet*, 335 (8696), 1037

McLaurin, J., Kierstead, M. E., Brown, M. E., Hawkes, C. A., Lambermon, M. H. L., Phinney, A. L., Darabie, A. A., Cousins, J. E., French, J. E., Lan, M. F., Chen, F., Wong, S. S. N., Mount, H. T. J.,

Fraser, P. E., Westaway, D. & George-Hyslop, P. S. (**2006**). Cyclohexanehexol inhibitors of A[beta] aggregation prevent and reverse Alzheimer phenotype in a mouse model. *Nature Medicine*, 12 (7), 801-808

McLellan, M. E., Kajdasz, S. T., Hyman, B. T. & Bacskai, B. J. (**2003**). In Vivo Imaging of Reactive Oxygen Species Specifically Associated with Thioflavine S-Positive Amyloid Plaques by Multiphoton Microscopy. *The Journal of Neuroscience*, 23 (6), 2212-2217

Meyer-Luehmann, M., Coomaraswamy, J., Bolmont, T., Kaeser, S., Schaefer, C., Kilger, E., Neuenschwander, A., Abramowski, D., Frey, P., Jaton, A. L., Vigouret, J.-M., Paganetti, P., Walsh, D. M., Mathews, P. M., Ghiso, J., Staufenbiel, M., Walker, L. C. & Jucker, M. (**2006**). Exogenous Induction of Cerebral ß-Amyloidogenesis Is Governed by Agent and Host. *Science*, 313 (5794), 1781-1784

Meyer-Luehmann, M., Mielke, M., Spires-Jones, T. L., Stoothoff, W., Jones, P., Bacskai, B. J. & Hyman, B. T. (**2009**). A Reporter of Local Dendritic Translocation Shows Plaque- Related Loss of Neural System Function in APP-Transgenic Mice. *The Journal of Neuroscience*, 29 (40), 12636-12640

Meyer-Luehmann, M., Mora, J. R., Mielke, M., Spires-Jones, T., de Calignon, A., von Andrian, U. & Hyman, B. (**2011**). T cell mediated cerebral hemorrhages and microhemorrhages during passive Abeta immunization in APPPS1 transgenic mice. *Molecular Neurodegeneration*, 6 (1), 22

Meyer-Luehmann, M., Spires-Jones, T. L., Prada, C., Garcia-Alloza, M., de Calignon, A., Rozkalne, A., Koenigsknecht-Talboo, J., Holtzman, D. M., Bacskai, B. J. & Hyman, B. T. (**2008**). Rapid appearance and local toxicity of amyloid-[bgr] plaques in a mouse model of Alzheimer/'s disease. *Nature*, 451 (7179), 720-724

Minoshima, S., Giordani, B., Berent, S., Frey, K. A., Foster, N. L. & Kuhl, D. E. (**1997**). Metabolic reduction in the posterior cingulate cortex in very early Alzheimer's disease. *Annals of Neurology*, 42 (1), 85-94

Moehlmann, T., Winkler, E., Xia, X., Edbauer, D., Murrell, J., Capell, A., Kaether, C., Zheng, H., Ghetti, B., Haass, C. & Steiner, H. (**2002**). Presenilin-1 mutations of leucine 166 equally affect the generation of the Notch and APP intracellular domains independent of their effect on Aβ42 production. *Proceedings of the National Academy of Sciences*, 99 (12), 8025-8030

Moreno-Gonzalez, I., Estrada, L. D., Sanchez-Mejias, E. & Soto, C. (**2013**). Smoking exacerbates amyloid pathology in a mouse model of Alzheimer's disease. *Nature Communications*, 4 1495

Morris, J. C., Aisen, P. S., Bateman, R. J., Benzinger, T. L. S., Cairns, N. J., Fagan, A. M., Ghetti, B., Goate, A. M., Holtzman, D. M., Klunk, W. E., McDade, E., Marcus, D. S., Martins, R. N., Masters, C. L., Mayeux, R., Oliver, A., Quaid, K., M Ringman, J., Rossor, M. N., Salloway, S., Schofield, P. R., Selsor, N. J., Sperling, R. A., Weiner, M. W., Xiong, C., Moulder, K. L. & Buckles, V. D. (**2012**). Developing an international network for Alzheimer's research: the Dominantly Inherited Alzheimer Network. *Clinical Investigation*, 2 (10), 975-984

Mudher, A. & Lovestone, S. (**2002**). Alzheimer's disease – do tauists and baptists finally shake hands? *Trends in Neurosciences*, 25 (1), 22-26

Mullan, M., Crawford, F., Axelman, K., Houlden, H., Lilius, L., Winblad, B. & Lannfelt, L. (**1992**). A pathogenic mutation for probable Alzheimer's disease in the APP gene at the N-terminus of [beta]-amyloid. *Nature Genetics*, 1 (5), 345-347

Müller, T., Meyer, H. E., Egensperger, R. & Marcus, K. (**2008**). The amyloid precursor protein intracellular domain (AICD) as modulator of gene expression, apoptosis, and cytoskeletal dynamics— Relevance for Alzheimer's disease. *Progress in Neurobiology*, 85 (4), 393-406

Nath, S., Agholme, L., Kurudenkandy, F. R., Granseth, B., Marcusson, J. & Hallbeck, M. (**2012**). Spreading of Neurodegenerative Pathology via Neuron-to-Neuron Transmission of β-Amyloid. *The Journal of Neuroscience*, 32 (26), 8767-8777

Natté, R., Maat-Schieman, M. L. C., Haan, J., Bornebroek, M., Roos, R. A. C. & Van Duinen, S. G. (**2001**). Dementia in hereditary cerebral hemorrhage with amyloidosis-Dutch type is associated with cerebral amyloid angiopathy but is independent of plaques and neurofibrillary tangles. *Annals of Neurology*, 50 (6), 765-772

Nikolaev, A., McLaughlin, T., O/'Leary, D. D. M. & Tessier-Lavigne, M. (**2009**). APP binds DR6 to trigger axon pruning and neuron death via distinct caspases. *Nature*, 457 (7232), 981-989

Nyström, S., Psonka-Antonczyk, K. M., Ellingsen, P. G., Johansson, L. B. G., Reitan, N., Handrick, S., Prokop, S., Heppner, F. L., Wegenast-Braun, B. M., Jucker, M., Lindgren, M., Stokke, B. T., Hammarström, P. & Nilsson, K. P. R. (**2013**). Evidence for Age-Dependent in Vivo Conformational Rearrangement within Aβ Amyloid Deposits. *ACS Chemical Biology*,

O'Brien, R. J. & Wong, P. C. (**2011**). Amyloid Precursor Protein Processing and Alzheimer's Disease. *Annual Review of Neuroscience*, 34 (1), 185-204

Oddo, S., Caccamo, A., Shepherd, J. D., Murphy, M. P., Golde, T. E., Kayed, R., Metherate, R., Mattson, M. P., Akbari, Y. & LaFerla, F. M. (**2003**). Triple-Transgenic Model of Alzheimer's Disease with Plaques and Tangles: Intracellular A[beta] and Synaptic Dysfunction. *Neuron*, 39 (3), 409-421

Oh, E. S., Savonenko, A. V., King, J. F., Fangmark Tucker, S. M., Rudow, G. L., Xu, G., Borchelt, D. R. & Troncoso, J. C. (**2009**). Amyloid precursor protein increases cortical neuron size in transgenic mice. *Neurobiology of Aging*, 30 (8), 1238-1244

Page, R. M., Gutsmiedl, A., Fukumori, A., Winkler, E., Haass, C. & Steiner, H. (**2010**). β-Amyloid Precursor Protein Mutants Respond to γ-Secretase Modulators. *Journal of Biological Chemistry*, 285 (23), 17798-17810

Parbhu, A., Lin, H., Thimm, J. & Lal, R. (**2002**). Imaging real-time aggregation of amyloid beta protein (1–42) by atomic force microscopy. *Peptides*, 23 (7), 1265-1270

Pasqualetti, P., Bonomini, C., Forno, G., Paulon, L., Sinforiani, E., Marra, C., Zanetti, O. & Maria Rossini, P. (**2009**). A randomized controlled study on effects of ibuprofen on cognitive progression of Alzheimer's disease. *Aging Clinical and Experimental Research*, 21 (2), 102-110

Pfeifer, M., Boncristiano, S., Bondolfi, L., Stalder, A., Deller, T., Staufenbiel, M., Mathews, P. M. & Jucker, M. (**2002**). Cerebral Hemorrhage After Passive Anti-Aβ Immunotherapy. *Science*, 298 (5597), 1379

Pham, E., Crews, L., Ubhi, K., Hansen, L., Adame, A., Cartier, A., Salmon, D., Galasko, D., Michael, S., Savas, J. N., Yates, J. R., Glabe, C. & Masliah, E. (**2010**). Progressive accumulation of amyloid-β oligomers in Alzheimer's disease and in amyloid precursor protein transgenic mice is accompanied by selective alterations in synaptic scaffold proteins. *FEBS Journal*, 277 (14), 3051-3067

Pimplikar, S. W. (**2009**). Reassessing the amyloid cascade hypothesis of Alzheimer's disease. *The International Journal of Biochemistry & Cell Biology*, 41 (6), 1261-1268

Postina, R., Schroeder, A., Dewachter, I., Bohl, J., Schmitt, U., Kojro, E., Prinzen, C., Endres, K., Hiemke, C., Blessing, M., Flamez, P., Dequenne, A., Godaux, E., van Leuven, F. & Fahrenholz, F. (**2004**). A disintegrin-metalloproteinase prevents amyloid plaque formation and hippocampal defects in an Alzheimer disease mouse model. *The Journal of Clinical Investigation*, 113 (10), 1456-1464

Praprotnik, D., Smith, M. A., Richey, P. L., Vinters, H. V. & Perry, G. (**1995**). Plasma membrane fragility in dystrophic neurites in senile plaques of Alzheimer's disease: an index of oxidative stress. *Acta Neuropathologica*, 91 (1), 1-5

Radde, R., Bolmont, T., Kaeser, S. A., Coomaraswamy, J., Lindau, D., Stoltze, L., Calhoun, M. E., Jaggi, F., Wolburg, H., Gengler, S., Haass, C., Ghetti, B., Czech, C., Holscher, C., Mathews, P. M. & Jucker, M. (**2006**). A[beta]42-driven cerebral amyloidosis in transgenic mice reveals early and robust pathology. *EMBO Reports*, 7 (9), 940-946

Radde, R., Duma, C., Goedert, M. & Jucker, M. (**2008**). The value of incomplete mouse models of Alzheimer's disease. *European Journal of Nuclear Medicine and Molecular Imaging*, 35 (1), 70-74

Rajendran, L., Honsho, M., Zahn, T. R., Keller, P., Geiger, K. D., Verkade, P. & Simons, K. (**2006**). Alzheimer's disease β-amyloid peptides are released in association with exosomes. *Proceedings of the National Academy of Sciences*, 103 (30), 11172-11177

Rak, M., Del Bigio, M. R., Mai, S., Westaway, D. & Gough, K. (**2007**). Dense-core and diffuse Aβ plaques in TgCRND8 mice studied with synchrotron FTIR microspectroscopy. *Biopolymers*, 87 (4), 207-217

Reitz, C., Cheng, R., Rogaeva, E. & et al. (**2011**). MEta-analysis of the association between variants in sorl1 and alzheimer disease. *Archives of Neurology*, 68 (1), 99-106

Ring, S., Weyer, S. W., Kilian, S. B., Waldron, E., Pietrzik, C. U., Filippov, M. A., Herms, J., Buchholz, C., Eckman, C. B., Korte, M., Wolfer, D. P. & Müller, U. C. (**2007**). The Secreted β-Amyloid Precursor Protein Ectodomain APPsα Is Sufficient to Rescue the Anatomical, Behavioral, and Electrophysiological Abnormalities of APP-Deficient Mice. *The Journal of Neuroscience*, 27 (29), 7817-7826

Roberson, E. D., Scearce-Levie, K., Palop, J. J., Yan, F., Cheng, I. H., Wu, T., Gerstein, H., Yu, G.-Q. & Mucke, L. (**2007**). Reducing Endogenous Tau Ameliorates Amyloid ß-Induced Deficits in an Alzheimer's Disease Mouse Model. *Science*, 316 (5825), 750-754

Rogaeva, E., Meng, Y., Lee, J. H., Gu, Y., Kawarai, T., Zou, F., Katayama, T., Baldwin, C. T., Cheng, R., Hasegawa, H., Chen, F., Shibata, N., Lunetta, K. L., Pardossi-Piquard, R., Bohm, C., Wakutani, Y., Cupples, L. A., Cuenco, K. T., Green, R. C., Pinessi, L., Rainero, I., Sorbi, S., Bruni, A., Duara, R., Friedland, R. P., Inzelberg, R., Hampe, W., Bujo, H., Song, Y.-Q., Andersen, O. M., Willnow, T. E., Graff-Radford, N., Petersen, R. C., Dickson, D., Der, S. D., Fraser, P. E., Schmitt-Ulms, G., Younkin, S., Mayeux, R., Farrer, L. A. & St George-Hyslop, P. (**2007**). The neuronal sortilin-related receptor SORL1 is genetically associated with Alzheimer disease. *Nature Genetics*, 39 (2), 168-177

Rogers, J., Cooper, N. R., Webster, S., Schultz, J., McGeer, P. L., Styren, S. D., Civin, W. H., Brachova, L., Bradt, B. & Ward, P. (**1992**). Complement activation by beta-amyloid in Alzheimer disease. *Proceedings of the National Academy of Sciences*, 89 (21), 10016-10020

Roher, A. E., Lowenson, J. D., Clarke, S., Woods, A. S., Cotter, R. J., Gowing, E. & Ball, M. J. (**1993**). beta-Amyloid-(1-42) is a major component of cerebrovascular amyloid deposits: implications for the pathology of Alzheimer disease. *Proceedings of the National Academy of Sciences*, 90 (22), 10836-10840

Rusanen, M., Kivipelto, M., Quesenberry, C. P., Jr, Zhou, J. & Whitmer, R. A. (**2011**). HEavy smoking in midlife and long-term risk of alzheimer disease and vascular dementia. *Archives of Internal Medicine*, 171 (4), 333-339

Saura, C. A., Choi, S.-Y., Beglopoulos, V., Malkani, S., Zhang, D., Rao, B. S. S., Chattarji, S., Kelleher Iii, R. J., Kandel, E. R., Duff, K., Kirkwood, A. & Shen, J. (**2004**). Loss of Presenilin Function Causes Impairments of Memory and Synaptic Plasticity Followed by Age-Dependent Neurodegeneration. *Neuron*, 42 (1), 23-36

Schellenberg, G. & Montine, T. (**2012**). The genetics and neuropathology of Alzheimer's disease. *Acta Neuropathologica*, 124 (3), 305-323

Schenk, D., Barbour, R., Dunn, W., Gordon, G., Grajeda, H., Guido, T., Hu, K., Huang, J., Johnson-Wood, K., Khan, K., Kholodenko, D., Lee, M., Liao, Z., Lieberburg, I., Motter, R., Mutter, L., Soriano, F., Shopp, G., Vasquez, N., Vandevert, C., Walker, S., Wogulis, M., Yednock, T., Games, D. & Seubert, P. (**1999**). Immunization with amyloid-[beta] attenuates Alzheimer-disease-like pathology in the PDAPP mouse. *Nature*, 400 (6740), 173-177

Selkoe, D. J. (**2001**). Alzheimer's Disease: Genes, Proteins, and Therapy. *Physiological Reviews*, 81 (2), 741-766

Selkoe, D. J. (**2011**). Resolving controversies on the path to Alzheimer's therapeutics. *Nature Medicine*, 17 (9), 1060-1065

Seubert, P., Vigo-Pelfrey, C., Esch, F., Lee, M., Dovey, H., Davis, D., Sinha, S., Schiossmacher, M., Whaley, J., Swindlehurst, C., McCormack, R., Wolfert, R., Selkoe, D., Lieberburg, I. & Schenk, D. (**1992**). Isolation and quantification of soluble Alzheimer's [beta]-peptide from biological fluids. *Nature*, 359 (6393), 325-327

Shankar, G. M., Li, S., Mehta, T. H., Garcia-Munoz, A., Shepardson, N. E., Smith, I., Brett, F. M., Farrell, M. A., Rowan, M. J., Lemere, C. A., Regan, C. M., Walsh, D. M., Sabatini, B. L. & Selkoe,

D. J. (**2008**). Amyloid-[beta] protein dimers isolated directly from Alzheimer's brains impair synaptic plasticity and memory. *Nature Medicine*, 14 (8), 837-842

Shen, J. & Kelleher, R. J. (**2007**). The presenilin hypothesis of Alzheimer's disease: Evidence for a loss-of-function pathogenic mechanism. *Proceedings of the National Academy of Sciences*, 104 (2), 403-409

Sheng, J. G., Price, D. L. & Koliatsos, V. E. (**2002**). Disruption of Corticocortical Connections Ameliorates Amyloid Burden in Terminal Fields in a Transgenic Model of Aβ Amyloidosis. *The Journal of Neuroscience*, 22 (22), 9794-9799

Shepherd, C. E., Gregory, G. C., Vickers, J. C., Brooks, W. S., Kwok, J. B. J., Schofield, P. R., Kril, J. J. & Halliday, G. M. (**2004**). Positional effects of presenilin-1 mutations on tau phosphorylation in cortical plaques. *Neurobiology of Disease*, 15 (1), 115-119

Singh, P. P., Singh, M. & Mastana, S. S. (**2006**). APOE distribution in world populations with new data from India and the UK. *Annals of Human Biology*, 33 (3), 279-308

Small, S. A. & Duff, K. (**2008**). Linking Aβ and Tau in Late-Onset Alzheimer's Disease: A Dual Pathway Hypothesis. *Neuron*, 60 (4), 534-542

Snider, B., Norton, J., Coats, M. A. & et al. (**2005**). NOvel presenilin 1 mutation (s170f) causing alzheimer disease with lewy bodies in the third decade of life. *Archives of Neurology*, 62 (12), 1821-1830

Snyder, S. W., Ladror, U. S., Wade, W. S., Wang, G. T., Barrett, L. W., Matayoshi, E. D., Huffaker, H. J., Krafft, G. A. & Holzman, T. F. (**1994**). Amyloid-beta aggregation: selective inhibition of aggregation in mixtures of amyloid with different chain lengths. *Biophysical Journal*, 67 (3), 1216-1228

Sofroniew, M. & Vinters, H. (**2010**). Astrocytes: biology and pathology. *Acta Neuropathologica*, 119 (1), 7-35

Spires, T. L., Meyer-Luehmann, M., Stern, E. A., McLean, P. J., Skoch, J., Nguyen, P. T., Bacskai, B. J. & Hyman, B. T. (**2005**). Dendritic Spine Abnormalities in Amyloid Precursor Protein Transgenic Mice Demonstrated by Gene Transfer and Intravital Multiphoton Microscopy. *The Journal of Neuroscience*, 25 (31), 7278-7287

Steiner, H., Revesz, T., Neumann, M., Romig, H., Grim, M. G., Pesold, B., Kretzschmar, H. A., Hardy, J., Holton, J. L., Baumeister, R., Houlden, H. & Haass, C. (**2001**). A Pathogenic Presenilin-1 Deletion Causes Abberrant Aβ42 Production in the Absence of Congophilic Amyloid Plaques. *Journal of Biological Chemistry*, 276 (10), 7233-7239

Stelzmann, R. A., Norman Schnitzlein, H. & Reed Murtagh, F. (**1995**). An english translation of alzheimer's 1907 paper, "über eine eigenartige erkankung der hirnrinde". *Clinical Anatomy*, 8 (6), 429-431

Strittmatter, W. J., Saunders, A. M., Schmechel, D., Pericak-Vance, M., Enghild, J., Salvesen, G. S. & Roses, A. D. (**1993**). Apolipoprotein E: high-avidity binding to beta-amyloid and increased frequency

of type 4 allele in late-onset familial Alzheimer disease. *Proceedings of the National Academy of Sciences*, 90 (5), 1977-1981

Sturchler-Pierrat, C., Abramowski, D., Duke, M., Wiederhold, K.-H., Mistl, C., Rothacher, S., Ledermann, B., Bürki, K., Frey, P., Paganetti, P. A., Waridel, C., Calhoun, M. E., Jucker, M., Probst, A., Staufenbiel, M. & Sommer, B. (**1997**). Two amyloid precursor protein transgenic mouse models with Alzheimer disease-like pathology. *Proceedings of the National Academy of Sciences*, 94 (24), 13287-13292

Tagliavini, F., Giaccone, G., Frangione, B. & Bugiani, O. (**1988**). Preamyloid deposits in the cerebral cortex of patients with Alzheimer's disease and nondemented individuals. *Neuroscience Letters*, 93 (2–3), 191-196

Takahashi, R. H., Almeida, C. G., Kearney, P. F., Yu, F., Lin, M. T., Milner, T. A. & Gouras, G. K. (**2004**). Oligomerization of Alzheimer's β-Amyloid within Processes and Synapses of Cultured Neurons and Brain. *The Journal of Neuroscience*, 24 (14), 3592-3599

Takahashi, R. H., Milner, T. A., Li, F., Nam, E. E., Edgar, M. A., Yamaguchi, H., Beal, M. F., Xu, H., Greengard, P. & Gouras, G. K. (**2002**). Intraneuronal Alzheimer Aβ42 Accumulates in Multivesicular Bodies and Is Associated with Synaptic Pathology. *The American journal of pathology*, 161 (5), 1869-1879

Takao, M., Ghetti, B., Hayakawa, I., Ikeda, E., Fukuuchi, Y., Miravalle, L., Piccardo, P., Murrell, J., Glazier, B. & Koto, A. (**2002**). A novel mutation (G217D) in the Presenilin 1 gene (PSEN1) in a Japanese family: presenile dementia and parkinsonism are associated with cotton wool plaques in the cortex and striatum. *Acta Neuropathologica*, 104 (2), 155-170

Terry, R. D., Masliah, E., Salmon, D. P., Butters, N., DeTeresa, R., Hill, R., Hansen, L. A. & Katzman, R. (**1991**). Physical basis of cognitive alterations in alzheimer's disease: Synapse loss is the major correlate of cognitive impairment. *Annals of Neurology*, 30 (4), 572-580

Thal, D. R., Rüb, U., Orantes, M. & Braak, H. (**2002**). Phases of Aβ-deposition in the human brain and its relevance for the development of AD. *Neurology*, 58 (12), 1791-1800

Thies, W. & Bleier, L. (**2011**). 2011 Alzheimer's disease facts and figures. *Alzheimer's & Dementia*, 7 (2), 208-244

Thornton, E., Vink, R., Blumbergs, P. C. & Van Den Heuvel, C. (**2006**). Soluble amyloid precursor protein α reduces neuronal injury and improves functional outcome following diffuse traumatic brain injury in rats. *Brain Research*, 1094 (1), 38-46

Townsend, M., Shankar, G. M., Mehta, T., Walsh, D. M. & Selkoe, D. J. (**2006**). Effects of secreted oligomers of amyloid β-protein on hippocampal synaptic plasticity: a potent role for trimers. *The Journal of Physiology*, 572 (2), 477-492

Tsai, J., Grutzendler, J., Duff, K. & Gan, W.-B. (**2004**). Fibrillar amyloid deposition leads to local synaptic abnormalities and breakage of neuronal branches. *Nature Neuroscience*, 7 (11), 1181-1183

Tyas, S. L. (**2001**). Alcohol use and the risk of developing Alzheimer's disease. *Alcohol research & health : the journal of the National Institute on Alcohol Abuse and Alcoholism*, 25 (4), 299-306

Urbanc, B., Cruz, L., Buldyrev, S. V., Havlin, S., Irizarry, M. C., Stanley, H. E. & Hyman, B. T. (**1999**). Dynamics of Plaque Formation in Alzheimer's Disease. *Biophysical Journal*, 76 (3), 1330-1334

Valenzuela, M. J. & Sachdev, P. (**2006**). Brain reserve and dementia: a systematic review. *Psychological Medicine*, 36 (4), 441-454

Vlad, S. C., Miller, D. R., Kowall, N. W. & Felson, D. T. (**2008**). Protective effects of NSAIDs on the development of Alzheimer disease. *Neurology*, 70 (19), 1672-1677

Walker, L. C., Callahan, M. J., Bian, F., Durham, R. A., Roher, A. E. & Lipinski, W. J. (**2002**). Exogenous induction of cerebral β-amyloidosis in βAPP-transgenic mice. *Peptides*, 23 (7), 1241-1247

Walsh, D. M., Hartley, D. M., Kusumoto, Y., Fezoui, Y., Condron, M. M., Lomakin, A., Benedek, G. B., Selkoe, D. J. & Teplow, D. B. (**1999**). Amyloid β-Protein Fibrillogenesis: STRUCTURE AND BIOLOGICAL ACTIVITY OF PROTOFIBRILLAR INTERMEDIATES. *Journal of Biological Chemistry*, 274 (36), 25945-25952

Walsh, D. M., Klyubin, I., Fadeeva, J. V., Cullen, W. K., Anwyl, R., Wolfe, M. S., Rowan, M. J. & Selkoe, D. J. (**2002**). Naturally secreted oligomers of amyloid [beta] protein potently inhibit hippocampal long-term potentiation in vivo. *Nature*, 416 (6880), 535-539

Walsh, D. M., Tseng, B. P., Rydel, R. E., Podlisny, M. B. & Selkoe, D. J. (**2000**). The Oligomerization of Amyloid β-Protein Begins Intracellularly in Cells Derived from Human Brain†. *Biochemistry*, 39 (35), 10831-10839

Wang, A., Das, P., Switzer, R. C., Golde, T. E. & Jankowsky, J. L. (**2011**). Robust Amyloid Clearance in a Mouse Model of Alzheimer's Disease Provides Novel Insights into the Mechanism of Amyloid-β Immunotherapy. *The Journal of Neuroscience*, 31 (11), 4124-4136

Webster, S., Lue, L. F., Brachova, L., Tenner, A. J., McGeer, P. L., Terai, K., Walker, D. G., Bradt, B., Cooper, N. R. & Rogers, J. (**1997**). Molecular and Cellular Characterization of the Membrane Attack Complex, C5b-9, in Alzheimer's Disease. *Neurobiology of Aging*, 18 (4), 415-421

Willem, M., Lammich, S. & Haass, C. (**2009**). Function, regulation and therapeutic properties of β-secretase (BACE1). *Seminars in Cell & Developmental Biology*, 20 (2), 175-182

Winblad, B., Andreasen, N., Minthon, L., Floesser, A., Imbert, G., Dumortier, T., Maguire, R. P., Blennow, K., Lundmark, J., Staufenbiel, M., Orgogozo, J.-M. & Graf, A. (**2012**). Safety, tolerability, and antibody response of active Aβ immunotherapy with CAD106 in patients with Alzheimer's disease: randomised, double-blind, placebo-controlled, first-in-human study. *The Lancet Neurology*, 11 (7), 597-604

Wu, H.-Y., Hudry, E., Hashimoto, T., Kuchibhotla, K., Rozkalne, A., Fan, Z., Spires-Jones, T., Xie, H., Arbel-Ornath, M., Grosskreutz, C. L., Bacskai, B. J. & Hyman, B. T. (**2010**). Amyloid β Induces

the Morphological Neurodegenerative Triad of Spine Loss, Dendritic Simplification, and Neuritic Dystrophies through Calcineurin Activation. *The Journal of Neuroscience*, 30 (7), 2636-2649

Wyss-Coray, T. (**2006**). Inflammation in Alzheimer disease: driving force, bystander or beneficial response? *Nature Medicine*, 12 (9), 1005-1015

Wyss-Coray, T., Loike, J. D., Brionne, T. C., Lu, E., Anankov, R., Yan, F., Silverstein, S. C. & Husemann, J. (**2003**). Adult mouse astrocytes degrade amyloid-[beta] in vitro and in situ. *Nature Medicine*, 9 (4), 453-457

Xie, H., Guan, J., Borrelli, L. A., Xu, J., Serrano-Pozo, A. & Bacskai, B. J. (**2013**). Mitochondrial Alterations near Amyloid Plaques in an Alzheimer's Disease Mouse Model. *The Journal of Neuroscience*, 33 (43), 17042-17051

Xie, H., Hou, S., Jiang, J., Sekutowicz, M., Kelly, J. & Bacskai, B. J. (**2013**). Rapid cell death is preceded by amyloid plaque-mediated oxidative stress. *Proceedings of the National Academy of Sciences*, 110 (19), 7904-7909

List of Figures

List of Tables

Eidesstattliche Versicherung/Affidavit

Hiermit versichere ich an Eides statt, dass ich die vorliegende Dissertation „Dynamics of Amyloid Plaque Formation in Alzheimer's disease" selbstständig angefertigt habe, mich außer der angegebenen keiner weiteren Hilfsmittel bedient und alle Erkenntnisse, die aus dem Schrifttum ganz oder annähernd übernommen sind, als solche kenntlich gemacht und nach ihrer Herkunft unter Bezeichnung der Fundstelle einzeln nachgewiesen habe.

I hereby confirm that the dissertation "Dynamics of Amyloid Plaque formation in Alzheimer's disease" is the result of my own work and that I have only used sources or materials listed and specified in the dissertation.

München, den

Munich, date   Unterschrift/Signature

Declaration of Results Contributions

For this thesis, the initial idea was conceived by Melanie Meyer-Luehmann; all experiments were carried out by Joanna McCarter; Sabine Liebscher, Teresa Bachhuber, Christian Haass and Magdalena Götz contributed analytical advice in discussion with Melanie Meyer-Luehmann and Joanna McCarter.

Curriculum Vitae

Joanna McCarter

joanna.mccarter@gmail.com

Geyerstrasse 9 RG, Munich 80469, Germany. +49 (0)1763 807 94 07

University Education

2010-Present PhD, Neurodegenerative Diseases

Adolf Butenandt Institute, Ludwig-Maximilians-University, Munich, Germany

2009-2010 Neuroscience PhD preparatory year

Graduate School of Neuroscience, Ludwigs-Maximilians-University, Munich, Germany

Part of the internationally-recognised IMPRS (International Max Planck Research School) PhD program.

2005–2009 BSc (Hons) Neuroscience (with Industrial Experience). First Class

Biomedical Faculty, University of Leeds, UK

International Research and Work Experience

2010-Present PhD Research

Adolf Butenandt Institute, Ludwig-Maximilians-University, Munich, Germany

Thesis Title: *Dynamics of Amyloid Plaques in a mouse model of Alzheimer's disease*

Gained wide-ranging knowledge about neurodegenerative diseases as well as the broader field of life science research in Munich. Developed communications skills by writing my own and editing several colleagues' scientific papers.

2009 BSc Dissertation

University of Leeds, Leeds, UK.

Wrote report and presented my project to a large audience of professors and students.

2007-2008 Industrial Placement

GlaxoSmithKline, Cognition and Neurodegeneration Centre, Singapore, Singapore.

12 month placement, had own project to developing a biochemical gene-expression assay for cognition enhancement. Learnt first-hand how drug development in a pharmaceutical company works. Experienced the scientific environment in the Asia-Pacific region.

Feb-Apr 2005 English Teacher

Tiny Tots School, Kurseong, West Bengal, India

Planned lessons and taught English to school children aged 4 to 18.

Publications

McCarter J.F., Liebscher S., Bachhuber T., Abou-Ajram C., Hübener M., Hyman B.T., Haass C., Meyer-Luehmann M., *Clustering of plaques contributes to plaque growth in a mouse model of Alzheimer's disease*. Acta Neuropathologica, 2013 (link).

Conferences attended

2013   Biovision, Lyon, France

2012   Society for Neuroscience, New Orleans, USA. Presented a poster of my research.

2012   Euroscience Open Forum, Dublin, Ireland

Additional Skills

Languages English: mother tongue; German: working knowledge

IT skills Excellent working knowledge of Microsoft Word, Excel and Powerpoint; Adobe Photoshop and Illustrator and Endnote reference manager. Highly proficient at scientific literature research.

Communication and Career Development Workshops

Careers Insight Workshop – Medical Writing in MedComms (2 days)

Advanced Scientific Writing (3 days)

How to Publish in Peer-reviewed Journals (3 days)

How to Present at International Scientific Conferences (3 days)